Published in final edited form as:
Curr Drug Deliv. 2011 January 1; 8(1): 79–134.

Bombesin receptor-mediated imaging and cytotoxicity: review and current status

Veronica Sancho[*,1], **Alessia Di Florio**[*,1], **Terry W. Moody**[2], and **Robert T. Jensen**[1]

[1] Digestive Diseases Branch, National Institutes of Diabetes, Digestive and Kidney Diseases, National Institutes of Health, Bethesda, MD, 20892

[2] Department of Health and Human Services, National Cancer Institute Office of the Director, Center for Cancer Research, National Cancer Institute, National Institutes of Health, Bethesda, MD 20892

Abstract

The three mammalian bombesin (Bn) receptors (gastrin-releasing peptide [GRP] receptor, neuromedin B [NMB] receptor, BRS-3) are one of the classes of G protein-coupled receptors that are most frequently over-express/ectopically expressed by common, important malignancies. Because of the clinical success of somatostatin receptor-mediated imaging and cytotoxicity with neuroendocrine tumors, there is now increasing interest in pursuing a similar approach with Bn receptors. In the last few years then have been more than 200 studies in this area. In the present paper, the *in vitro a*nd *in vivo* results, as well as results of human studies from many of these studies are reviewed and the current state of Bn receptor-mediated imaging or cytotoxicity is discussed. Both Bn receptor-mediated imaging studies as well as Bn receptor-mediated tumoral cytotoxic studies using radioactive and non-radioactive Bn-based ligands are covered.

Keywords

bombesin; gastrin-releasing peptide; neuromedin B; BRS-3; receptor-mediated imaging; tumor cytotoxicity; DOTA; DTPA; NOTA

I. Bombesin (Bn) receptor family-General (Table 1,2)

The mammalian Bn receptor family is receiving increased attention as a means of localizing tumors or other disease processes by receptor-mediated imaging or for receptor-mediated cytotoxicity of tumors [1–5]. This family got its unusual name, because the original members of this peptide family were isolated from various frog skins and were named after the frog they were isolated from, with the original amidated tetradecapeptide isolated from the European frog, Bombina bombina in 1970 [6–8] (Table 2). Subsequently, a large number of related peptides were isolated which were divided into three groups: the Bn-related peptides with a COOH terminal, Gly-His-Leu-Met-NH_2, the ranatesin-litorin group with a COOH terminus of Gly-His-Phe-Met-NH_2 and the phyllolitorin group with a COOH terminus ending in Gly-Ser-Phe/Leu-Met-NH_2 (Table 2) [6–8]. Subsequently two mammalian equivalent peptides were isolated, gastrin-releasing peptide (GRP), a 27 amino

Corresponding author: Dr R.T. Jensen, Building 10, Room 9C-103, National Institutes of Health, Bethesda, MD 20892, Phone-301-496-4201, Fax-301-402-0600, robertj@bdg10.niddk.nih.gov.

*Both authors contributed equally to this work

Conflict of Interest: None

acid peptide which shares the same seven COOH terminal amino acids with Bn (Table 2)[9] and the decapeptide, neuromedin B (NMB) (Tables 1,2) which shares 6 of the 7 COOH terminal amino acids with litorin (Table 2)[10]. Each of these peptides is widely distributed in both the central nervous system (CNS) and peripheral tissues, especially in the gastrointestinal (GI) tract [8]. Numerous studies demonstrate these two peptides are involved in a wide range of physiological and pathophysiological processes which include: in the CNS (circadian rhythm, TSH release, behavior control, thermoregulation, satiety), in the immune system [effects on macrophages, lymphocytes, leukocytes, dendritic cells], endocrine effects [release of numerous hormones/neurotransmitters], GI tract [motility, secretion, growth], as well as urogenital tract and respiratory system [8,11–13]. They have important pathophysiological effect on growth and differentiation of a number of important human tumors [colon, prostate, lung, head/neck squamous cell, CNS, pancreatic and some gynecologic cancers] and in some cases function as autocrine growth factors [5,11,14,15]. In mammals, the Bn receptor family consists of three hepata-helical, G-protein-coupled receptors, which include the 384 amino acid gastrin-releasing peptide receptor (GRPR), which has 55% amino acid identities to the 390 amino acid neuromedin B receptor (NMBR), and a 399 amino acid orphan receptor, bombesin receptor subtype 3 (BRS-3) [8]. The BRS-3 receptor is included in the mammalian Bn receptor family because it has 47–52% homology to the GRPR and NMBR even though its natural ligand is still unknown [5,8,15]. The BRS-3 has a more limited distribution than the GRPR and NMBR, but is found in both the CNS and peripheral tissues, especially the GI tract [8]. Each of these receptors is coupled to phospholipase C signaling cascades as well as activates a number of tyrosine kinase cascades [5,8,13,15].

II. Why there is special interest in Bombesin (Bn) receptor family-mediated imaging/cytotoxicity

The presence of bombesin receptors (Bn) receptors on tumor tissues is receiving increased attention, both for its possible utilization to image tumors as well as to target cytotoxic agents either using radiolabeled Bn analogues or other cytotoxic agents formed by coupling various Bn receptor ligands by with various linkers to various cytotoxic agents[1–5,16–18] (Fig. 1,Table 1). While this receptor-mediated targeting approach is being used with many regulatory peptides [1–5,17,18], there is particularly interest with this receptor family for a number of reasons. First, the Bn receptor family of receptors, particularly GRPR, has been shown to be one of most over-expressed or ectopically expressed family of G protein-coupled receptors by small lung cancer cells [GRPR - 85–100%, NMBR-55%, BRS-3–25%]; nonsmall cell lung cancer [GRPR – 74–78%, NMBR-67%, BRS-3–8%]; pancreatic cancer [GRPR - 75%, NMBR-100%]; prostate cancer [GRPR – 60–100%, 0%-NMBR, BRS-3]; head/neck squamous cell cancers [GRPR - 100%]; glioblastomas [GRPR - 85%]; neuroblastomas [GRPR-72% NMBR - 46%, 0% BRS-3]; breast cancer [GRPR – 40–70%, NMBR-0%, BRS-3]; intestinal carcinoids [NMPR - 46%, 0%-GRPR, BRS-3]; and bronchial carcinoids [35%-BRS-3, 4%-NMBR, GRPR -0%][11,16,19,21]. Many of these malignancies have a poor prognosis with advanced disease, current treatments are suboptimal, and therefore there is heightened interest in developing newer, novel treatments, of which the utilization of the over-expression/ectopic expression of this family of receptors could be one useful approach. Second, this approach has proven merit. In the case of somatostatin receptors, receptor-mediated imaging and cytotoxicity has been shown to be safe, clinically useful and is now being widely used in clinical practice [22,23]. In the case of neuroendocrine tumors (carcinoids, pancreatic endocrine tumors), in most studies the majority (>80%) over-express or ectopically express one or more of the five classes of G protein-coupled somatostatin receptors (sst1–5), usually the sst2 subtype [17,22–25], in an analogous fashion to the tumors listed above, over-expressing one of the Bn receptor family.

The use of ^{111}In-penetreotide for somatostatin receptor scintigraphy (SRS) is now a standard clinical method to image these tumors [26–28]. Studies have shown SRS is more sensitive than conventional methods used for neuroendocrine tumor localization (computed tomographic scanning, MRI scanning ultrasound) of the primary tumor and metastatic disease [26–29]. Figure 2 shows an example of its sensitivity and usefulness in a typical patient with a neuroendocrine tumor. In this patient the CT scan was negative however, the SRS showed tumor presence in the liver and lymph nodes. This figure illustrates the selectivity and sensitivity of using somatostatin receptor over-expression to target these tumors [26–29]. A similar strategy is now being used to target tumoricidal doses of radiolabeled somatostatin analogs (^{90}Y, ^{177}Lu, ^{111}In-labeled) to treat patients with advanced malignant neuroendocrine tumors [22,23]. Such a strategy could also be used to target nonradioactive cytotoxic agents (i.e. chemotherapeutic agents, toxins, immunological agents, etc) to tumor cells [30–34]. Unfortunately, many of the common lethal tumors do not over-express somatostatin receptors, as occurs in the neuroendocrine tumors. Therefore if receptor-mediated imaging or cytotoxicity is going to be used for these tumors, some other family of receptors needs to be considered. As discussed above, the Bn family of receptors could fulfill this requirement for a number of these tumors [1–5,16–18]. Third, Bn-related peptides also function as potent growth factors, sometimes in an autocrine fashion, for many common malignant tumors including those of lung, pancreas, head/neck, CNS (glioblastomas), kidney, prostate, breast, colon/rectum, ovary and stomach [11,21,35,36]. This raises the possibility that receptor antagonists of Bn receptors may have cytotoxic effects for a number of theses tumors, as well as raises the possibility that targeting Bn receptors on these tumor cells may have additional cytotoxic effects by interrupting this autocrine stimulatory effect. Four, although there are no effective nonpeptide antagonists or agonists for GRPR or NMBR, which are primarily over-expressed by tumors, the pharmacology of these receptors has been well studied, especially in nonhuman cells. Both selective agonists and at least eleven chemical classes of antagonists, with varying degrees of selectivity, have been described [8,14,37]. Therefore, pharmacological, both agonists and antagonists exist that can be used for Bn receptor targeting strategies.

III. Bn receptor-mediated imaging/cytotoxicity. Review of studies and current status

III. A. General (Fig. 1, Tables 1–12)

In this paper the important results of studies of Bn receptor-mediated imaging or cytotoxicity are summarized in the accompanying tables and briefly reviewed in the text. Both studies dealing with radiolabeled Bn analogs for either imaging or cytotoxic studies (Table 3–11) and studies investigating nonradioactive Bn receptor-mediated cytotoxicity are reviewed (Table 12). In the tables, results of *in vitro* and *in vivo* studies are considered in separate tables, because of the different questions frequently addressed. Furthermore, human studies are included in a separate section (Table 11). The radiolabeled Bn peptide studies (Tables 3–11) are divided by the type of isotope used. A wide range of different linkers to couple the isotopes to the Bn-related peptides were used in different studies and their structures are shown in Fig. 1. Their abbreviations as well as those of various spacers used in the different studies are summarized in Table 1.

III. B. Pharmacology of Bn analogs used for receptor-mediated imaging/cytotoxicity studies

Bn is a 14 amino acid COOH terminal amidated peptide; GRP has 27 amino acids and NMB 10 amino acids (Table 2)[8]. The COOH terminus with amidation is needed for high affinity and biological activity, whereas the NH_2 terminal is not need for high affinity receptor interaction, and COOH modified analogues can function as potent antagonists [8,37–39].

Therefore the NH_2 terminal of various Bn COOH terminal peptides can be attached to coupling agents or radiolabeled with full retention of biological activity. Bn and GRP have 8- and 1000-fold selectivity for the hGRPR over the hNMBR, respectively, whereas NMB has 1000-fold selectivity for the hNMBR over the hGRPR [14]. GRP, NMB, as well as all other natural occurring Bn-related peptides interact with hBRS-3 only with very low affinity (>1 uM)[8,40–42]. The novel, synthetic Bn analog, [D-Tyr^6, β-Ala^{11}, Phe^{13}, Nle^{14}]Bn(6–14)(Table 2) has the unique property of having high affinity for all three human receptor subtypes, functions as a potent agonist at each of these receptors and is rapidly internalized by each receptor [30,34,40–42].

Because the GRPR is the principal Bn receptor subtype over-expressed by most cancers, almost all Bn receptor-mediated imaging studies and cytotoxicity studies have concentrated on developing ligands that interact with this receptor with high affinity (Tables 2–12). Because previous studies demonstrate that the COOH terminal Bn hepapetide is largely inactive, most studies used at least Bn octapeptide (BN (7–14) or longer Bn peptides for their studies (Tables 2–12). Bn (7–14) analogs were the most frequently used Bn related peptide for these studies[8,43], followed by longer Bn peptides (Tables 2–12). Most studies used Bn receptor agonists for both Bn receptor-mediated imaging and cytotoxicity studies, however, a number of more recent studies used radiolabeled antagonists for imaging studies (Tables 2–12). Recent studies have reported that radiolabeled antagonists with various G protein-coupled receptors, even though not internalized, may give better images than radiolabeled agonists [44,45]. Similarly, with Bn analogs, a number of radiolabeled Bn antagonists were reported in various studies to give excellent imaging of various tumors *in vivo* [2,45–51].

III. C. Review of ^{99M}Tc-labeled Bn analog *in vitro* (Table 3) and *in vivo* (Table 4) studies of Bn receptor-mediated imaging/cytotoxicity studies

^{99m}Tc is the most used radioisotope worldwide for diagnosis in nuclear medicine, as it is used in 85% of diagnostic imaging. This is due to its availability (^{99}Mo/^{99m}Tc generator system), well-established labeling chemistry, good labeling efficiency, half life (6.01 h) and 140 keV gamma energy. Among its applications are included: bone scanning (^{99m}Tc-MDP), myocardial perfusion imaging (^{99m}Tc-retrofosmin and ^{99m}Tc-sestambi), functional brain imaging (^{99m}Tc-HMPAO and ^{99m}Tc-EC), immunoscintigraphy (^{99m}Tc-scintium), red cells blood labeling to localize gastrointestinal bleeding, imaging of heart damage (^{99m}Tc-pyrophosphate) and liver-spleen scanning (^{99m}Tc-sulfur colloids).

Bn (1–14)—The first study using a ^{99m}Tc radiolabeled bombesin analog is from 1998 [52]. The authors tested the agonist [Lys^3]Bn (Table 2) coupled to the isotope through 2 different linkers (Pm-DADT or Hx-DADT, DADT= diaminedithiol, Table 1, Fig. 1). Binding studies in rat brain membranes with ^{99m}Tc-Pm-DADT-[Lys^3]Bn or ^{99m}Tc-Hx-DADT-[Lys^3]Bn showed Ki values not different (3.5±0.7 nM and 5.2±1.5 nM, respectively) from natural bombesin (4.3±1.0 nM). *In vivo* biodistribution experiments in normal animals showed that the ^{99m}Tc-Hx-DADT linked [Lys^3]Bn analog had 4-fold greater accumulation in the intestine due to its more lipophilic character than ^{99m}Tc-Pm-DADT-[Lys^3]Bn, making the latter more suitable for imaging in the abdominal area.

In another study from the same group [53], ^{99m}Tc-Pm-DADT-[Lys^3]Bn showed high accumulation in the intestine, which the authors attempted to decreased by introducing a DTPA moiety (Fig. 1, Table 2) in position 1 of [Lys^3, Tyr^4]Bn [Analog #70, Table 3] (Table 2). Binding experiments [Analog #70, Table 3] with PC-3 membranes showed Ki values for the new Bn agonist of 4.1±1.4 nM, slightly higher than Bombesin (1.7±0.6 nM). *In vivo* biodistribution experiment with normal and PC-3 cell xenografts bearing rats demonstrated

the introduction of DTPA in this Bn analog produced decreased radioactivity accumulation in the abdominal region, increased renal clearance, as well as, high and specific uptake by pancreas and PC-3 tumor cells, which could be clearly observed by scintigraphy [Analog #70, Table 4].

Another study using the Bn agonist [Lys^3]Bn (Table 2) coupled to ^{99m}Tc by the linker EDDA/HYNIC (Fig. 1, Table 1) using an instant freeze-dried kit formulation [Analog #62, Table 3], showed high stability either in human serum or a cysteine solution. *In vivo* biodistribution and imaging studies [Analog #62, Table 4] with ^{99m}Tc-EDDA/HYNYC-[Lys^3]Bn in normal and PC-3 tumor bearing rats demonstrated rapid clearance from blood with renal excretion of the Bn analog, and significant uptake by both the pancreas and the tumor cells, which could be observed by scintigraphy and highlighted after the removal of the internal viscera. This study proved the possibility of creating a ^{99m}Tc Bn analog using this instant freeze-dried kit.

In a study from the same group [54], ^{99m}Tc-EDDA/HYNYC- [Lys^3]Bn (Table 2) was compared with ^{99m}Tc- N_2S_2-Tat (49–57) -[Lys^3]Bn (N_2S_2=Cys (Acm)-Gly-Cys (Acm); Tat (49–57)=Arg-Lys-Lys-Arg-Arg-Gln-Arg-Arg-Arg, Table 1) [Analogs #21–22, Table 3 and 4]. This hybrid Bn analog was obtained by coupling the Bn agonist to the Tat (49–57) HIV peptide through the spacer Glu-Gly-Cys-Gly and the linker N_2S_2 bound to ^{99m}Tc. With this approach the authors tried to increase the internalization of the Bn analog using the HIV peptide Tat, because it has been used to deliver a large variety of cargoes into cells. In fact, this hybrid Bn analog showed higher internalization values than ^{99m}Tc-EDDA/HYNYC-[Lys^3]Bn in 3 different cell lines: PC-3, MCF7 and MDA-MB231 [Analogs #21–22, Table 3], although it presented lower stability in human serum and/or cysteine solution. When comparing these two radiolabeled peptides in biodistribution and imaging studies [Analogs #21–22, Table 4], the hybrid Bn analog also showed rapid clearance from blood with renal excretion, significant uptake by the pancreas and tumor, but a higher uptake in non-targeted organs and kidneys, thus producing a higher background.

Bn (2–14)—Bn agonist Bn (2–14) (Table 2) has also been radiolabeled with ^{99m}Tc and studied for its possible use in nuclear medicine. One study from Gourni *et al.* [55] studied this Bn agonist linked through 4 different amino acid sequences to the ^{99m}Tc isotope (Gly-Gly-Cys-Aca, MeGly-Gly-Cys-Aca, Me_2Gly-Gly-Cys-Aca or Mac-Gly-Gly-Aca; Aca=aminohexanoic acid, Table 1) [Analogs #63–69, Tables 3 and 4]. Binding studies with these Bn (2–14) analogs in PC-3 cells showed no difference in the IC_{50} values. *In vivo* biodistribution studies performed in normal animals showed that the 4 radiolabeled Bn (2–14) analogs had rapid blood clearance, were elimination mainly through the renal/urinary pathway, and had high and specific pancreatic uptake [Analogs #63–69, Table 4].

In later paper from Gourni *et al.* [56], the previously tested ^{99m}Tc- Gly-Gly-Cys-Aca-Bn (2–14) was compared to ^{99m}Tc- Gly-Gly-Cys-Aca-Bn (7–14), in order to determine if the shorter sequence in the latter compound produced any improve in the properties of the radiopeptide [Analogs #18–19, Tables 3 and 4]. It was found that the IC_{50}'s, internalization and efflux values were not different between them, and the Bn (2–14) analog was more stable after 2 h in human plasma [Analogs #18–19, Table 3]. Biodistribution studies with both ^{99m}Tc-Bn analogs demonstrated they had fast blood clearance, no uptake or retention in the stomach, low accumulation in the liver, but high uptake in the intestine, high accumulation in the pancreas and good tumor uptakes, but also both produced clear images of the tumors in dynamic planar studies. The only difference found between them was a slower washout from the pancreas and slightly higher liver excretion rate by ^{99m}Tc-Gly-Gly-Cys-Aca-Bn(7–14) [Analogs #18–19, Table 4].

The Bn analog Gly-Gly-Cys-Aca-Bn (2–14) also has been studied using as a linker, N_3S (2‴,2″,2‴-nitrotriethanethiol, Table 1) and the effect of the introduction of 3 basic amino acids (Orn-Orn-Orn) in the sequence of the spacer [Analogs #16–17, Tables 3,4] studied. It was found that the analog N_3S-Orn-Orn-Orn-Gly-Gly-Cys-Aca-Bn (2–14) had higher stability and internalization rate in PC-3 cells than the N_3S-Gly-Gly-Cys-Aca-Bn (2–14) [Analogs #16–17, Table 3]. *In vivo* biodistribution/imaging experiments [Analogs #16–17, Table 4]. showed that the radiopeptide ^{99m}Tc-N_3S-Orn-Orn-Orn-Gly-Gly-Cys-Aca-Bn(2–14), compared to ^{99m}Tc-N_3S-Gly-Gly-Cys-Aca-Bn(2–14), produced a better uptake in pancreas and tumor tissues and had a higher tumor/non tumor ratio, as well as produced quality SPECT images with clear PC-3 cell tumor visualization and low background as early as 10 min p.i.

Bn (7–14)—Among the ^{99m}Tc radiolabeled Bn analogs studied, Bn (7–14) (Table 2) has been the most widely used, being studied with different linkers in 41% of the publications [Tables 3 and 4].

Smith *et al.*[57] tested the radiolabeled Bn analog Dpr-Ser-Ser-Ser-Bn (7–14) (Dpr=1,2-diaminopropionic acid, Table 1) coupled to ^{99m}Tc by the moiety $(H_2O)(CO)_3$ or $(CH_2CH_3)(CO)_3$. They observed that $(H_2O)(CO)_3$-Dpr-Ser-Ser-Ser-Bn (7–14) had an IC_{50} value in the nanomolar range (0.86±0.22), was stable in aqueous solution for more than 24 h and had a 55% internalization rate after a 90 min incubation [Analogs #76, Table 3]. *In vivo* experiments in normal or PC-3 cell tumor bearing mice [Analog #76–77, Table 4] comparing these two radiolabeled Bn agonists showed fast blood clearance, high renal excretion, high pancreatic and tumor uptake with both, but the ^{99m}Tc-$(H_2O)(CO)_3$ Bn analog's values were higher than those of either 99mTc-$(CH_2CH_3)(CO)_3$-Bn analog or the previously reported Bn analog, 99mTc-N_3S-5-Ava-Bn(7–14) [58].

In another study from the same group [59], Alves *et al.* studied 3 different Bn (7–14) analogs, coupled to ^{99m}Tc with the same linker PZ1 (pyrazolyl, Table 1), but using 3 different spacers (Gly-Gly-Gly, Ser-Ser-Ser or β-Ala=β-Alanine, Table 1) [Analogs #67–69, Table 3 and 4]. Among them, the one with the highest affinity was the PZ1-Gly-Gly-Gly-Bn (7–14) agonist (IC_{50}: 0.2±0.02 nM), which was 10-fold higher than Bn (7–14). ^{99m}Tc-PZ1-Ala-Ala-Ala-Bn(7–14) showed the highest internalization value with 90% of the cell-associated activity remaining internalized even at 90 min [Analogs #67–69, Table 3]. When these Bn (7–14) agonists were tested in *in vivo* biodistribution/imaging studies [Analogs #67–69, Table 4] in SCID mice bearing xenografted human PC-3 cell tumors, all of them showed rapid blood clearance, minimal gastric accumulation, renal excretion and high accumulation in pancreas, but the tumor uptake observed was lower than seen with ^{99m}Tc-$(H_2O)(CO)_3$-Dpr-Ser-Ser-Ser-Bn (7–14) [57].

One year later, the same group [60] studied the possibility of improving the characteristics of the Bn (7–14) analog by coupling it to the linker DPR (Table 1) using different spacers (Asn-Asn-Asn, Asn-Asn-Asn-βAla, Asn-Asn-Asn-5Ava, Arg-Arg-Arg, Arg-Arg-Arg-βAla or Arg-Arg-Arg-5Ava; where βAla: β-Alanine and 5Ava: 5-aminovaleric acid, Table 1) [Analogs #54–59, Tables 3, 4]. The different spacers did not produce any significant change either in binding affinity [IC_{50} ranging from 0.2±0.02 for DPR-Arg-Arg-Arg-βAla-Bn(7–14) to 3.6±2.2 nM for DPR- Asn-Asn-Asn-5Ava-Bn(7–14)], or stability (>75% after 4h in human serum). When all analogs were tested for 1 h p.i. *in vivo* biodistribution experiments in normal CF-1 mice [Analogs #54–59, Table 4], the one with the amino acid Arg in the spacer showed hepatobiliary clearance, while those with Asp had renal excretion of the radiolabeled peptide. All of them showed high pancreas uptake with the highest values with ^{99m}Tc-DPR-Asn-Asn-Asn-βAla-Bn(7–14) and ^{99m}Tc-DPR-Asn-Asn-Asn-βAla-Bn (7–14) [Analogs #55–56, Table 4]. The latter two Bn analogs were tested for longer periods of

time (4h and 24h), and demonstrated that the radiolabeled agonist, ^{99m}Tc-DPR-Asn-Asn-Asn- βAla-Bn (7–14) showed the best pancreatic uptake, so it was chosen for *in vivo* biodistribution experiments with animal bearing PC-3 cell tumor xenografts and for imaging studies [Analog #55, Table 4]. This Bn analog had good tumor uptake values and the tumors were clearly visualized, however the GI uptake was higher than with the previously studied Bn analog ^{99m}Tc-DPR-Ser-Ser-Ser-Bn(7–14) [57].

In another study with ^{99m}Tc and a Bn (7–14) analog [61], the analog was bound to the isotope ^{99m}Tc by a different linker, NS_3 (2′,2″,2‴-nitrotriethanethiol, Table 1, Fig. 1) and 3 different spacers (βAla, Gly-Gly-Gly and Ser-Ser-Ser) combined with 4-(isocyanomethy)benzoic acid or 4-isocyonobutanoic acid [Analogs #48–53, Table 3, 4]. When the 6 Bn analogs were tested in binding studies in PC-3 cells [Analogs #48–53, Table 3], no significant difference in the IC_{50} values were found [values ranging from 0.2±0.04 for Analog #48 to 1.9±0.4 nM for Analog #49] and the highest internalization value was observed with Analog #51. The two Bn analogs showing the best values for cellular binding and internalization [Analogs #48, Table 4): ^{99m}Tc- NS_3-4-(isocyanomethy)benzoic acid-βAla-Bn (7–14) and analog #51, Table 4): ^{99m}Tc-NS_3-4-(isocyanomethy)benzoic acid-βAla-Bn (7–14), were used in *in vivo* biodistribution studies in normal animals. These analogs showed rapid accumulation in the liver, excretion to the intestine, and low pancreatic uptakes, making poor candidates to be used in the nuclear medicine.

Another linker, DMTA (2-(N,N″-bis(tert-butoxycarbonyl)diethylenetriamine)acetic acid, (Table 1, Fig. 1), has been used to bind ^{99m}Tc. In this study [62], DMTA was linked to Bn (7–14) through 4 different spacers: βAla, Gly-Gly-Gly, Gly-Ser-Gly or Ser-Ser-Ser [Analog #33–36, Tables 3, 4]. Binding studies were performed with each Bn analog [Analog #33–36, Table 3], and in all cases a nM IC_{50} were obtained, ranging from 0.28±0.2 with DMTA-βAla-Bn (7–14) to 2.56±1.3 nM with DMTA-Gly-Gly-Gly -Bn (7–14). The highest internalization value, though, was observed with ^{99m}Tc-DMTA-βAla-Bn(7–14) (23.8±0.03% after 2h incubation). All of the Bn analogs were tested for *in vivo* biodistribution studies in normal animals [Analog #33–36, Table 4]. ^{99m}Tc-DMTA-Ser-Ser-Ser-Bn(7–14) had prolonged retention in the circulation, the more hydrophilic radiolabeled agonist (serine-containing spacer) were predominantly excreted by the kidneys, while the more hydrophobic conjugates were excreted by the hepatobiliary system. The highest pancreas uptake was observed with the agonist ^{99m}Tc-DMTA-βAla-Bn(7–14). This radiolabeled Bn agonist was selected for biodistribution studies in animals bearing PC-3 tumors. This radioconjugate showed high affinity and internalization values in PC-3 cells. In another study from the same group [63], two different ^{99m}Tc radiolabeled βAla-Bn (7–14) analogs were studied and compared, one coupled to the linker HYNIC (Table 1, Fig. 1) and the other to N(PN6)-Cys, [Analogs #25–26, Tables 3,4]. Comparing the results obtained with each Bn analog, the value of all the parameters studied (stability, amount of receptor internalization in PC-3 cells, pancreas and tumor uptake in normal and PC-3 tumor bearing animals, higher uptake in scintigraphy image studies) were more favorable with ^{99m}Tc-HYNIC-βAla-Bn(7–14) than ^{99m}Tc≡N(PN6)-Cys- βAla-Bn (7–14).

HYNIC (Fig. 1) has been also used in another study as a linker between for ^{99m}Tc and a Bn (7–14) analog. ^{99m}Tc-HYNIC/Tricine/TPPS-Bn (7–14) [Analog #61, Tables 3, 4] [64] had a nM IC_{50} value in PC-3 cells, although it was16-fold higher than that of Bn (7–14) analog; it showed good stability and internalization values. *In vivo* biodistribution studies/imaging with this Bn analog radio-conjugate demonstrated that xenografted HT-29 tumors in BALB/c nude mice were clearly visualized at 1 h p.i. with excellent tumor/background ratio, although at this time the highest uptake areas were in the kidneys and bladder due to the renal excretion. After 4 h p.i. the background radioactivity in the chest region disappeared due to the high renal excretion rate, but the tumors were still clearly seen.

In a recent study [65], 14 Bn (7–14) analogs were studied [Analogs #1–14, Tables 3,4], comparing the linker DPR or PZ1 and 7 different spacers (βAla, Gly-Gly-Gly, Gly-Ser-Gly, PEG5, PEG8, Ser-Gly-Ser, Ser-Ser-Ser; PEG=ethylene glycol [2-aminoethylcarboxymethylether] (Table 1). *In vitro* binding experiments with T47-D and MDA-MB-231 cells [Analogs #1–14, Table 3] showed that, although all of the had IC_{50} values in the nM range, the PZ1-Bn (7–14) analogs had higher binding affinities. In all cases these analogs were stable more than 24h in PBS with or without HSA (human serum albumin) and the amount of receptor internalized was similar. *In vivo* biodistribution experiments in normal and tumor bearing animals were performed with all the analogs. All the PZ1-Bn (7–14) radioconjugates showed low tumor uptake, and among the DPR linked radiopeptides all of them showed high pancreatic uptake, but only one showed high tumor uptake and accumulation, which was ^{99m}Tc-DPR-Ser-Ser-SerBn(7–14). This radiolabeled Bn analog when used in imaging studies and produced favorable tumor/background ratios and clear visualization of the tumor tissue.

In several studies the possibility of using the linker (NαHis)Ac (Nα-carboximethylhistidine, Table 1, Fig. 1) to the Bn (7–14) analog through several spacers has been examined. In one study from 2006 [66] Bn (7–14) and 3 other Bn analogs ([Cha^{13}]Bn (7–14), [Nle^{14}]Bn (7–14) and [Cha^{13}, Nle^{14}]Bn (7–14)) were tested using none or 2 different spacers (βAla-βAla or NH-CH_2-CH_2-O-CH_2-CH_2O-CH_2CO) [Analogs #42–47, Tables 3, 4]. Bindings studies showed that all the Bn analogs showed IC_{50} values in the nM range, with (NαHis)Ac-Bn (7–14) having the highest affinity (IC_{50}: 0.19±0.09 nM) and (NαHis)Ac- [Nle^{14}]Bn (7–14) the lowest (IC_{50}: 15.7±6.0 nM), but stability studies in human plasma or using PC-3 cells showed the contrary, with the more stable molecule being (NαHis)Ac- [Nle^{14}]Bn (7–14) [Analogs #42–47, Table 3]. Internalization/efflux experiments showed a similar pattern for all the Bn (7–14) analogs. When all of the radiopeptides were tested in *in vivo* biodistribution studies, the ^{99m}Tc-(NαHis)Ac- NH-CH_2-CH_2-O-CH_2-CH_2O-CH2CO-[Cha^{13}, Nle^{14}]Bn (7–14) and ^{99m}Tc-(NαHis)Ac-βAla-βAla- [Cha^{13}, Nle^{14}]Bn (7–14) showed improved biodistribution and much higher tumor/blood ratios, with the latter one also showing increased tumor/kidney and tumor/liver values [Analogs #42–47, Table 4].

A later study from the group of Garcia-Garayoa *et al.* [67] tried to improve the biodistribution of the ^{99m}Tc-(NαHis)Ac-βAla-βAla- [Cha^{13}, Nle^{14}]Bn (7–14) analog (Fig. 1, Table 2) by introducing a positive or negative charged amino acid in the spacer sequence (β^{3}hGlu-β^{3}Glu-β^{3}Glu, β^{3}hGlu-β^{3}Glu-βAla, β^{3}hGlu-βAla-βAla, β^{3}hLys-βAla-βAla, β^{3}hSer-βAla-βAla and βAla-βAla) [Analogs #27–32 Tables 3, 4]. They found that the binding affinity of (NαHis)Ac-β^{3}hGlu-β^{3}Glu-β^{3}Glu- [Cha^{13}, Nle^{14}]Bn (7–14) to PC-3 cells was reduced (IC_{50}: 634±221.7 nM) having an affinity 317-fold lower than Bn (7–14) and 124-fold lower than (NαHis)Ac-βAla-βAla- [Cha^{13}, Nle^{14}]Bn (7–14), while the latter's affinity, was not different from that of (NαHis)-βAla-βAla- [Cha^{13}, Nle^{14}]Bn (7–14) (IC_{50}: 5.1±1.7 nM) or (NαHis)Ac-β^{3}hSer-βAla-βAla- [Cha^{13}, Nle^{14}]Bn (7–14) (IC_{50}: 6.8±3.2 nM). Introduction of the negative or positive charged amino acid in the spacer structure did not produce any significant modification in the stability of the molecules, but did alter the internalization values [Analogs #27–32 Table 3]. In fact, ^{99m}Tc-(NαHis)Ac-β^{3}hGlu-β^{3}Glu-β^{3}Glu -[Cha^{13}, Nle^{14}]Bn (7–14) was not internalizated (1% after 1 h incubation), ^{99m}Tc-(NαHis)Ac-β^{3}hGlu-β^{3}Glu-βAla- [Cha^{13}, Nle^{14}]Bn (7–14) had half of the internalization value (15%) observed with ^{99m}Tc-(NαHis)Ac-β^{3}hGlu-βAla-βAla- [Cha^{13}, Nle^{14}]Bn (7–14) (30%) and ^{99m}Tc-(NαHis)Ac-β^{3}hLys-βAla-βAla-[Cha^{13}, Nle^{14}]Bn (7–14) had a higher rate (40%). *In vivo* biodistribution/SPECT imaging studies performed in normal and PC-3 cell bearing tumor SCID mice showed that ^{99m}Tc-(NαHis)Ac-β^{3}hGlu-β^{3}Glu-βAla- [Cha^{13}, Nle^{14}]Bn(7–14) demonstrated the best properties compared to the other radiopeptides. In fact, this radiolabeled bombesin agonist had the highest tumor uptake and retention, and fast

clearance from non-targeted tissues, with clearer visualization of the tumors and lower renal and hepatic uptakes [Analogs #27–32 Table 4].

Another strategy to improve the characteristics of the Bn analog ^{99m}Tc-(NαHis)Ac-βAla-βAla- [Cha^{13}, Nle^{14}]Bn (7–14) (Fig. 1, Table 2) was performed by Schweinsberg *et al.* [68] by the insertion of a polar carbohydrate (Lys (sha), Lys (Amd) or Ala(NTG), Table 1) between the linker ((NαHis)Ac) and the spacer (βAla-βAla) [Analogs #37–40, Tables 3, 4]. Binding affinities and internalization studies in PC-3 cells showed no differences among the 4 Bn agonists, but differences were found *in vivo* biodistribution and imaging studies. In fact, all of the glycated analogues showed higher tumor/background ratio compared with the non-glycated. The best results were obtained with the ^{99m}Tc-(NαHis)Ac-Ala(NTG)-βAla-βAla- [Cha^{13}, Nle^{14}]Bn(7–14) which had a 4-fold increase in uptake and retention in the tumor and significant less accumulation in the tumor. All 3 new glycated Bn analogs produced a clear image of the tumor with a low abdominal background [Analogs #37–40, Table 4].

Maes *et al.* [69] also tried to improved the characteristics of the radiolabeled Bn analog ^{99m}Tc-(NαHis)Ac-βAla-βAla-[Cha^{13}, Nle^{14}]Bn(7–14) (Fig. 1, Table 2) by introducing the carbohydrate moiety Pra(Glu) (Table 1). This modification did not change the IC_{50} value obtained with ^{99m}Tc-(NαHis)Ac-βAla-βAla- [Cha^{13}, Nle^{14}]Bn (7–14), but produced an increase in the tumor uptake, tumor retention and excretion via kidneys [Analog #20, Tables 3, 4].

Bn Antagonist—In different studies ^{99m}Tc radiolabeled Bn antagonists have been used to study the possibility they could be used as a radiotracer in prostate and breast tumor cancer over-expressing bombesin receptors due to their proven high affinities.

In a paper from Maina *et al.* the Bn antagonist Demobesin 1 (Table 1) was coupled to ^{99m}Tc and its binding capacity and biodistribution properties in a mouse (AR42J) and a human (PC-3) tumor cell line were measured and compared to the radiopeptide, ^{111}In-Z-070 (Table 1). Binding studies showed that Demobesin 1 had IC_{50} 11–14-fold lower than Z-070 in PC-3. *In vivo* biodistribution studies showed that although both Bn analogs showed similar tumor uptake in AR42J bearing mice, ^{99m}Tc-Demobesin 1 had 2–3-fold higher tumor uptake in PC-3 xenografted mice, revealing the importance of the selection of the experimental tools testing the radiolabeled peptide [Analog #75, Tables 3, 4 and #7, Tables 3, 4].

Another study from the same group [70] compared 4 different Demobesin analogs (Demobesin 3–6, Table 1) coupled to ^{99m}Tc. All of these are agonists and each had similar IC_{50} values (in the nM range), stability and internalization rates [Analogs #71–75, Table 3]. When comparing the results from biodistribution studies (Table 4), radiolabeled Demobesin 5 and 6 were rapidly cleared via liver and had a high percentage of intestinal uptake, while ^{99m}Tc-Demobesin 3 and 4 were renally excreted and which produced lower background activity. Uptake by PC-3 tumors in xenografted animals was higher with ^{99m}Tc-Demobesin 3 and it was selected for imaging studies which showed clear tumor uptake and low kidney retention.

Cescato *et al.* [45] compared Demobesin 1 (Bn antagonist) and Demobesin 4 (Bn agonist) (Tables 1,2) coupled to ^{99m}Tc through the linker tetraamine-benzyllaminidiglycolic acid. *In vitro* experiments showed that both of them had similar IC_{50} values, however, Demobesin 1 showed a higher percent of membrane binding, but this Bn antagonist was not internalized [Analogs #23–24, Table 3]. Biodistribution studies (Table 4) in normal and PC-3 bearing SCID mice showed good pancreatic uptake and fast clearance in blood and non-target tissues. ^{99m}Tc-Demobesin 1 (antagonist) had a higher tumor accumulation and faster

pancreatic washout, but also had higher liver and intestinal uptake values than ^{99m}Tc-Demobesin 4 [Analogs #23–24, Table 4]. It was concluded that the radiolabeled antagonist is the preferable candidate as radiotracer.

RM1 (Tables 1,2), another Bn antagonist, has also been tested as a possible ^{99m}Tc radiotracer [49] coupled to the isotope by the linker N4-Gly-aminobenzoyl. IC_{50} values of 3.7±1.3 nM were measured, not different from that with Bn (7–14), and high membrane bound values were obtained, but it was not internalized [Analog #15, Table 3]. When ^{99m}Tc-RM1 was injected into PC-3 bearing nude mice, high tumor and pancreatic uptake was observed with fast washout in the non-expressing GRPR tissues producing high tumor/non tumor ratios. SPECT/CT studies in animal bearing PC-3 tumors resulted in images with a clear delineation of the tumor with low abdominal and kidney uptake 12 h p.i. [Analog #15, Table 4].

Litorin (Table 2)—Litorin (Table 2) belongs to the ranatensin peptide family and it has high amino acid sequence similar to bombesin. This bombesin related peptide has been also coupled to ^{99m}Tc and its possibility as a radiopeptide investigated. Durkan *et al.*[71] coupled litorin directly, with no linker or spacer, to ^{99m}Tc. The resulting agonist radiopeptide had high stability after incubation with high concentration of Cys solution. Injecting normal Wistar rats with this radiolabeled Bn-related peptide produced a high and specific uptake in the pancreas, and excretion of ^{99m}Tc-Litorin by kidneys [Analog #41, Tables 3, 4].

III. D. Review of ^{111}In-labeled Bn analog *in vitro* (Table 5) and *in vivo* (Table 6) studies of Bn receptor-mediated imaging/cytotoxicity studies

^{111}Indium is a very useful tool in nuclear medicine for the imaging of tumors due to its half life (67 h), gamma energy of 247 keV and the type of disintegration producing an electron making it suitable for SPECT studies. In fact it is the isotope used for the radiolabeling of the first somatostatin analog available in the market for scintigraphic localization of primary and metastatic neuroendocrine tumors bearing somatostatin receptors, Octreoscan [^{111}In-pentreotide]. Another routinely used application of this radioisotope is for evaluating patients suspected of having abscesses with autologous human leukocytes labeled *in vitro* with (^{111}In)-oxine.

In the literature there are 17 experimental studies using this isotope in combination with different Bn analogs and linkers in order to obtain a radiopeptide suitable for its use in nuclear medicine for imaging, primarily concentrating on the detection of prostate or breast cancer by SPECT imaging (Tables 5, 6). Among all the Bn analogs tested two agonist were present in 71% of the studies: Bn (7–14) or [Pro^1, Tyr^4]Bn (Table 2, Fig. 1).

In an early study [72] with Bn (7–14) the characteristics of 5 ^{111}In-DOTA-radiolabeled peptides [Analogs #12–16, Tables 5,6], which were conjugated by different spacers, were analyzed. In each of the 5 peptides ^{111}In was bound to the linker DOTA (Fig. 1), but the spacer between DOTA and the Bn analog ranged between no spacer to one of 5 to 8 carbon atoms. Three of them showed a nanomolar IC_{50} [β-alanine [βAla], 5-aminopentanoic acid [5-Ava] and 8-aminooctanoic acid [8-Aoc] spacers, Table 1], which was similar to Bn (7–14) (IC_{50}: 1–3 nM), one had a 32.5-fold decreased affinity (65 nM) (11-aminoundecanoic acid [11-Aun], Table 1) and the DOTA-peptide without a spacer showed a 55-fold decrease (IC_{50}: 111 nM) compared to Bn (7–14). Cell internalization was measurement with just one of the analogs [^{111}In-DOTA-8-Aoc-Bn(7–14)] [Analog #15, Table 5] and was high (72% after 2h). Biodistribution was studied with all 5 Bn derivatives in normal animals [Analogs #12–16, Tables 6] [72], and the 8-Aoc derivative demonstrated the highest pancreatic uptake. In mice bearing PC-3 xenografts biodistribution was determined just for the ^{111}In-

DOTA-8-Aoc-Bn(7–14) [Analog #15, Table 6] and high tumor uptake and tumor/non-tumor ratio were found [72].

In another study from the same group [73], the same radiolabeled Bn derivative (^{111}In-DOTA-8-Aoc) was compared with another set of Bn derivatives [Analogs #19–24, Table 5, 6], each containing DOTA as the linker, but varying in the spacer structure (5-amino-3, 6-dioxaoctyl-succinamic acid [5-Aos], 8-amino-3-oxapentyl-succinamic acid [8-Ads], aminobenzoyl [AMBA], glycine-aminobenzoyl [Gly-AMBA] (Table 1) and glycine-p-aminomethylbenzoic acid [Gly-AM2BA] (Table 1). In most cases the IC_{50} obtained was in the nM range and was similar to Bn (7–14), however with 5-Aos as the spacer, a 3-fold decrease in affinity (6.2 nM) was seen compared to Bn (7–14). The 8-Aoc and Gly-AM2BA derivatives demonstrated a 4 and 2.9-fold increase in affinity compared to Bn (7–14) (0.51 and 0.7 nM respectively) [Analogs #19 and 24, Table 5]. The Gly-AM2BA analog showed the lowest rate of internalization. When *in vivo* biodistribution and imaging studies of these analogs were performed [Analogs #19–24, Table 6], in normal animals the highest pancreas uptake was observed with Gly-AMBA and AMBA, followed by the 8-Aoc derivative, which had the highest tumor uptake rate. When SPECT studies were performed with 8-Aoc, AMBA, Gly-AMBA and Gly-AMB2A radiolabeled analogs [Analogs #19, 23 and 24, Table 6], each produced a clear image of the tumor. The analogs with an aromatic group demonstrated higher GI retention (AMBA, Gly-AMBA and Gly-AM2BA).

In another set of studies [2,46] different Bn (7–14) radioconjugate derivatives [Analogs #1,2 and #8–11, Table 5, 6] were compared with each other and also with the ^{111}In labeled Bn antagonist [H-DPhe^6, Sta^{13}, Leu^{14}]Bn (7–14) [RM1, Table 1,2] and a ^{99m}Tc labeled Bn antagonist [$(N_4\text{-bzlg})^0$, DPhe^6, LeuNHEt^{13}, desMet^{14}]Bn (6–14), Fig. 1 [^{99m}Tc-Demobesin1, Table 1,2]. When studies of binding were performed, affinity was high (IC_{50}: 0.8 nM) for the Bn agonist (AMBA, #1, Table 5), near that seen with Bn(7–14), and was 40-fold greater than with the antagonist RM1 (IC_{50}: 35 nM). The same difference was observed for the internalization rates, but when the *in vivo* biodistribution and imaging studies were performed [Analogs #1,2 and #8–11, Table 6], the radiolabeled antagonists (^{111}In-RM1 and ^{99m}Tc-Demobesin1) [Analog #2, Table 6] had greater tumor uptake, tumor/non tumor ratio and tumor retention.

The first study using a [Pro^1, Tyr^4]Bn analog radiolabeled with ^{111}In by the linker DTPA (Table 2, Fig. 1) was published in 1999 [48][Analog #34, Table 5], in which this radiolabeled Bn analog was compared with a Bn antagonist [[Tyr^5, DPhe^6]Bn(5–13)ethyl amide, (Table 1, Analog #35, Table 5)], also radiolabeled with ^{111}In using a DTPA linker, and both were tested in the 7315b rat pituitary tumor cell line, AR42J cells and CA20948 cells. The results demonstrated that the Bn agonist ([Pro^1, Tyr^4]Bn) had a slightly higher affinity for the GRP receptor (8 *vs* 11 nM) and the agonist was internalizated, whereas the radiolabeled antagonist [Tyr^5, DPhe^6]Bn(5–13)ethyl amide, was not. This was also demonstrated by biodistribution studies [Analog #34, Table 6] that the Bn agonist showed a much higher specific uptake by GRP receptor tissues and by tumors, which could be detected by *ex-vivo* scintigraphy.

The same group published another biodistribution study [74] [Analog #31, Table 6] with this radiolabeled Bn agonist (^{111}In-DPTA-[Pro^1, Tyr^4]Bn), using as xenograft tumors the colon cancer cell line CC531 and the pancreatic cancer cell line CA20948. The results showed that in normal animals the highest uptake was observed in the pancreas, followed by kidneys and bladder (demonstrating a renal clearance of the radiopeptide). When the radioconjugate was injected into animals bearing the CC531 cancer cell line or the CA20948 cancer cell line, it was taken up by the tumor in a specific way and it was visualized scintigraphically. When this Bn radiopeptide was compared with other ^{111}In hormone radiopeptides (^{111}In-DPTA-

Octreotide, ^{111}In-DOTA-CCK, ^{111}In-DTPA-[Arg^1]Substance P) [75] [Analog #29, Table 5] in the pancreatic cancer cell line CA20948, the Bn derivative had the highest internalization rate, and the second highest tumor uptake ratio in Lewis rat bearing CA20948 tumors, after ^{111}In-DPTA-Octreotide [Analog #29, Table 6].

In another study four [76] ^{111}In radiolabeled [Tyr^4]Bn analogs [Analogs #3–6, Table 5] were tested ([Pro^1, Tyr^4]Bn or [εLys^1, Tyr^4]Bn) (Table 2) which were linked to the isotope with DOTA or DPTA. All the Bn analogs had an IC_{50} of 3–9 nM near that of the [^{4}Tyr]Bn (Table 2) value (1 nM). When the analogs were labeled with the isotope through the linker, the 4 resultant radiopeptides agonists were all internalized with the DPTA-[Pro^1, Tyr^4]Bn having the highest value. The biodistribution study [Analogs #3–6, Table 6] showed that DOTA-[Pro^1, Tyr^4]Bn had the highest tumor uptake and tumor/blood ratio, followed by the DPTA-[Pro^1, Tyr^4]Bn radiopeptide. However, the authors concluded that, as ^{111}In labeled DTPA-[Pro^1, Tyr^4]Bn is easier to handle, this should be the radiopeptide chosen for future studies.

Attempting to improve some characteristics of this radiopeptide (^{111}In- DTPA- [Pro^1, Tyr^4]Bn), it was compared with 2 others Bn agonist analogs ([βAla^{11}, Phe^{13}, Nle^{14}]Bn(7–14) and [βAla^{11}, Tha^{13}, Nle^{14}]Bn(7–14); Nle: Norleucine, Tha: β-(2-thienyl)alanine; Tables 1,2) [Analogs #36–41, Table 5] [77] which were combined with different DPTA-spacers (1,2-diaminopropionic acid ($_D$Dpr), 4-aminocarboxymethylpiperidine-Tha (ACMpip-Tha), 1-aminoethy-l,4-carboxymethylpiperazine (Acp) and DTha, Table 1). Among them, the best affinity, internalization and stability values were obtained with DPTA-ACMpip-Tha-[βAla^{11}, Phe^{13}, Nle^{14}]Bn(7–14) in both prostate PC-295 or pancreatic CA20948 cancer cell lines, with a 25-fold (IC_{50}: 0.1 nM) and 5.6-fold increase (IC_{50}: 0.4 nM) in the GRP receptor affinity with respect that of Bn(7–14). *In vivo* biodistribution studies in rats bearing PC-3 cell xenografts [Analogs #36 and #38, Table 6] comparing ^{111}In-DPTA-ACMpip-Tha-[βAla^{11}, Phe^{13}, Nle^{14}]Bn(7–14) with ^{111}In-DPTA-[Pro^1, Tyr^4]Bn, demonstrated that the former analog had higher pancreatic and tumor uptake, tumor/non-tumor ratio and lower kidney retention. Furthermore with ^{111}In-DPTA-ACMpip-Tha-[βAla^{11}, Phe^{13}, Nle^{14}]Bn(7–14), tumors were clearly visualized by SPECT/CT, suggested this new radiolabeled Bn analog as a new candidate for use in nuclear medicine.

^{111}In-DPTA-[Pro^1, Tyr^4]Bn has been also use in one study [Analog #33, Table 5][78]. The results showed that androgen ablation in animals bearing PC-3 tumor cells produced a decreased in the expression of GRP receptor in the tumor, and it also reduced the radiopeptide uptake by the tumor. This suggests that hormonal therapy may affect GRP receptor expression in prostate cancer tissue making GRP receptor-based imaging and therapy especially suitable for non-hormonally treated prostate cancer patients.

Another Bn analog that has been tested as a ^{111}In-radiolabeled agonist peptide is [DTyr^6, βAla^{11}, Thi^{11}, Nle^{14}]Bn(6–14) Table 2; Thi: 3-(2-thienyl)alanine, Table 1). In one study [50] [Analog #7, Table 5] this Bn analog was linked to the isotope by the linker DOTA$^{0–1}$, PEG^0 (Z-070) and it was compared with another Bn analog that was labeled with ^{99m}Tc (^{99m}Tc-Demobesin1, Table 1,2). The results demonstrated that Demobesin1 had 11–14 fold higher affinity for the GPRP receptor in PC-3 cells, but had a similar affinity in AR42J cells compared to Z-070. The same result was observed in the case of mice bearing PC-3 or AR42J xenografts [Analog #7, Table 6]. In another study with [DTyr^6, βAla^{11}, Thi^{11}, Nle^{14}]Bn(6–14) [79][Analogs 17–18, Table 5] the effect of two different linkers (DOTA-γ-aminobutyric acid (GABA) or DPTA-GABA, Table 1) was examined. The DOTA linked Bn analog had a lower affinity (1.4±0.1 nM *vs.* 3.5±0.32 nM), but both of them showed similar internalization rates and their half-life were similar. *In vivo* biodistribution studies [Analogs

#17–18, Table 6] showed a high uptake by GRP receptor expressing tissues and tumor with also high values in the ratio tumor/non-tumor.

Another ^{111}In labeled Bn antagonist studied was Bomproamide [47] ([DPhe^{6}, Leu-NHEt^{13}, des-Met^{14}]Bn(6–14), Table 2), a GRP receptor antagonist, coupled to the isotope by the linker DOTA-aminohexanoyl. This radiolabeled Bn antagonist analog [Analog #26, Table 5] showed a nM IC_{50} value (1.36±0.09 nM) similar to that of Bn(7–14), but had a low internalization level. *In vivo* experiments with mice bearing PC-3 xenografts demonstrated that the Bn antagonist radiopeptide [Analog #26, Table 6] showed high and rapid uptake by pancreas and tumor, which could be clearly visualized by SPECT/CT.

^{111}In-DPTA-[Lys^{3}, DTyr^{4}]Bn(2–14) [Analog #32, Table 5, Table 2] is another radiopeptide Bn agonist tested [80] for its possible use in imaging and treating tumors expressing GRP receptors. The experiments with this compound showed an IC_{50} of 1.05 nM in PC-3 cells, similar to that of Bn(7–14), with internalization values near 60% and a long half-life (59.4% after 8 h in rat plasma). When the radiopeptide was injected into mice bearing PC-3 cell xenografts [Analog #32, Table 6], a high uptake by tumor, adrenal gland, pancreas and intestine was observed.

III. E. Review of ^{64}Cu -labeled Bn analog *in vitro* (Table 7) and *in vivo* (Table 8) studies of Bn receptor-mediated imaging/cytotoxicity studies

Studies attempting to identify useful Bn analogs for imaging studies using Positron emission tomographic scanning (PET) of bombesin receptors started lately compared to the development of Bn radiolabeled analogs for SPECT imaging. ^{64}Cu is a positive charged radioisotope, which is used both for imaging (PET scanning) and therapy [81,82]. It is produced using a medical cyclotron, and has a half-life of 12.7 h, with an emission at 0.651MeV and decay at 0.578 MeV β^- [81]. The first study that attempted to identify a Bn analog labeled with ^{64}Cu was in 2003[83], subsequently 13 additional studies (Tables 7 and 8) reported different ^{64}Cu-radiolabeled Bn analogues and their pharmacokinetics properties and imaging efficacy. Finding in these studies are summarized in Tables 7 and 8, for *in vitro* and *in vivo* results, respectively.

Roger *et al.*, studied the *in vitro* and *in vivo* characteristics of the ^{64}Cu-DOTA-Aoc-Bn(7–14) (Aoc=aminooctanoic acid) analog [Analog #59. Table 7, 8] (Tables 1, 2,, Fig. 1.) [83]. This analog showed in the prostate cancer cell line, PC-3, high affinity for the hGRP receptor (K_d 6.1±2.5 nM) and a rapid internalization rate [Analog #59, Table 7]. *In vivo* biodistribution studies and microPET imaging, performed in athymic mice bearing human prostate cancer xenografts, PC-3, showed a rapid tumor uptake as well as in other tissues such as liver, pancreas and intestine, resulting in a low tumor-non-tumor ratio [Analog #59, Table 8] [83]. Therefore, the authors performed an *in vivo* determination of blood flow, finding that it is 2.6-fold lower to the PC-3 tumor than to the pancreas. These results could explain a limited diffusion of the ^{64}Cu-DOTA-Aoc-Bn(7–14) analog and, consequently, a low uptake and binding of the radioligand by the tumor [83]. Finally, the authors suggest modifying the charge of the peptide and the peptide linker group, in order to reduce the amount of the ^{64}Cu-radiolabeled peptide taken up by normal tissues [83].

To improve the specificity of the ^{64}Cu- DOTA-Aoc-Bn(7–14) analog the same group modified it by substituting PEG (ethylene glycol [2-aminoethylcarboxymethylether]) instead of Aoc (Table 1, Fig. 1.). The hypothesis was that this modification could improve the pharmacokinetics of the conjugate, in particular, for its delivery to the tumor site [84]. The authors evaluated *in vivo* and *in vivo* properties of ^{64}Cu-DOTA-PEG–Bn(7–14) *vs* ^{64}Cu-DOTA-Aoc-Bn(7–14) analogs [Analogs #60–61, Tables 7,8], using the PC-3 cell line and normal athymic nude mice. Competitive binding assay results for [Tyr^{4}]-Bn (used as

control), DOTA-Aoc-Bn(7–14) and DOTA-PEG-Bn(7–14) showed a strong reduction of binding affinity toward hGRP receptor of the new conjugates (IC_{50} 18.8±2.3 nM, 90.5±22 nM, 3.9±0.6 μM, respectively) [Analogs #60–61, Table 7]. Furthermore, ^{64}Cu-DOTA-PEG–Bn(7–14) also showed a reduction in the internalization rate compared to ^{64}Cu-DOTA-Aoc–Bn(7–14) analog, mostly due to the lack of affinity of PEG-conjugate [84]. Finally, *in vivo* studies found ^{64}Cu-DOTA-PEG-Bn(7–14) had a faster blood clearance than expected and a specific, but reduced pancreatic uptake compared to ^{64}Cu-DOTA-Aoc-Bn(7–14) (1.3-fold less) [Analogs #60–61, Table 8] [84].

Chen *et al.* studied the *in vitro* and *in vivo* characteristics of the ^{64}Cu-DOTA-[Lys^3]Bn agonist conjugate [Analogs #35–36, Tables 7, #35 Table 8] (Tables 1,2, Fig. 1.) [85]. Using the human androgen independent (AI) prostate cancer cell line PC-3, they found a high binding affinity to hGRP receptor (IC_{50} 2.2±0.5 nM) and internalization rate [Analogs #35–36, Table 7] [85]. *In vivo* studies were performed in human prostate cancer carcinoma xenografts induced by injection of either the AI-PC-3 cell line or the androgen dependent (AD) CWR22 cell line. The radiopeptide uptake was specific and it displayed a predominant renal clearance. Interestingly, the uptake was higher in the AI-PC-3 xenografts than in AD-CWR22 xenografts [Analog #35, Table 8] [85]. MicroPET and autoradiography imaging for both models showed a very high tumor-to- background ratio, although tumor and pancreas accumulation was lower compared to normal biodistribution studies [Analog #35, Table 8] [85].

To investigate the possibility whether a truncated coupled Bn analog, Bn(7–14) was more suitable for PET imaging purposes than full-length Bn, Yang *et al.* performed a compared *in vivo* and *in vitro* evaluation of ^{64}Cu-DOTA-Aoc-Bn(7–14) and ^{64}Cu-DOTA-[Lys^3]Bn agonist conjugates [Analogs #62–63, Table 7; #62–65, Table 8] (Tables 1,2, Fig. 1.) [86]. In PC-3 cells the DOTA-[Lys^3]Bn compound displayed a higher binding affinity than the DOTA-Aca-Bn(7–14) compound (IC_{50} 2.2±0.5 *vs.* 18.4±0.2 nM) [Analogs #62–63, Table 7]. Moreover, the internalization rate and retention was much higher for the full-length compound [Analogs #62–63, Table 7] [86]. *In vivo* studies showed more stability in mouse blood, urine, tumor, liver and kidney samples from PC-3 tumor bearing mice for the full length Bn compound and a higher liver and intestinal uptake for the Bn(7–14) analog [Analogs #62–65, Table 8] [86]. MicroPET images showed a low background radioactivity for ^{64}Cu-DOTA-[Lys^3]Bn but it still displayed a significant accumulation in intestine and rapid renal clearance [Analogs #62–65, Table 8] [86].

In a study aimed to identify a new Bn radioligand labeled with ^{111}In, the agonist DOTA-[Pro^1, Tyr^4]Bn(1–14) (MP23436) was synthesized and characterized (Tables 1,2. Fig. 1.) [76]. Next, Biddlecombe *et al.* evaluated both ^{64}Cu and ^{86}Y-radiolabeld MP2346 conjugates [Analogs #34 and 71, Table 7; #34, 71,72, Table 8] [87]. An *in vitro* study in the PC-3 cell line showed a good internalization rate for both compounds, with an initial slower rate for ^{86}Y-MP23436 that becomes 3-fold higher at 20 h with the ^{64}Cu-radioligand [Analogs #34 and 69, Table 7] [87]. The *in vivo* biodistribution in PC-3 tumor bearing mice was associated with a higher uptake for the ^{86}Y-conjugate and consistent levels of ^{64}Cu compound in liver, mostly caused by transchelation of the copper [Analogs #34 and 69, Tables 8]. Finally, PET images showed a better tumor-normal tissue ratio for ^{86}Y-MP23436. These results were attributed to the physical and chemical properties of ^{64}Cu and ^{86}Y metals [Analogs #34 and 69, Table 8] [87].

Parry *et al.* evaluated a series of Bn analogs coupled to 4 to 12-carbon linkers in the human breast cancer cell line, T-47D [Analogs #50–54, Tables 7, 8] [88]. *In vitro* binding affinity in these cells showed a high affinity of the DOTA-Aoc-Bn(7–14) compound (Table 1,2. Fig. 1.) (IC_{50} 6.7 nM) compared to others and a very low affinity for the Aba-linker containing

compound (4-carbons) (IC_{50} 78.5 nM) [Analogs #50–54, Table 7] [88]. The internalization rate displayed a very low value for DOTA-Ado-Bn(7–14) compound (12-carbons), in spite of its binding affinity. The authors concluded that the presence of 12 carbon spacer in Ado-compound could improve the GRP receptor affinity, but lead to a tridimensional conformation that inhibited its internalization [Analogs #50–54, Table 7] [88]. *In vivo* experiments in T-47D tumor bearing mice showed that Aoc, the 8-carbon linker compound had the highest tumor uptake, but also had high liver uptake. Moreover, PET images showed that 6-and 8- carbon containing linkers had a good tumor uptake suggesting that further modifications are necessary to optimize the use of Bn radiolabeled analogs for breast cancer imaging [Analogs #50–54, Table 8] [88].

The same group studied the effect of the presence of various amino acid spacers between DOTA and truncated Bn(7–14) compound when labeled with ^{64}Cu [89]. ^{64}Cu-DOTA-X-Bn(7–14) (Tables 1,2. Fig. 1.) containing in the X-position three amino acid combinations of non polar glycine (G), polar serine (S) or negatively charged glutamic acid (E) [Analogs #45–49, Table 7; #45–47, Table 8] [89]. The presence of a negative charged E strongly reduced GRP receptor binding affinity and the internalization rate of the compound in PC-3 cell lines, so the author focused their *in vivo* studies using GGG, GSG and GSS- containing conjugates [Analogs #45–49, Table 7] [89]. MicroPET images from PC-3 tumor bearing mice, displayed a high tumor, liver and kidney uptake for the GGG-containing radioligand, while the two GSG- and GSS- radioligand showed a better tumor-normal tissues ratio. In particular, ^{64}Cu-DOTA-GSS-Bn(7–14) had the longer retention compared to the other two conjugates [Analogs #45–47, Table 8] [89]. The presence of a serine amino acid linker seemed to decrease the lipophilicity and liver uptake; on the other hand, there was an increase of abdominal accumulation, compromising the tumor-non-tumor ratio [89].

To reduce transchelaton of ^{64}Cu, Garrison *et al.* attempted to use a different chelator, CB-TE2A (1,4,8,11-tetraazabicyclo[6.6.2]hexadecane-4,11-diacetic acid) (Table 1, Fig. 1) [90]. They compared *in vitro* and *in vivo* properties of -8-Aoc-Bn(7–14) either chelated with CB-TE2A or DOTA [Analogs # 37–38, Tables 7,8]. In PC-3 cells, ^{64}Cu-CB-TE2A-8-Aoc-Bn(7–14) showed higher binding affinity than ^{64}Cu-DOTA-8-Aoc-Bn(7–14) (IC_{50} 0.5 *vs.* 1.4 nM, respectively) [Analogs # 37–38, Table 7] [90]. Furthermore, in internalization experiments performed in the same cell line, the ^{64}Cu-CB-TE2A radioconjugate showed a faster internalization rate than ^{64}Cu-DOTA radioconjugate [Analogs # 37–38, Table 7] [90]. *In vivo* experiments conducted in SCID mice bearing PC-3 xenografts, showed a rapid uptake for both compounds, but a significant rapidly clearance for the ^{64}Cu-CB-TE2A-compound. Moreover, microPET images displayed a tumor-non-tumor ratio higher for ^{64}Cu-CB-TE2A-8-Aoc-Bn(7–14) [Analogs #37–38, Table 8] [90].

Another group conjugated the 8-Aoc-Bn(7–14) compound with ^{64}Cu-NOTA (1,4,7-triazacyclononanetriacetic acid) [Analog #55, Table 7; analogs #55–56, Table 8] (Table 1, Fig. 1.) [91]. *In vitro binding* affinity of ^{64}Cu-NOTA -8-Aoc-Bn(7–14) in PC-3 cell line displayed an IC_{50} of 3.1 nM, very close to the Bn and Bn(7–14) affinities to hGRP receptors [Analog #55, Table 7] [91]. *In vivo* studies in CF-1 normal mice demonstrated very fast blood clearance and a significance renal excretion [Analogs #55–56, Table 8]. Moreover, ^{64}Cu-NOTA-8-Aoc-Bn(7–14) (Fig. 1,Table 2) displayed a specific uptake in GRP receptor-expressing tissues such as mouse pancreas. MicroPET images and *in vivo* biodistribution studies in SCID mice bearing PC-3 tumors also showed high and specific uptake of ^{64}Cu-NOTA -8-Aoc-Bn(7–14) in tumors, with a reduced liver accumulation, which points out that the use of NOTA as chelator strongly reduces the possibility of any dissociation phenomenon for ^{64}Cu [Analogs #55–56, Table 8] [91]. The same group, has recently reported another study in a breast cell cancer model, using the ^{64}Cu-NO2A-8-Aoc-Bn(7–14) conjugate [Analog #57, Table 7; Analogs #57–58, Table 8], where the chelator is

NO2A (1,4,7-triazacyclononane-1,4-diacetate) (Table 1,Fig. 1) and compared it with a ^{64}Cu-DOTA-8-Aoc-Bn(7–14) compound[92]. *In vitro* binding affinity studies were performed in the human breast cancer cell line T-47D and showed a 3-fold decrease in affinity compared to Bn(7–14) (i.e. 7.6 nM), but a very fast internalization rate [92] [Analog #57, Table 7]. *In vivo* evaluation of ^{64}Cu-NO2A-8-Aoc-Bn(7–14) in normal CF-1 mice showed a fast and specific uptake in tissues expressing GRP receptors [Analogs #57–58, Table 8]. Moreover, microPET/CT and microMRI images of SCID mice bearing T-47D tumors showed high tumor-non tumor ratios for most of the tissues, with a reduced abdominal and liver accumulation, probably due to the hydrophobicity of the NOA2 chelators [Analogs #57–58, Table 8] [92].

Gasser *et al.* recently reported in a study a new ligand derivative TACN ((2-[4,7-bis(2-pyridylmethyl)-1,4,7-triazacyclononan-1-yl]acetic acid) (Table 1,, Fig. 1) coupled to the Bn agonist analog, βAla-βAla – [Cha^{13}, Nle^{14}]Bn(7–14) (Tables 1, 2) [Analog #39, Tables 7, 8] [93]. *In vitro* stability studies showed that ^{64}Cu-TACN- βAla-βAla–[Cha^{13}, Nle^{14}]Bn(7–14) had high stability in presence of an excess of either the competing ligand (cyclam) or the copper-seeking superoxide dismutase (SOD). Similar results were obtained by *in vivo* stability studies in rat plasma [Analog #39, Table 7] [93]. Furthermore, the authors performed *in vivo* biodistribution studies in Wistar rats and showed a high uptake in pancreas with a predominant renal excretion [Analog #39, Table 8] [93].

A similar study was also performed using the same Bn agonist analog [Cha^{13}, Nle^{14}]Bn(7–14) (Tables 1,2) but using as a chelator, a bispidine derivative (3,7-diazabicyclo[3.3.1]nonane) [Analogs #40–41, Tables 7, 8] [94]. *In vivo* studies in Wistar rats showed a very fast blood clearance and renal excretion, with low liver accumulation. Furthermore, NMRI nu/nu mice bearing PC-3 humane prostate tumors, displayed a tumor accumulation [Analogs #40–41, Tables 8] [94].

Liu *et al.* analyzed the synergistic effect of the dual-receptor targeting of a ^{64}Cu-X-RGD-Bn radioligand targeting GRP receptors and $\alpha_v\beta_3$ integrin, using as chelators either DOTA or NOTA [Analogs #42–42, Tables 7, 8] (Table 1,2. Fig. 2) [95]. In PC-3 cells both ^{64}Cu-DOTA-RGD-Bn and ^{64}Cu-–NOTA-RGD-Bn conjugates displayed a comparable affinity to both the integrin $\alpha_v\beta_3$ and the hGRP receptor. They targeted $\alpha_v\beta_3$ integrin, because it has been demonstrated this integrin is involved in tumor angiogenesis in several tumors [95–97]. Although the IC_{50} values for hGRP receptor were relatively high (85.8 nM for DOTA compound and 92.7 nM for NOTA compound) [Analogs #42–42, Table 7], *in vivo* PET images in PC-3 bearing tumor mice showed a specific tumor uptake and lower liver accumulation for NOTA-compound (Fig. 1) [Analogs #42–42, Table 8]. In addition, biodistribution studies in normal Balb/c mice, confirmed high uptake in GRP receptors-expressing tissues, such as murine pancreas and a fast excretion, mostly by kidneys [Analogs #42–42, Table 8] [95].

Finally, Ma *et al.*, recently, reported a study in which the Bn agonist [Lys^3]Bn (Tables 1,2) and the somatostatin derivative [Tyr^3]octreotate were compared. Each showed high stability in human serum for a long time period [Analog #44, Table 7] [98].

III. F. Review of ^{18}F -labeled Bn analog *in vitro* (Table 7) and *in vivo* (Table 8) studies of Bn receptor-mediated imaging/cytotoxicity studies

^{18}F is a suitable isotope used in positron emission tomography (PET) with a short half-life (110 minutes), used for labeling small molecules such as biologically active peptides and produced in small biomedical cyclotrons [82,99]. The radiolabeling process is complex but, since ^{18}F has a small prosthetic group, coupling to the peptide or the chelator, strongly reduces the chance that alterations in the coupled peptides change biological properties [82].

Findings from studies reporting *in vitro* and *in vivo* use of ^{18}F-Bn-radiolabeled conjugates are summarized in Tables 7 and 8.

Zhang *et al.* analyzed the properties of two Bn-derivatives, [Lys^3]Bn and Aca-Bn(7–14), both coupled with ^{18}F-SFB (N-succinimidyl-4–^{18}F-fluorobenzoate) [Analogs #30–33, Table 7; analogs #30–31, Table 8] (Table 2, Table 1, Fig. 1)[99]. *In vitro* studies, performed in the human prostate cell line PC-3, showed that ^{18}F-[Lys^3]Bn had a higher affinity for GRP receptors than ^{18}F-Aca-Bn(7–14) (IC_{50} 3.3 *vs* 20.8 nM, respectively) [Analogs #30–33, Table 7]. Moreover, when coupling with FB (fluorobenzoate), the resulting conjugates, ^{18}F-FB-[Lys^3]Bn and ^{18}F-FB-Aca-Bn(7–14) (Table 2,Table 1,Fig. 1) had IC_{50} values of 5.6 nM and 48.7 nM, respectively [Analogs #30–33, Table 7] [99]. Internalization experiments in PC-3 cells demonstrated these radioligands showed a rapid uptake rate, although this was followed by a high efflux rate, probably due to the strong lipophilic properties of the radioconjugates [Analogs #30–33, Table 7]. *In vivo* studies were performed only with ^{18}F-FB-[Lys^3]Bn and ^{18}F-FB-Aca-Bn(7–14) conjugates. Biodistribution and microPET images studies in PC-3 tumor bearing athymic mice displayed a rapid blood clearance, an excretion through kidneys for both radiolabeled compounds and a significant liver and gallbladder accumulation for ^{18}F-FB-Aca-Bn(7–14) compound [Analogs #30–31, Table 8]. This latter finding strongly reduces the suitability of its use for detecting orthopic prostate cancer, located very close to the urinary bladder [99]. The tumor uptake and the tumor-non tumor ratios were higher for ^{18}F-FB-[Lys^3]Bn than for ^{18}F-FB-Aca-Bn(7–14) [99].

The same group reported another study aimed to increase the tumor-non-tumor tissues ratios synthesizing a dual-receptor targeting radioligand by targeting the GRP receptor and $\alpha_v\beta_3$ integrin, since $\alpha_v\beta_3$ is involved in the angiogenesis of most solid tumors [96,97,100]. The resulting ligand, ^{18}F-FB-Bn-RGD (FB=fluorobenzoate; RGD=arginine-glycine-aspartate) (Table 2,Table 1,Fig. 1) was studied in comparison with the monomeric forms, ^{18}F-FB-Bn and ^{18}F-FB-RGD [Analogs #26–27, Tables 7,8]. *In vitro* internalization rate in the human prostate cancer cell line PC-3, showed comparable behavior between ^{18}F-FB-Bn and ^{18}F-FB-Bn-RGD conjugates [Analogs #26–27, Table 7] [100].

Moreover, *in vivo* experiments in PC-3 tumor bearing mice, displayed a higher tumor uptake compared to the monomeric forms [Analogs #26–27, Table 8] [100]. To improve the *in vivo* kinetics, the same group synthesized another radioconjugate adding PEG_3 (11-amino-3,6,9-trioxaundecanoic acid) (Table 1) as a spacer [Analogs #28–29, Tables 7, 8] [101]. In PC-3 cell line, the authors found that FB-PEG_3-Glu-RGD-Bn (Glu=glutamate) (Table 2, Table 1, Fig. 1) had comparable binding affinity to GRP receptor with Aca-Bn(7–14) and PEG_3-Glu-RGD-Bn (Tables 1,2) [Analogs #28–29, Table 7] [101]. Moreover, internalization studies in PC-3 cells showed that ^{18}F-FB-PEG_3-Glu-RGD-Bn had a fast internalization rate, mostly due to the binding to GRP receptors rather then integrin binding [Analogs #28–29, Table 7]. MicroPET images in PC-3 tumor bearing mice showed that ^{18}F-FB-PEG_3-Glu-RGD-Bn showed renal excretion, with a fast accumulation in kidneys. It also had a low accumulation in liver and high tumor-non-tumor tissues ratios [Analogs #28–29, Table 8] [101].

Höhne *et al.* synthesized ^{18}F-Bn-derivatives radioligand using a silicon one-step method [Analogs #24–25, Tables 7, 8] [51]. The *in vitro* behavior of the GRP receptor antagonists ^{18}F-2-(4-(di-tert-butylfluorosilyl)phenyl) acetyl-Arg-Ava- [NMeGly^{11}, Sta^{13}, Leu^{14}] Bn(7–14) and the ^{18}F-2-(4-(di-tert-butylfluorosilyl)phenyl) acetyl-Arg-Ava-[His(3Me)^{11}, Sta^{13}, Leu^{14}]Bn(7–14) (Tables 1,2) was studied in PC-3 cells and revealed a very different GRP receptor affinity, (IC_{50} 22.9 and 267.7 nM, respectively) [Analogs #24–25, Table 7] [51]. *In vitro* stability studies in PBS (phosphate buffered saline), mouse or human plasma showed no degradation products within 2 h for ^{18}F-2-(4-(di-tert-butylfluorosilyl)phenyl) acetyl-Arg-Ava-[NMeGly^{11}, Sta^{13}, Leu^{14}] Bn(7–14). Moreover,

this result was supported by *ex vivo* stability studies in mouse blood at 10 and 30 minutes post-injection [Analogs #24–25, Table 7] [51]. Finally, *in vivo* biodistribution studies with the ^{18}F-2-(4-(di-tert-butylfluorosilyl)phenyl) acetyl-Arg-Ava-[NMeGly^{11}, Sta^{13}, Leu^{14}] Bn(7–14) antagonist, performed in PC-3 tumor bearing mice, displayed a low tumor uptake, however pancreatic uptake was high [Analogs #24–25, Table 8]. This study confirmed the use of a silicon-based one-step method to synthesize ^{18}F-labeled Bn derivatives. Furthermore, the authors suggested an increase of lipophilic characteristics be considered to improve tumor uptake and, consequently, suitability for prostate tumor imaging, for these Bn radiolabeled compounds [51].

Becaud *et al.*, from the same group, recently reported a study on the synthesis of two new ^{18}F-radiolabeled Bn-derivatives: the antagonist ligand, 3-Cyano-4-[^{18}F] fluorobenzoyl-Ava-[NMeGly^{11}, Sta^{13}, Leu^{14}]Bn(7–14) and the agonist ligand, 3-Cyano-4-[^{18}F] fluorobenzoyl-Ava- [FA(01010)^{13}, Leu^{14}] Bn(7–14) [Analogs #22–23, Table 7] (Tables 1,2) [102]. *In vitro* binding assay in PC-3 cells, showed a good affinity of these two radioligands for the GRP receptor compared to Bn and Bn(7–14) with IC_{50} of 2.7 nM for 3-Cyano-4-[^{18}F] fluorobenzoyl-Ava-[NMeGly^{11}, Sta^{13}, Leu^{14}]Bn(7–14) and 9.2 nM for 3-Cyano-4-[^{18}F] fluorobenzoyl-Ava- [FA(01010)^{13}, Leu^{14}] Bn(7–14) [Analogs #22–23, Table 7] [102]. Mouse plasma stability studies indicated an excellent stability for both radioligands, especially for 3-Cyano-4-[^{18}F] fluorobenzoyl-Ava-[NMeGly^{11}, Sta^{13}, Leu^{14}]Bn(7–14). The results of this study pointed out that the one-step ^{18}F-fluorination of Bn peptides is practical under mild conditions and produces a good yield of radiochemical compounds [102].

III. G. Review of ^{68}Ga -labeled Bn analog *in vitro* (Table 7) and *in vivo* (Table 8) studies of Bn receptor-mediated imaging/cytotoxicity studies

The positron emitter ^{68}Ga is a high β^+ energy emitter ($E_{\beta^+_{max}}$=1.9 MeV) with a short half-life ($t_{1/2}$= 68 minutes) [82,103]. It has been used to label Bn analogs for PET imaging purposes because of its ease of production from ^{68}Ge/^{68}Ga generators. There are only three studies assessing the *in vitro* and *in vivo* properties of various ^{68}Ga-Bn analogs conjugates and their results are summarized in Tables 7 and 8 [Analogs #66–68] [103–105].

In 2004, Shuhmacher *et al.* analyzed the Bn radiolabeled agonists $^{68/67}$Ga-DOTA-PEG_2-[D-Tyr^6,β-Ala^{11}, Thi^{13}, Nle^{14}] Bn(6–14) (DOTA=1,4,7,10-tetraazacyclododecane-N,N′,N″,N‴-tetraaceticacid; PEG_2 = (2-aminoethyl)-carboxymethyl ether; $^{68/67}$Ga-BZH3) [Analog # 68, Table 7, 8] (Tables 1,2, Fig. 1) *in vitro* and *in vivo* behavior and compared the results obtained with the same peptide radiolabeled with the radiolanthanide ^{177}Lu [104]. *In vitro* studies were performed in the pancreatic tumor rat cell line AR42J, using the ^{67}Ga-BZH3 conjugate. They reported an hGRP receptor binding affinity of 0.46 nM for the new Bn analog [Analog #68, Table 7], which is three times higher affinity than that for the ^{125}I-[Tyr^4]Bn radiocompound, used as standard control. The internalization rate, in AR42J cells, was rapid and high (88% after 2 hours), confirming the agonistic nature of ^{67}Ga-BZH3 radiopeptide [104]. Moreover, ^{67}Ga-BZH3, as well as the ^{177}Lu-BZH3 peptide, showed a high retention rate ($t_{1/2}$=13.5 hours compared to ^{125}I-[Tyr^4]Bn for 3 hours), probably due to the linker used for coupling. Biodistribution studies, in AR42J tumor bearing mice, displayed a dose-dependent uptake for ^{67}Ga-BZH3 in hGRP receptor positive tissues (tumor and pancreas), with a fast blood clearance. However, the intestinal uptake was still high [Analog #68, Table 8]. PET images were obtained using the ^{68}Ga-BZH3 radioconjugate and indicated a very sensitive localization of hGRP receptor positive tumors in the mediastinal area [Analog #68, Table 8]. On the other hand, this $^{67/68}$Ga-radiolabeled compound could show some limitations in detection of metastatic prostate carcinoma, because of its high background signal in the abdomen [104].

The same group reported another study in which they designed and developed the new Bn analogue agonist, DOTA-PEG_4-Bn(7–14) (PEG_4=15-amino-4,7,10,13 tetraoxapentadecanoic acid; DOTA-PESIN) [Analog #69, Table 7, 8] (Tables 1,2, Fig. 1) and coupled it with either ^{68}Ga or ^{177}Lu[103]. In an *in vitro* analysis in the human prostate cancer PC-3 cell line, they found a high hGRP receptor binding affinity for ^{68}Ga-DOTA-PESIN conjugate (IC_{50} 6.6±3.0 nM). Moreover, as well as the ^{177}Lu-radio-compound, a specific analysis demonstrated selectivity for the hGRP receptor subtype (10.0 nM), and the hNMB receptor (12 nM) over the hBRS-3 receptor (>1000 nM) [103]. The internalization and retention rates, after 2 hours, were much higher for ^{177}Lu-DOTA-PESIN than ^{68}Ga-DOTA-PESIN. On the other hand, a longer time period (4 hours) showed a higher ^{68}Ga-DOTA-PESIN uptake [Analog #69, Table 7] [103]. *In vivo* biodistribution and scintigraphy experiments using PC-3 cell xenografts showed a fast tumor uptake and high level of tumor-liver ratio [Analog #69, Table 8]. Moreover, they found a fast renal excretion and a lower background for PET imaging [103].

Finally, Liu *et al.*, recently, reported a study with the dual radiocompound ^{68}Ga-NOTA-RGD-Bn [Analog # 69, Table 7, 8; NOTA=1,4,7-triazacyclononanetriacetic acid; RGD=arginine-glycine-aspartate] (Tables 1,2, Fig. 1), directed against both the $\alpha_v\beta_3$ integrin and hGRP receptors. The use of $\alpha_v\beta_3$ integrin is justified by several studies that demonstrated its involvement in the angiogenesis of most solid tumors [96,97,100]. The *in vitro* affinity for hGRP receptor was evaluated in the human prostate cancer cell line, PC-3. Compared to the native Bn and the compound with no linker (RGD-Bn), ^{68}Ga-NOTA-RGD-Bn showed comparable affinity with IC_{50} values of 67.9 nM for RGD-Bn, 55.9 nM for NOTA-RGD-Bn and 78.9 nM for Bn [Analog #66, Table 7] [105]. Cell uptake in PC-3 cells was higher for ^{68}Ga-NOTA-RGD-Bn than for those of ^{64}Cu and ^{18}F labeled Bn reported previously [95,100], but lower than ^{68}Ga-NOTA-Bn compound. MicroPET images, biodistribution studies and immunofluorescence analysis in PC-3 tumor bearing mice showed slightly higher tumor uptake of ^{68}Ga-NOTA-RGD-Bn than ^{68}Ga-NOTA-Bn [Analog #66–67, Table 8]. The difference between *in vitro* and *in vivo* results was probably due to several factors including the presence of integrin receptors, which is much higher in the PC-3 tumor than in *in vitro* cells and the possibility that RGD was able to recognize the murine integrin β3, which is strongly expressed on tumor vasculature (as demonstrated by the immunofluorescence study). Moreover, the author hypothesized an *in vivo* synergistic interaction of the two motifs of the heterodimer compound that improved its binding affinity [105].

III. H. Review of ^{177}Lu-labeled Bn analog *in vitro* (Table 9) and *in vivo* (Table 10) studies of Bn receptor-mediated imaging/cytotoxicity studies

Radiolanthanides are a family of trivalent radiometals ($*M^{3+}$), β- and γ-emitters, primarily used for both imaging and therapy. They are easily available and possess high stability in aqueous solutions creating stable conjugates [81].

In order to coupled to peptides and inhibit their *in vivo* transchelation activity, radiolanthanides require multidentate chelators, usually macrocyclic, poliamino-carboxilate ligands such as DTPA (2-[bis[2-[bis(carboxymethyl)amino]ethyl]amino]acetic) or DOTA (1,4,7,10-tetraazacyclododecane-N,N′,N″,N‴-tetraaceticacid) (Tables 1,2. Fig. 1)[103,106–109]. ^{177}Lu coupling has been also reported with the use of the asymmetrically substitute chelator DO3A (1,4,7-tris(carboxymethyl)10-(aminoethyl)-1,4,7,10-tetraazacyclododecaneOH) (Tables 1,2,Fig. 1). Coupling to DO3A is reported to have some favorable features compared to DTPA and DOTA chelators, in terms of greater stability and inertia to metal dissociation [3,110–113]. ^{177}Lu is the lanthanide that is frequently used as a "no carrier added" isotope, and is widely used for imaging studies, although it is also used as

a therapeutic agent [82,114]. It has excellent stability ($t_{1/2}$=6.7 days) and emits both medium energy β-emissions (133 and 412 keV) and γ-emissions (113 and 208 keV) [114].

To try to develop targeting and therapeutic ^{177}Lu labeled Bn analogues, there have been 12 studies attempting to optimize the balance between tumor uptake, tumor retention and chemical properties (Tables 10 and 9). The *in vitro* results of these studies are summarized in Table 9 and *in vivo* results in Table 10.

Since the conjugate DOTA-8-Aoc-Bn(7–14) (Aoc=aminooctanoic acid) (Tables 1, 2), in previous studies, showed very high affinity for GRP receptors and stability, Smith *et al.*, labeled it with ^{177}Lu. [72,108]. ^{177}Lu -DOTA-8-Aoc Bn(7–14) [Analog #10, Tables 9, 10] has high affinity and specificity, displaying an IC_{50} value of 0.3 ± 0.1nM, in PC-3 cells, which possess hGRPR receptors and which is similar to the affinity of Bn and Bn(7–14) for hGRP receptors [108]. Moreover, it showed 73% cell retention after 2 hours post-internalization and very low efflux levels [108]. *In vivo* studies in CF-1 and PC-3 bearing tumors mice models demonstrated good tumor uptake in GRP receptor expressing tissues and in tumors, as well as an efficient clearance by renal system [Analog #10, Tables 9, 10] [108]. Subsequently, the same group evaluated the efficacy of a combined GRP receptor targeted radiotherapy (TRT)/chemotherapy approach, using this new conjugate, in androgen independent prostate cancer [109]. Using as a model, the GRP receptor containing prostate cancer cells, PC-3 in xenografts, they found that a combined therapy with the two microtubule inhibitors, docetaxel and estamustine with^{177}Lu -DOTA-8-Aoc-Bn(7–14) [Analog #6, Table 10] increased by 30% the mean survival compared to targeted radiotherapy or chemotherapy used as single agents [109].

Based on well-known Bn analogs, which have high affinity for all human Bn, receptors [40,115], Zhang *et al.*, developed radiolabeled ^{111}In-, ^{90}Y- and ^{177}Lu- pan-Bn agonist conjugates having high affinity for all the three Bn receptors [79]. Specifically, they studied, *in vivo*, the properties of ^{177}Lu-DOTA-BZH2 (BZH2=[DTyr^{6},βAla^{11}, Thi^{13}, Nle^{14}])Bn(6–14))[Analog # 16, Tables 9,10;Table 2] and found that it had specific, high uptake in rat pancreatic GRP receptor bearing AR-42J tumors in rats, both in GRP receptor positive tissues and in xenograft tumors. Moreover, it displayed a rapid blood clearance with a <0.015% ID/g remaining amount at 4 hours [79]. Unfortunately, preclinical studies showed this compound had a fast washout. To overcome that disadvantage, the same group designed a new conjugate, DOTA-PEG_4-Bn(7–14) (PEG_4=15-amino-4,7,10,13-tetraoxapentadecanoic acid; DOTA-PESIN) [Analog #11, Table 9;Tables 1,2,Fig. 1] and labeled it either with ^{177}Lu or ^{68}Ga [103]. In PC-3 cells, using the universal agonist ligand ^{125}I-([DTyr^{6},βAla^{11}, Thi^{13}, Nle^{14}]Bn(6–14) which has high affinity for human Bn receptors [103] as preferring ligand in competitive experiments, both ^{177}Lu-and ^{68}Ga- radiolabeled Bn showed high affinity for human GRP receptors (IC_{50} 6.1±3.0 nM and 6.6±3.0 nM, respectively) and demonstrated some selectivity for the hGRP receptor subtype (8.3±1.7 nM and 10.0 nM, respectively), over than hNMB receptor (15±4, nM and 12±4.0 nM, respectively) and had no affinity for the hBRS-3 receptor (>1000 nM) [103]. The internalization and retention rates were much higher compared to other pan-Bn analogues [103]. These latter results were confirmed by *in vivo* biodistribution and scintigraphy experiments in PC-3 xenografts, in which they revealed a superior tumor to liver ratio than seen with other radiolabeled peptides and a clear contrast from the background [Analog # 11, Table 10] [103].

A recent study reported divalent DOTA-Bn conjugates could improve targeted imaging compared to monovalent analogues [106]. Specifically, in this study the authors evaluated the amount of receptor internalization in PC-3 cells, of four different ^{177}Lu-labeled compounds: monovalent DOTA-Ahx-Bn(4–14) (06), DOTA-[Lys^{3}]Bn(1–14) (07) and

divalents DOTA-Ahx-Bn(4–14) (08) and DOTA-[Lys^3]Bn(1–14) (09) [Analogs #1–4, Table 9]. Interestingly, after 4 hours, the 08 and 09 divalent conjugates showed a better internalization rate (41.9± 2.1% and 35.9±1.5%, respectively) than the monovalent compounds. At the same time, 08 and 09 compounds showed high cell retention [106].

Recently, Koumarianou *et al*. analyzed and compared the *in vitro* and *in vivo* behavior of ^{90}Y- and ^{177}Lu-DOTA-Bn(2–14) agonist analogues [Analog #7, Tables 9,10] (Table 2) [107]. The ^{177}Lu-labeled compound showed high affinity with an IC_{50} of 1.34± 0.1 nM and good *in vitro* stability (85.6% in serum after 24 hours) [Analog #8, Table 9]. *In vivo* studies in normal mice demonstrated a rapid blood clearance, primarily by renal excretion [Analog #7, Table 10]. However, they found a high uptake in large intestine, probably due to the expression of GRP receptors in this organ. The authors concluded that the ^{177}Lu- labeled compound was preferable compared to the ^{90}Y labeled compound [107].

The use of an asymmetric chelator such as DO3A was first evaluated by Hu *et al.* in a comparative analysis between DO3A-amide-Bn(7–14) and DO3A-amide-βAla-Bn(7–14) (three carbon spacer) conjugates [Analogs #21–24, Table 9] (Tables 1,2, Fig. 1) [113]. The authors labeled these compounds with three different lanthanides, ^{149}Promethium [^{149}Pm], ^{153}Samarium [^{153}Sm] and ^{177}Lu. *In vitro* analysis in PC-3 cells showed that the β-alanine spacer-containing compound had a higher binding affinity (IC_{50} 1.8±0.2 nM) compared with the no spacer compound (IC_{50} 59.8±23.1 nM) [Analogs # 23, 24, Table 9]. On that basis, *in vivo* analyses in normal mice were performed only with the DO3A-amide βAla-Bn [7–14] compound [Analogs # 5 and 22, 23, Table 10]. The ^{149}Pm -labeled compound showed very similar behavior compared to the same compound labeled with ^{153}Sm and ^{177}Lu. The authors considered that the use of the three different radiolanthanides for the same conjugate could be interchangeable, depending on the nuclear properties required for a particular disease target [113].

Lantry's group synthesized and characterized a new conjugate radiolabeled Bn agonist analog, ^{177}Lu-DO3A-glycyl-4-aminobenzoyl-Bn(7–14) (^{177}Lu-AMBA) and compared both its *in vitro* and *in vivo* characteristics to ^{177}-Lu-DOTA-8-Aoc-Bn(7–14) (^{177}Lu-Bn8) [Analogs # 8, 9, Tables 9,10] (Tables 1,2, Fig. 1)[110]. Binding affinity assessed in PC-3 cells showed that ^{177}Lu-AMBA had a similar affinity, compared to the ^{177}Lu-Bn8 compound (IC_{50} 2.50±0.5 *vs* 3.10±0.99, respectively), as well as, a similar degree of internalization and retention [110]. *In vivo* studies in athymic mice showed a similar biodistribution and mechanism of excretion, however ^{177}Lu-AMBA displayed higher levels of accumulation and retention after 1 h and 24 h, respectively [Analogs # 8, 9, Table 10] [110]. In PC-3 tumor-bearing mice treatment with ^{177} Lu-AMBA resulted in a significant increase in survival and a reduction of PC-3 growth rate in treated mice *vs* non-treated, in a single dose treatment [Analogs #8. 9, Table 9]. Moreover, the survival rate and the tumor growth rate of tumor-bearing mice increased with a second dose treatment after 14 days [Analogs #8, 9, Table 9] [110].

Since the prostate cancer cell line PC-3 displays a high expression of GRP receptors (2.5×10^5/cells), Maddalena *et al.* evaluated ^{177}Lu-AMBA tumor binding and imaging potential in low GRP receptors expressing models, such as the prostate cancer cell lines, LNCaP and DU145 cells (an early androgen-sensitive prostate cancer and an androgen insensitive metastatic cell line, respectively) [Analogs #13–15, Table 9] [112]. LNCaP expressed 5.9×10^3 GRP receptors per cell, while DU145 expresses 1.2×10^4 GRP receptors per cell. ^{177}Lu-AMBA showed a very high affinity for all the cell lines tested (K_d of LNCaP, 0.65 nM, of DU145, 0.53 nM, of PC-3 1.01 nM) [Analogs # 13–15, Table 9]. Moreover, both using autoradiography and γ-images, in LNCaP and DU145 xenografts models, ^{177}Lu-AMBA showed a clear identification of tumors [Analogs #13–15, Table 10].

Finally, radiotherapy studies using either LNCaP- or DU145- tumor-bearing mice demonstrated a strong effect in decreasing tumor proliferation rates compared to PC-3 xenografts models [110,112]. Interestingly, in LNCaP model, ^{177}Lu-AMBA was able to normalize tumor microvasculature phenotype, reducing tumoral blood pooling [Analog #13, Table 10] [112].

To further investigate the *in vitro* binding properties of ^{177}Lu-AMBA [Analog #17, Table 9], a series of human neoplastic and non-neoplastic tissues were evaluate by autoradiography, for their bombesin-related receptor expression [116]. ^{177} Lu-AMBA demonstrated a number of GRP and NMB receptors- expressing tumors, including various prostate, mammary and renal cell carcinomas, as well as gastrointestinal stromal tumors. On the other hand, ^{177}Lu-AMBA was not able to identify BRS-3 receptor expressing tumors and Bn receptors on pancreatic islets [116]. Interestingly, this compound demonstrated no binding to normal human pancreas, unless chronic pancreatitis was present [116]. Thomas *et al.*, performed a similar analysis using GRP- or NMB- or BRS-3- receptors over-expressing cell lines and human normal and tumor tissues, obtaining very similar results [Analogs#18–20, Table 9 and analog #18, Table 10] [117].

To further explore the *in vitro* and *in vivo* behavior of ^{177}Lu-AMBA, its stability was studied in mouse, rat and human [Analog #12, Table 9] by analyzing the generation of a series of metabolites derived from this compound [111]. A rapid cleavage of the peptide was seen in mouse, rat and human plasma as well as mouse kidney homogenates. A rapid *in vivo* clearance of the entire conjugate and radioactivity was also found in mouse and rat blood [Analog #12, Table 10]. No unmetabolized drug was excreted in mouse and rat urine [111]. Furthermore, *in vitro* binding affinity in PC-3 cells and *in vivo* biodistribution and clearance in PC-3 xenografts of all metabolites derived from ^{177}Lu-AMBA were evaluated [Analog #13, Table 10]. The results showed the ^{177}Lu-AMBA metabolites all had a low affinity for hGRP receptors and a very fast renal excretion (within an hour), demonstrating that the tumor uptake observed in this study and in previous ones, was only due to ^{177}Lu-AMBA and not to any radiolabeled metabolites [Analog #12, Table 10] [111].

III. I. Review of ^{125}I, ^{86,90}Y, ^{186,187,188}Re -labeled Bn analog *in vitro* (Table 7) and *in vivo* (Table 8) studies of Bn receptor-mediated imaging/cytotoxicity studies

III. I. 1. ^{125}I studies—These are a few studies in which Bn-analogs were radiolabeled with ^{125}I, $^{86/90}$Y or $^{186/188}$Re. The *in vitro* and *in vivo* results of these studies are summarized in Tables 7 and 8, respectively.

Two studies investigated the possibility of radiolabeled Bn-analogs involved the use of radio-iodinated conjugates [118,119]. Rogers *et al.*, analyzed the Bn analog antagonist ^{125}I-mIP-[des-Met^{14}]Bn(7–14) (mIP=meta-iodophenyl and desMet= methionine removed) (Table 1,2) compared with the agonist ^{125}I-[Tyr^{4}]Bn [Analogs #3–10, Table 7; analogs #6–9, Table 7] [118]. Using as model the BALB/B1 mouse fibroblast cell line, BNR-11 that has a stably transfected murine GRP receptor, the authors found that the *in vitro* internalization rate was high for both compounds (≈40% after 5 minutes) [Analogs #3 and 8, Table 7]. However, they found a high efflux rate for both, but it was much higher with ^{125}I-[Tyr^{4}]Bn [118]. Next, the authors evaluated the *in vitro* binding affinity of ^{125}I-mIP-[des-Met^{14}]Bn(7–14) in the human carcinoma cell lines A427 (lung), SKOV3.ip1 (ovary), and HeLa cells (cervical epithelium) over-expressing a recombinant adenoviral vector containing the murine GRP receptor gene (AdCMVGRPr), using BNR-11 cells as control. For both radioconjugates in all the transfected cell lines the binding was greater than in BNR-11 cells [Analogs #3–10, Table 7]. *In vivo* studies were, initially, performed in normal BALB/c mice and showed a fast uptake and clearance from normal tissues. Moreover, ^{125}I-mIP-[des-Met^{14}]Bn(7–14) displayed lower levels of deiodination [Analogs #7 and 8, Table 8].

Biodistribution studies in SKOV3.ip1 tumor bearing mice showed that ^{125}I-mIP-[des-Met^{14}]Bn(7–14) and ^{125}I-[Tyr^{4}]Bn had high uptake with a greater tumor localization for the first radioligand [Analogs #6 and 9, Table 8] [118].

The same group reported another study in the human ovarian cancer cell line SKOV3.ip1 over-expressing the AdCMVGRPr vector, comparing the two Bn agonist radioligands ^{125}I-mIP-Bn and ^{125}I-[Tyr^{4}]Bn [Analogs #1 and 2, Tables 7, 8] (Tables 1,2) [119]. The live-cell binding assay showed high binding in these cells for ^{125}I-[Tyr^{4}]Bn with 80% of radioligand bound after 2 days [Analog #1, Table 7] [119]. Biodistribution studies in SKOV3.ip1 tumor bearing nude mice indicated a greater tumor localization of ^{125}I-mIP-Bn than ^{125}I-[Tyr^{4}]Bn, although the tumor uptake was comparable [Analogs #1 and 2, Table 8] [119].

III. I. 2. ^{86,90}Y studies—^{86}Y is a pure β-emitter, with half-life of $t_{1/2}$=64 h and $E_{\beta max}$=2.27 MeV, used for imaging purposes in PET scanning as a surrogate for ^{90}Y, which is also used as a therapeutic nuclide. Unfortunately, since it has a large range in tissues and can cause hematological toxicity, its use in radiotherapeutical procedures is not still clear [87,107].

As described in the ^{177}Lu –radioligands paragraph, Zhang *et al.* performed a comparative study of the Bn agonist, BZH2 (BZH2=DOTA-GABA-[DTyr^{6},βAla^{11}, Thi^{13}, Nle^{14}]Bn(6–14)) (DOTA= 1,4,7,10-tetraazacyclododecane-N,N′,N″,N‴-tetraaceticacid; GABA=γ-aminobutyric acid) (Tables 1,2, Fig. 2) compound, labeling it either with ^{90}Y, ^{111}In or ^{177}Lu [Analogs # 70, 71, Table 7 and # 16, Tables 9,10 and # 17, Tables 5, 6]. *In vitro* binding receptor autoradiography on human tumors, each expressing a single bombesin receptor subtype, showed higher affinity and selectivity of ^{90}Y-BZH2 for the GRP receptor, NMB receptor and BB3 (IC_{50} 1.4 nM, 4.9 nM and 10.7 nM, respectively), probably due to the extra negative charge at the NH_2 terminus of ^{90}Y-BZH2[79]. Internalization studies performed in the pancreatic tumor rat cell line AR42J, showed that radiolabeled BHZ2 Bn-analog had a comparable internalization rate when radiolabeled either with ^{90}Y, ^{111}In or ^{177}Lu [Analogs # 70–71, Table 7 and # 16, Table 9 and # 17, Table 7] [79].

Similarly, in the comparative study between ^{177}Lu-and ^{90}Y-DOTA-Bn(2–14) agonist analogues [Analog #7, Tables 9,10; analog #73, Tables 7, 8] (Tables 1,2. Fig. 2) Koumarianou *et al.* found *in vitro*, similar affinity to hGRP receptor (IC_{50} 1.3 and 1.99 nM, respectively) and serum stability (85.6% and 79.1%, in serum after 24 hours. respectively) [107]. However, the ^{90}Y-radioligand had a faster efflux rate than the ^{177}Lu-Bn analog [Analog #7, Table 10–1; analog #74, Table 7]. Moreover, *in vivo* studies in normal mice demonstrated specific binding to the GRP receptor, a fast blood clearance and renal excretion [Analog #7, Table 9; analog #74, Table 8]. Nevertheless, ^{177}Lu-DOTA-Bn(2–14) had more specific uptake in *in vivo* blocking experiments with the native Bn, than ^{90}Y-DOTA-Bn(2–14) [107].

Biddlecombe *et al.* compared both ^{64}Cu and ^{86}Y-DOTA-[Pro^{1}, Tyr^{4}]Bn(1–14) (DOTA-[Pro^{1}, Tyr^{4}]Bn(1–14) =MP23436) (Table 1,2 Fig. 2) [Analogs #34 and 72, Table 7; #34, 72 and 73, Table 8] [87]. The *in vitro* study in the PC-3 cell line displayed 3-fold higher internalization rate for ^{86}Y-MP23436 at 20 h than ^{64}Cu-radioligand [Analogs #34 and 72, Table 7] [87]. An *in vivo* biodistribution in the PC-3 tumor bearing mice showed a higher uptake for the ^{86}Y- than ^{64}Cu-MP23436 [Analogs #34, 72 and 73, Table 8]. Biodistribution results were confirmed by PET images where ^{86}Y-MP23436 had a better tumor-normal tissue ratio [Analogs #34, 72 and 73, Table 8] [87].

III. I. 3. ^{186,187,188}Re studies—Rhenium is a transition metal that shares several chemical properties with technetium (^{99m}Tc). Rhenium radioisotopes, ^{186}Re and ^{188}Re, are β-emitters

with half-lives of $t_{1/2}$=90.6 and 16.9 hours, respectively [114,120]. $^{188}W/^{188}Re$ generators produce both radioisotopes. The drawback of ^{186}Re is its low specific activity due to the production method, while for ^{188}Re, its short half-life is a drawback for some studies [121].

Safavy *et al.* coupled the trihydroxamate bifunctional chelating agent trisuccin to the Bn-analog antagonist [des Met^{14}] Bn(7–14) (Tables 1,2) and radiolabeled with ^{188}Re [Analogs #18–21, Table 7] [120]. In a cell binding assay in the BNR-11 cell line, which is a 3T3 mouse fibroblast cell line stably transfected with the murine GRP receptor, the ^{188}Re-Tris-[des Met^{14}] Bn(7–14) and ^{188}Re-Tris-C_6-[des Met^{14}]Bn(7–14) (C_6 = 6 carbons, as linker) radioligands showed 14% and 13% binding, respectively, compared with 21% for the control, ^{125}I-[Tyr^4]Bn [Analogs #18–19, Table 7] [120]. Comparable results were obtained using the PC-3 cell line for ^{188}Re-Tris-[Des Met^{14}] Bn(7–14) which bound a 10% compared with 20% for ^{125}I-[Tyr^4]Bn [Analog #20, Table 7]. The reduced binding could be a consequence of the labeling process [120].

Moustapha *et al.* performed an *in vivo* study in CF-1 normal mice, with the radiolabeled compounds ^{188}Re-N_3S -5-Ava-Bn(7–14) non-carried (NCA), ^{186}Re-N_3S-5-Ava-Bn(7–14) carried (CA) and ^{186}Re-N_3S-5-Ava- Bn(7–14) non-carried (NCA) (N_3S= dimethylglycyl-L-seryl-L-cysteinglycinamide; Ava=5-aminopentanoic acid; [Analogs #15–17, Table 8] (Tables 1,2, Fig. 2) [121]. Biodistribution studies of all three radioligands displayed an efficient blood clearance after 4 hours with high affinity and specificity in pancreas [Analogs #15–17, Table 8] rising the possibility to use NCA $^{188/186}$Re-Bn-derivatives for targeting GRP receptor expressing tumors [121].

Finally, Gourni *et al.* evaluated the *in vitro* features of a series of Bn compounds labeled either with ^{99m}Tc or $^{185/187}Re$, which have similar chemical properties [55]. They synthesized four labeled Bn agonists, where the pyroglutamic acid of Bn was replaced by different chemical groups that were able to bind radiometals: Aca-Gly-Gly-Cys-Bn(2–14) (Bn1.1), Aca-MeGly-Gly-Cys-Bn(2–14) (Bn1.2), Aca-Me2Gly-Gly-Cys-Bn(2–14) (Bn1.3) and Aca-Mac-Gly-Cys-Bn(2–14) (Bn1.4) (MeGly=methylglicine; Me_2Gly=dimethylglycine; Mac=mercaptoacetic acid; [Analogs #11–14, Table 7] (Tables 1,2. Fig. 2) [55]. *In vitro* binding to the hGRP receptor, in PC-3 cells, showed high affinity for the three radioligands (IC_{50} 1.13 nM for Bn1.1; 0.76 nM for Bn1.2 and 1.42 nM for Bn1.4) [55]. Assuming that ^{99m}Tc and $^{185/187}Re$ are comparable radioisotopes and consequently, give similar GRP receptor affinity to the radioligands, the authors performed *in vivo* experiments in mice with the all four ligands labeled with ^{99m}Tc, concluding that the Bn1.1 derivative seems to be the more promising compound (see the ^{99m}Tc paragraph)[55].

IV. Review of human radiolabeled studies of Bn receptor-mediated imaging/ cytotoxicity studies (Table 11)

IV. A. Human studies using radiolabeled bombesin analog (Table 11)

12 studies has been published (Table 11) where different radiolabeled bombesin analogues were tested in human healthy volunteers or patients suspected or confirmed to have breast, prostate, gastrointestinal or lung cancer, the radiolabeled Bn analogs were examined for diagnostic purposes, alone or comparing with another radiolabeled compound used in nuclear medicine. In 83% of studies ^{99m}Tc was used and in 17% ^{68}Ga was the isotope selected to be coupled to the Bn analog. The most frequent Bn analog used was [Cys^0-Aca^1]Bn(2–14) also called [Leu^{13}]Bn (Table 2) (50% of cases), which is a Bn receptor agonist.

IV. B. Human ^{99m}Tc bombesin analog studies

In 2002 Scopinaro *et al*. [122], tested for the first time ^{99m}Tc-[Leu^{13}]Bn [Study #4, Table 11] in 5 patients suspected to have breast cancer, and after 2 days the same patients were injected with ^{99m}Tc-Sestamibi, a routinely used radiotracer for the detection of breast cancer, in order to compare the results with that obtained with radiolabeled [Leu^{13}]Bn. They observed by planar scintigraphy that ^{99m}Tc-Sestamibi detected 4 of the lesions, while ^{99m}Tc-[Leu^{13}]Bn showed 5 lesions (100%) and all the lymph node affected. No side effects were observed. Apart from the tumor, the radiolabeled bombesin agonist was also taken up by the thyroid gland, liver and kidneys. In both cases, with sestamibi and [Leu^{13}]Bn, there was no uptake by a fibroadenoma lesion.

The same group [123] studied 3 healthy subjects and 2 patients, 1 with prostate cancer and 1 with small cell lung cancer (SCLC), injected with ^{99m}Tc-[^{13}Leu]Bn, and images were obtained by SPECT and planar scintigraphy [Study #1, Table 11]. The patient with SCLC was also studied with ^{99m}Tc-Sestamibi. Side-effects after the injection of the radiolabeled Bn analog were not observed. ^{99m}Tc-[Leu^{13}]Bn imagined both prostate cancer and SCLC. Prostate cancer was visualized as soon as 1 and 2 min after injection and then was progressively masked by radioactivity accumulating in the bladder. The patient with SCLC after injection with ^{99m}Tc-[Leu^{13}]Bn four uptake zones were detected by SPECT and 3 by planar scan, while after ^{99m}Tc-Sestamibi 3 and 2 hot zones were detected, respectively. ^{99m}Tc-[Leu^{13}]Bn imagined SCLC from minute 1 to 3 hours. ^{99m}Tc-[Leu^{13}]Bn was also taken up by liver and kidneys, faintly by the thyroid gland, and appeared into duodenum and jejunum at 3 h p.i.

In 2003 ^{99m}Tc-[^{13}Leu]Bn was used for biopsy site localization driven by the use of an imaging probe combined with X-ray in 5 patients, suspicious for breast cancer [124][Study #2, Table 11]. Patients were injected with ^{99m}Tc-[Leu^{13}]Bn and the biopsy samples obtained were measured for radioactivity. 48 samples were obtained, 19 of them with high ^{99m}Tc-[Leu^{13}]Bn, 21 with intermediate and 8 with low uptake. Histochemical studies performed in these samples showed that cancer was found in all the samples with high ^{99m}Tc-[^{13}Leu]Bn uptake and 19/21 with intermediate and 2/8 with low uptake.

In 2004, De Vincentis *et al.* [125] studied 14 patients with a prostatic lesion by performing trans-rectal ultrasonography-guided biopsy, CT, MRI and as well as ^{99m}Tc-[Leu^{13}]Bn scintigraphy [Study #3, Table 11]. The radiolabeled bombesin analog detected all the cancer cases (12/14 cases, confirmed by histopathology), and also the lymph nodes involved (4 cases, confirmed by histopathology study after operation), while CT and MRI only were positive in 3/4 cases. Studies in 5 patients with ^{111}In-Octreoscan detected only 2/3 cases of cancer and no lymph node involvement.

Scopinaro *et al.* [126][Study #5, Table 11] used the same approach as the previous study to assess whether or not ^{99m}Tc-[Leu^{13}]Bn scan was able to detect not only prostate cancer but also invasion of pelvic lymph nodes, in 10 patients suspected to have prostate cancer. They observed that ^{99m}Tc-[Leu^{13}]Bn visualized 100% of the cancers (8/10 patients) and lymph node invasion (3/10). No positive uptake was seen in the 2 cases of adenoma, with results confirmed by pathology evaluation. With MRI no lymph node invasion was found.

In a later study Scopinaro *et al.* [127] [Study #6, Table 11] used ^{99m}Tc-[Leu^{13}]Bn to test whether or not this radiolabeled Bn analog can detect colon cancer, as it is known this type of cancer, as well as breast and prostate cancer, can over-express bombesin receptors. For that, 13 patients, 7 of them known to have colon cancer, were subjected to SPECT and planar scintigraphy with ^{99m}Tc-[Leu^{13}]Bn. Images were taken before 1 h p.i., before discharge of radioactivity from the liver to the duodenum. Cancer was detected in 11/11

patients; it showed 2 false positives (1 Crohn's disease and 1 with polyp showing mild dysplasia). ^{99m}Tc-[Leu^{13}]Bn detected invasion of lymph nodes in 5 patients (100% of the cases).

Another Bn analog (N_3S-5Ava-Bn(7–14) also know as RP527, Table 1) coupled to ^{99m}Tc has been used 3 in human studies. In the first study, from 2000 (Van de Miele *et al.* [58] [Study #8, Table 11]), 10 patients with prostate (4 patients with bone metastasis with androgen resistant prostate cancer) or suspected of breast cancer (6 patients) were subjected to planar scintigraphy after injection of ^{99m}Tc-RP527. None of the patients had an adverse reaction. After injection of the radiolabeled Bn analog renal and hepatic clearance and pancreatic uptake, but not blood accumulation was observed. Positive imaging of the bone metastasis in a patient with androgen resistant prostate cancer with ^{99m}Tc-RP527 was obtained (1/4 patients) and in this case just half of the lesions were visualized. However, in 4/5 patients ^{99m}Tc-RP527 showed positive uptake by breast cancer and all lymph nodes involved. In the breast cancer patient with bone metastasis there was no clear ^{99m}Tc-RP527 uptake by the primary tumor, lymph nodes involved or the metastasis.

The same group published a second study [128] [Study #9, Table 11] with the radiolabeled Bn analog ^{99m}Tc-RP527, but in this case just healthy subjects were included in order to study the biodistribution and dosimetry of the radiotracer by planar scintigraphy images from 30 min to 24h p.i., and to assess blood and urine samples. They found low accumulation of ^{99m}Tc-RP527 in brain, lung, myocardium, breast and testis, with hepatobiliary and renal clearance and extensive bowel uptake. The authors concluded that the biodistribution characteristics of ^{99m}Tc-RP527 made it suitable for the tumor detection in the suprabdominal region, but imaging of the abdominal region more problematic, due to the intestinal accumulation.

In 2008 Van de Wiele *et al.* [4] published another human study [Study #10, Table 11] using ^{99m}Tc-RP527. 9 patients with suspected breast cancer and 5 with tamoxifen-resistant bone-metastasized breast carcinoma underwent ^{99m}Tc-RP527 scintigraphy. The results showed that in 8/9 patients the radiolabeled Bn analog visualized the tumor, lymph node involved and part of the bone metastasis when present (1 patient). However, ^{99m}Tc-RP527 did not visualize any of the bone metastasis in the 5 tamoxifen-resistant bone-metastasized breast carcinoma patients. In no case was any adverse reaction to ^{99m}Tc-RP527 seen.

Another ^{99m}Tc-Bn analog has been studied [129] [Study #7] in humans, [Lys^3]Bn (Table 2) coupled to the isotope by the linker EDDA/HYNIC (Table 1, Fig, 1). It was injected in 11 patients (3 with proven and 8 suspected to have breast cancer) and SPECT and planar scintigraphy images were taken from 20 min to 24 h p.i.. After injection none of the patients suffered from side-effects. ^{99m}Tc-EDDA/HYNIC-[Lys^3]Bn had a rapid blood clearance and was mainly renal excretion. The images obtained showed that patients with cancer presented asymmetrical uptake by the breast tissue and higher accumulation in the breasts with malignant tumors.

IV. C. Human ^{68}Ga bombesin analog studies

The Bn analog BZH3 ([DTyr^6, βAla^{11}, Thi^{13}, Nle^{14}]Bn(6–14), Tables 1,2) coupled to the ^{68}Ga isotope through the linker DOTA-PEG_2 has been tested in 2 studies with cancer patients [130,131]. One study involved 17 patients with gastrointestinal stromal tumors (GIST) [Study #11, Table 11] and the other [Study #12, Table 11] involved 9 patients with low grade gliomas. In both cases patients underwent PET scans with ^{68}Ga-BZH3 and the radiotracer ^{18}F-FDG and results were compared. In the study with the GIST patients [130] ^{68}Ga-BZH3 localized 8/30 lesion (positive tumor uptake in 7/17 patients) while ^{18}F-FDG was positive in 25/30 lesion (14/17 patients). In one case the radiolabeled Bn analog

was able to detect one tumor in the stomach not detected by ^{18}F-FDG. In the study performed in low grade gliomas [131], in all cases (9/9) the combination of both radiotracer, ^{68}Ga-BZH3 and ^{18}F-FDG, was able to detect the tumors.

V. Nonradioactive Bn cytotoxic analogs (Table 12)

Many cancer patients are treated with cytotoxic chemotherapeutic drugs. For example, each year over 170,000 patients in the United States are diagnosed with lung cancer but unfortunately 160,000 lung cancer patients die from this disease annually [132]. Small cell lung cancer (SCLC), which kills approximately 25,000 patients, is treated with chemotherapy and/or radiation therapy, but relapse frequently occurs and the median survival time is less than 1 year. Non-SCLC (NSCLC), which kills approximately 135,000 patients, is treated with combination chemotherapy but the 5-year survival rate is only approximately 15%. Cancer cells take up chemotherapeutic drugs; however, they are internalized by rapidly growing normal cells such as white blood cells causing toxic side effects. Chemotherapy effectiveness in cancer patients is limited by toxicity to normal cells and multidrug resistance [4]. It is possible to target drugs to cancer cells using cell surface peptide receptors. Bombesin (Bn)-like peptides and receptors are present in many cancer cells including lung cancer and Bn stimulates their growth [11,19,21,133,134]. Thus attempts have been made to develop cytotoxic Bn-conjugates, which will kill cancer cells, but not normal cells.

Camptothecin is a topoisomerase I inhibitor binding directly to the topoisomerase I-DNA complex, resulting in DNA damage and apoptosis. Two camptothecin analogs (topotecan and irinotecan) are used for ovarian, cervical, SCLC and colon cancer treatment. Apart from its anticancer properties, camptothecin has low aqueous solubility. BA0, (DTyr^{6}, β-Ala^{11}, Phe^{13}, Nle^{14})Bn-(6–14) (Table 2), is a universal agonist, which binds with high affinity to BRS-3 as well as NMB and GRP receptors [30,34,40,135]. In 2007, in order to improve camptothecan's solubility Shun *et al.* [136] coupled camptothecin to the Bn agonist analog, [DSer^{5}, DTyr^{6}, βAla^{11}, Phe^{13}, NLe^{14}]Bn(5–14) (BA3) [Analog #2, Table 12] using various built in nucleophile-assisted releasing (BINAR) linkers (L1-L3)): analogs of N-(N-methyl-amino-ethyl)-glycine carbamate. The carbamate linkage in CPT-L2-BA3 is metabolized by P450 enzymes, which are enriched in cancer cells, resulting in L2-BA3 and CPT [137]. CPT diffuses into the nucleus where it can inhibit cancer cell replication [30]. In particular, CPT inhibits topoisomerase I, which unwinds DNA prior to replication. *In vitro* cytotoxicity studies [136] in different cell lines were performed and results showed that the conjugated Bn analog had a tumoricidal IC_{50} in the μM range with values 10-fold higher than camptothecin alone [Analog #2, Table 12]. The CPT-Bn analog in PC-3 cells inhibited adhesion to collagen type I, $\alpha_V\beta_3$ and $\alpha_V\beta_5$, at 10–20 μM, also in HUVECs inhibited capillary-like tube formation and *in vivo* angiogenesis, at 10–20 μM and 40 μM, respectively [Analog #2, Table 12].

The synthetic analog of Bn, (DSer^{5}, DTyr^{6}, β-Ala^{11}, Phe^{13}, Nle^{14})Bn-(5–14) (BA3) coupled at the N-terminal to camptothecin (CPT), was studied in more detail for its ability to interact with Bn receptors in other studies [30,34,138]. Results in study #1 (Table 12) [30] demonstrate CPT-L2-BA3 can inhibit specific binding of ^{125}I-BA0 to Balb/c 3T3 cells transfected with GRP receptors, NMB receptors or BRS-3 (IC_{50} = 0.012, 0.035 and 0.031 nM, respectively) [Analog #1, Table 12]. Because BA0 had IC_{50} values of 0.32, 0.74 and 0.25 nM for GRP receptors, NMB receptors or BRS-3 respectively, CPT-L2-BA3 bound with approximately 1-order of magnitude greater affinity than did BA0 [Analog #1, Table 12]. This may result because CPT interacts with additional hydrophobic amino acids present in Bn receptors in addition to the essential Bn receptor amino acids, which interact with Bn agonists. For GRP receptors Gln^{122}, Phe^{185}, Ala^{198}, Pro^{199}, Arg^{288} and Ala^{308} are important for residues for binding GRP with selectivity and with high affinity [8,139,140].

CPT-L2-BA3 was internalized at 37°C but not 4°C [Analog #1, Table 12]. [30]. Using Balb-3T3 cells transfected stably with the GRP receptor, NMB receptor or BRS-3 33% of the ^{125}I-CPT-L2-BA3 added to the cells was internalized after 10 min at 37°C [30] [Analog #1, Table 12]. As a control, CPT-L2-(DSer^{5}, ^{125}I-DTyr^{6}, β-Ala^{11}, DPhe^{13}, Nle^{14})Bn-(5–14) was not internalized. CPT-L2-(DSer^{5}, DTyr^{6}, β-Ala^{11}, Phe^{13}, Nle^{14})Bn-(5–14) functioned as a weak Bn receptor agonist which bound with over 2-orders of magnitude lower affinity to GRP receptors than did CPT-L2-BA3 [Analog #1, Table 12]. [30].

CPT-L2-BA3 is a potent Bn receptor agonist [30,34] [Analog #1, Table 12]. CPT-L2-BA3 increased phosphatidylinositol turnover and the ED_{50} for GRP receptors, NMB receptors and BRS-3 was 1, 1 and 11 nM respectively [Analog #1, Table 12] [30]. CPT-L2-BA3 inhibited the growth of lung cancer cells *in vitro* using the MTT assay as well as the clonogenic assay (IC_{50} = 70 nM) [30]. CPT-L2-BA3 (0.8 mg/kg, subcutaneous injection) slowed the growth of NCI-H1299 xenografts in nude mice *in vivo* by 38%[30][Analog #1, Table 12]. In addition, CPT-L2-BA3 inhibited the growth of CFPAC-1 (pancreatic cancer) and PC-3 cells (prostate cancer) *in vitro* and *in vivo* [30] [Analog #1, Table 12). Nanomolar concentrations of CPT-L2-BA3 were present in the plasma of nude mice treated with CPT-L2-BA3 and the half-life of CPT-L2-BA3 was approximately 20 min. in the mouse plasma [30] [Analog #1, Table 12]. In a separate study the mechanism of action CPT-L2-BA3 was investigated by comparing its behavior to a chemically identical compound, but with very low affinity for Bn receptors and which failed to activate Bn receptors (DPhe^{13}-CPT-2-BA3)[34]. This study demonstrated that the inactive analog was not internalized and in both the MTT assay and clonogenic assays on NCI-1299 cells, which possess Bn receptors, the active analog was more potent than the inactive analog [34]. Furthermore, *in vivo* studies of the growth of H1229 xenografts in nude mice demonstrated that the active compound CPT-L2-BA3 was more potent than the inactive compound, at inhibiting tumor growth [34]. These results provide strong evidence that the cytotoxicity of CPT-L2-BA3 is mediated by interaction with Bn receptors on the tumor. A goal is to develop a high affinity Bn conjugate that has a prolonged half-life *in vivo*. It remains to be determined if CPT-L2-BA3 will benefit patients with lung cancer.

A chemotherapeutic doxorubicin (DOX) analog was conjugated to GRP receptor antagonist RC-3095 (Table 3) using an ester linkage [141,142] [Analog #5, Table 12]. Specifically, the cytotoxic Bn conjugate, AN-215 was prepared by coupling the NH_2 terminus of des-DTpi-RC-3095 through a glutaric spacer to the 14-OH group of 2-pyrrolino-DOX (AN201) giving the structure: 2-pyrrolino-DOX-14-O-gl- [Leu^{13}ψ-Leu^{14}]Bn (7–14) [141,142]. The resulting AN-215 bound with high affinity to Swiss 3T3 cells containing BB_2 receptors (IC_{50} = 1.6 nM) whereas RC3095 alone had an IC_{50} value of 1.6 nM for the GRP receptor [14,141]. AN-215 inhibited the growth of CFPAC-1 pancreatic cancer, DMS-53 SCLC, PC-3 prostate cancer and MKN-45 gastric cancer cell lines with IC_{50} values of 0.3, 0.04, 0.7 and 0.2 nM respectively [141]. AN-215 also inhibited growth of H-69 small cell lung cancer cells, U-87-MG glioblastoma tumors, as well as NCI-N87 and HS-746 gastric cancers [Analog #5, Table 12] [141]. AN215 inhibited the growth of PC-3 tumors in nude mice whereas the DOX analogue (AN201) had little effect on tumor growth, but was toxic [142,143]. A key question is if AN-215, which is a Bn receptor antagonist, is internalized by cancer cells. Also, it remains to be determined if AN-215 is rapidly degraded by blood esterases.

The mitotic inhibitor paclitaxel (Taxol) is widely used in the treatment of breast, ovarian, lung and head and neck cancer, and also in advanced forms of Kaposi's sarcoma, but it has limited aqueous solubility and it is not targeted to any particular tissue. In order to improve solubility and efficiency in the drug delivery, Safavy *et al*. [144] coupled the Bn analog Bn(7–13)-NH_2[Analog #3, Table 12] (Table 2) directly to paclitaxel using PEG as linker, and studied the binding properties of the molecule and its cytotoxic activity. They found that

the conjugated Bn analog was soluble in water at a concentration of 250 mg/mL, in GRP receptor bearing BNR-11 cells it inhibited ^{125}I-[Tyr^4]Bn-binding to the same extent as Bn(7–13)NH_2, and it had $t_{1/2}$ of 154 min and 113 in PBS (phosphate buffered saline) and human plasma, respectively. When cytotoxic activity of the conjugated Bn analog was studied in NCI-H1299 cells, an increase in the cytotoxicity was found, with tumoricidal IC_{50} values after 24 h incubation of 14±1.1 nM *vs* 35±1.8 nM with paclitaxel alone.

In 2006, the same group published a study [145] using the same Bn analog (7–13)-NH_2 [Analog #4, Table 12], but as dipeptide, coupled to paclitaxel through PEG or Glu, and studied their cytotoxic activity in different cell lines. They found that the highest cytotoxic effect was obtained with paclitaxel-Glu-(Bn(6–14)$_2$) achieving 64–93% of growth inhibition.

The Bn receptor antagonists RC-3095 (Table 2) or RC-3940, (Hca^6, Leu^{13}, ψTac^{14})Bn(6–14) inhibited the growth of non-small cell lung cancer (NSCLC) cell lines NCI-H460 and A549 in orthotopically xenografted mice [146]. This resulted in a reduction of K-ras, COX-2 and pAkt in the tumors. Similarly, RC-3940 inhibited the growth of PC-3 and DU-145 prostate cancer tumors in nude mice [147]. This treatment resulted in a reduction in VEGF, bFGF, EGFR and HER2. In NSCLC, Bn and NMB were found to increase transactivation of the EGFR, which is inhibited by the tyrosine kinase inhibitor gefitinib. The Bn receptor antagonists PD176252 and PD168368 potentiate the growth inhibitory effects of gefitinib on cancer cells [148,149]. These results suggest that many of the effects of Bn may be mediated by the EGFR. The marine toxins hemiasterlin (Hem) and dolastatin (Dol) were coupled to a universal Bn agonist using an amide linkage [33]. The resulting Hem-LA-BA1 inhibited specific binding to NCI-H1299 lung cancer with an IC_{50} value of 15 nM [Analog #6, Table 12]. Hem-LA-BA1 was an agonist, which elevated cytosolic Ca^{2+} after addition to lung cancer cells. Hem-LA-BA1, but not BA1 inhibited the proliferation of NCI-H1299 cells *in vitro* [33]. The results indicate that marine toxin Bn conjugates kill cancer cells enriched in GRP receptors *in vitro* [33]. It remains to be determined if Hem-LA-BA1 inhibits lung cancer growth *in vivo*.

A diphtheria toxin-GRP fusion protein was cytotoxic and inhibited protein synthesis in cancer cells [150] [Analog #8, Table 12]. The catalytic and transmembrane domains of diphtheria toxin (DAB) were fused to GRP using molecular biology techniques. DAB_{389}GRP inhibited protein synthesis (IC_{50} = 0.02 nM) [150]. The cytotoxicity of DAB_{389}GRP resulted from receptor-mediated endocytosis through acidic vesicles and was blocked by 10 uM chloroquine [150] [Analog #8, Table 12]. DAB_{389}GRP inhibited the proliferation of SCLC cell line NCI-H345 which possess GRP receptors, with an IC_{50} of 1 nM, whereas the IC_{50} was 100 nM for NIH/3T3 cells, which lack GRP receptors [150]. It remains to be determined if DAB_{389}GRP inhibits the growth of SCLC tumors *in vivo* and does not cause toxic side effects in the host.

Mitochondria-disrupting peptides such as KLAKLAKKLAKLAK (KLA), GRFKRFRKKRKKLFKKLS (B27) and GGLRSLGRKILRAWKKYG (B28) were coupled to the N-terminal of Bn (2–14) [151] [Analog #7, Table 12] (Table 2). The resulting KB, BB27 and BB28 were evaluated [151]. BB28 half maximally inhibited the death of MCF-7 and CEM cells at 4 and 6 μM, respectively. Treated CEM cells had increased numbers of apoptotic and necrotic cells, loss of mitochondrial membrane potential and release of cytochrome C [151] [Analog #7, Table 12]. The effects of BB28 on CEM cells were inhibited by z-VAD-Fmk, a pan-caspase inhibitor. Intratumoral or intraperitoneal injection of BB28 (10 mg/kg) significantly slowed the growth of K562 tumors in nude mice [151]. Unfortunately relatively high doses of BB28 were used and it remains to be determined if lower doses are effective [151].

Another approach is to couple Bn antagonists to agents, which activate polyclonal T lymphocytes [152][Analog #9, Table 12]. Monoclonal antibody to OKT3 (anti-CD3) was coupled to [Cys^5, $DPhe^6$, Bn(5–13)ethyl amide](EA)[151]. EA binds with high affinity (IC_{50} = 1.7 nM) to Balb/3T3 cells containing GRP receptors and similar to other Bn des Met^{14} ethyl amide analogs functions as a Bn receptor antagonist [14,37,38,152]. The resulting bispecific molecule caused apoptosis and necrosis of NCI-H345 and DMS273 cells [152]. The bispecific molecule killed SCLC cells *in vivo* by activating allogeneic T cells through the CD2/TCR complex utilizing Il-2 [152] [Analog #9, Table 12]. The results suggest that bispecific molecules may stimulate the immune response against SCLC tumors.

In 1995 Chen *et al.* published a paper [153,154] using Bn analog ([Lys^3]Bn, (Table 2) [Analog #10, Table 12] coupled to an antibody anti-FcγRI as an immunotherapeutic approach to the treatment of SCLC. This bispecific immunoconjugate should bind by one side to the GRP receptor expressed in SCLC cells and by the other to the FcγRI expressed in cells such as activated monocytes or neutrophils and produce lysis of the cancer cells. In fact, the authors found [154] that binding to the SCLC cells was proportional to the immunoconjugate concentration and to the number of GRP receptors on the cell surface, and it also bound to monocytes and neutrophils. When the monocytes/neutrophils were previously activated and then coincubated with the SCLC and in the presence of the immunoconjugate, an increase in the lysis of the cancer cells was observed. In another study from the same group [155] they examined the effect of a different immunoconjugate composed of a Bn antagonist ([$DTrp^6$, Leu^{13}-ψ(CH_2NH)Phe^{14}]Bn(6–14), [Analog #11, Table 12] or agonist ([Lys^3]Bn, (Table 2) [Analog #9 Table 12] coupled to an antibody, anti-FcγRI or- FcγRIII, and the results showed that both immunoconjugates bound to SCLC cells in a dose-related manner, and none of them produced an alteration in the clonogenic growth of the cells. When the SCLC cells were coincubated in the presence of either immunoconjugate with activated monocytes or natural killer cells, a clear increase in cytotoxicity of SCLC was observed.

Another approach to attempt to decrease growth of tumor cells expressing GRP receptors was the synthesis of a 40 residue precursor peptide by linking together 4 designed anticancer peptide analogs including a VIP binding receptor inhibitor, a somatostatin agonist, a substance P receptor antagonist and a Bn receptor antagonist ([$DPhe^6$, Aib^{11}, $desMet^{14}$]Bn(6–14), [Analog #20, Table 12] through enzyme cleavable Lys-Lys linkers [156,157]. Treatment with this precursor peptide produced the release of each individual peptide analog by the action of enzymes such as PC1 or PC2, so each neuropeptide analog will bind its receptor and inhibit tumor growth. In fact, it was found that incubation of the precursor peptide with trypsin produced the release of all the individual peptides. Also treatment with this precursor peptide inhibited cell proliferation in all cancer cell lines tested. When Balb C nude mice xenografted with primary colon tumor cells were treated with the peptide precursor [Analog #20, Table 12], inhibition in tumor growth of 73.7% *vs* no treated animals was found. When the molecular pathway used to inhibit cellular proliferation in tumors by the precursor peptide was studied [157] in different cancer cell lines, the results showed that the precursor peptide down-regulated cAMP, EGF-dependent cell proliferation and the phosphorylation pERK1/2 in GI carcinomas. It also produced an activation of the apoptotic caspase-3 dependent pathway and induced the p53 tumor suppressor protein. In endothelial cells it inhibited the formation of capillary-like tubes and reduced VEGF levels.

Bn analog 8-Aoc-Bn(7–14) [Analog #21, Table 12] has been studied coupled to the photosensitizer Mono-carbohexyl-tetrasulfonated aluminium phthalocyanine in order to improve the site-delivery of the drug in prostate cancer [155]. Binding studies revealed that conjugated Bn analog [Analog #21, Table 12] had lower affinity than Bn analog alone in

PC-3 cells (IC_{50}: 29.4 nM *vs* 0.37 nM, respectively), but when photodynamic efficacy was tested in PC-3 cells *in vitro*, it was improved by a 2.5-fold compared to the Mono-carbohexyl- tetrasulfonated aluminium phthalocyanine alone.

Bn analogs have been also used to improve gene delivery into the cells by siRNA or adenovirus. In the first case [158], the Bn agonist analog Bn(7–14) [Analog #22, Table 12] (Table 2) was coupled to maleimide-PEG and combined with EHCO nanoparticles containing siRNA; the inclusion of the Bn conjugated to the nanoparticle produced a gene silencing efficiency of 91.9% and cell uptake of 73.9%, which was significantly higher than with EHCO nanoparticles without the Bn analog. In order to increase adenovirus-mediated gene delivery Hong *et al.* [158] conjugated a human GRP analog (13–27) [Analog #22, Table 12] to the N or C terminal of MH20 (an icosapeptide that mimics a portion of the α2 domain of human MHC class I molecules which are receptors for the entrance of the adenovirus in the cell). With this approach it was proposed that the conjugated GRP analog [Analog #22, Table 12] would bind the GRP receptor with the MH20 free to bind the adenovirus which will increase the number of adenovirus receptors in the cell and enhance virus entrance and gene delivery. In fact, while the GRP analog bound to the C side of the MH20 had no effect on adenovirus infection and gene transfer, the GRP-N′-MH20 showed a significant enhancement (8–15-fold) in adenovirus-mediated gene transfer in all cell lines tested when cells were pretreatment with the GRP conjugate [Analog #22, Table 12] at 25 μM. The increase in entry was proportional to the amount GRP receptor in the cell membrane.

Eleven different classes of Bn receptor antagonists have been developed [8,14,37–39] and members of some classes have been shown to be cytostatic for lung cancer cells. Peptide receptor antagonists for GRP receptors were developed by eliminating the C-terminal methionine or reducing the penultimate peptide bond before the C-terminal methionine [8,14,37–39,159]. BW2258U89 and RC-3095 (Table 2) are two such Bn antagonists which bind with high affinity (IC_{50} = 0.2 nM and 1.4 nM respectively) to GRP receptors [160]. BW2258U89, 1 uM, inhibited the growth of lung cancer cells. In nude mice bearing NCI-H1299 xenografts, tumor growth was slowed significantly if BW2258U89 was administered subcutaneously (0.8 mg/kg) [160]. The tumors rapidly regrew, however, if BW2258U89 administration was discontinued [160]. For NMB receptors, nonpeptide antagonists have been developed such as PD168368 and PD176252 (Table 2) [14,161]. PD168368 and PD176252 bind with high affinity (IC_{50} = 0.51 and 0.53 nM respectively) to Balb/3T3 cells transfected with NMB receptors [14]. PD168368 is slowly metabolized by proteolytic enzymes and hence can be administered orally. Gavage administration of PD168368 (0.8 mg/kg) inhibited the growth of tumors in nude mice [162]. PD168368 has limited solubility in water and permeates the brain after crossing the blood-brain barrier. In contrast, BW2258U89 is water-soluble and does not readily cross the blood-brain barrier.

In another study [163] using the Bn antagonists [$DPhe^6$, Aib^{11}, $desMet^{14}$]Bn(6–14) and [$DPhe^6$, $desMet^{14}$]Bn(6–14) analogs [Analogs #13–19, Table 12] (Table 2), the anti-proliferative properties of these peptides were tested in different cancer cell lines [163]. *In vitro* MTT results showed that all Bn antagonists had cytotoxic effects in these cancer cells, specifically the highest values in cell proliferation inhibition were found with [$DPhe^6$, Aib^{11}, Ile^{13}, $desMet^{14}$]Bn(6–14) at 0.1 nM in MiaPaCa-2 cell line, [$DPhe^6$, Aib^9, Aib^{11}, Ile^{13}, $desMet^{14}$]Bn(6–14) at 0.1 nM in SW620, [$DPhe^6$, Aib^9, Ile^{13}, $desMet^{14}$]Bn(6–14) at 1 μM in HT29 cells and Butanoyl[$DPhe^6$, Aib^{11}, $desMet^{14}$]Bn(6–14) at 0.01 nM in PTC[Analogs #13–19, Table 12]. Butanoyl[$DPhe^6$, Aib^{11}, $desMet^{14}$]Bn(6–14) [Analog #19, Table 12] was chosen to treat PTC cell tumor xenograft mice as the butanoyl moiety may protect the N′ terminal end of the molecule and improve its *in vivo* stability and biodistribution. After 29 days of treatment, tumor growth was inhibited by 44.3% in the treated animals.

VI. Conclusions

The discovery of the frequent over-expression and/or ectopic expression of various peptide/neurotransmitter receptors on many neoplasms have opened the potential for a new approach to both imaging these tumors and for targeted delivery of cytotoxic agents. The results using radiolabeled somatostatin analogs to target somatostatin receptors (sst1–5) which are over-expressed/ectopically expressed in various neuroendocrine tumors (primarily carcinoids, pancreatic endocrine tumors) [1,22,23] have clearly established the clinical usefulness of somatostatin receptor-mediated imaging and cytotoxicity for treatment of these malignancies. Unfortunately, many of the common neoplasms (lung, gastric, pancreatic, breast, prostate, CNS tumors, etc) for which limited treatments exist for advanced disease, do not over-express/ectopically express somatostatin receptors, however they frequently over-express other G protein-coupled receptors, particularly those of the Bn family of receptors (GRPR, NMBR, BRS-3) [11,19,20].

Unfortunately, at present except for the use of radiolabeled somatostatin analogs in patients with neuroendocrine tumors, the approach of using the tumor receptor over-expression/ectopic expression for receptor-mediated imaging or cytotoxicity with any of the other peptide receptors, including Bn receptors, has not yet been demonstrated to be clinically useful. The studies reviewed here have identified a number of radiolabeled Bn analogs that could be used for standard nuclear medicine imaging (^{99m}Tc-, ^{111}In-, $^{185/7}$Rh-labeled analogs, ^{125}I), for PET imaging (^{18}F, ^{68}Ga, ^{64}Cu) or for radiation-mediated cytotoxicity (^{90}Y, ^{111}In, ^{64}Cu, ^{177}Lu, ^{125}I). Both *in vitro* and *in vivo* studies in animals show a number of these radiolabeled Bn analogs have many properties that should allow them to be useful for studies in patients with these neoplasms. These results including identifying a number of radiolabeled analogs with high Bn receptor affinity, particularly for the GRP receptor, which is most frequently over-expressed in these tumors; that show stability in plasma or *in vivo* and that function as Bn receptor agonists and are rapidly internalized by the tumors. Furthermore, in *in vivo* studies, a number of these radiolabeled Bn analogs imaged tumors, were internalized and the radiolabeled ligand was retained in the tumor, properties that are thought necessary for effective receptor-mediated cytotoxicity. Although the clinically relevant studies in patients with neuroendocrine tumors using radiolabeled somatostatin analogs have all used radiolabeled agonists, recent studies show that radiolabeled antagonists of the somatostatin receptor give even better imaging results even though they are not internalized [44]. Whether they will also be more effective for radiation-induced cytotoxicity in patients with neuroendocrine tumors is not established at present. Similarly, a number of radiolabeled Bn analogs, which function as receptor antagonists, are also reported to give excellent imaging, although they are not internalized [2,45–51].

At present there are only 12 studies of radiolabeled Bn analogs (all agonists) in humans, which in most cases are performed on patients with known Bn receptor containing tumors and are either standard nuclear medicine imaging or PET imaging studies (Table 11). While some of these studies show promising results, they include only small numbers of patients and much more systematic studies involving larger numbers of patients will need to be performed to assess the potential value of this approach. Future studies will need to establish the sensitivity of the radioligands used; their specificity because false positives can have a marked effect on their general utility, and whether their use changes clinical management to justify the full development of Bn receptor-mediated imaging agents. Furthermore, the question of whether a radiolabeled agonist or Bn antagonist is best will need to be resolved. Additional detailed studies will need to be done to evaluate the possible use of radiolabeled Bn analogs for receptor-mediated cytotoxic in human malignancies.

A number of *in vitro* and *in vivo* studies are suggesting various approaches for Bn receptor-mediated cytotoxicity using nonradiolabeled analogues (Table 12). These include coupling of Bn analogs to chemotherapeutic agents (camptothecin, paclitaxel); to novel marine cytotoxic peptides (hemiasterlin, dolistatin); to various cytotoxins (diphtheria toxin); to mitochondria disruptive peptides; to immune activating agents; to agents enhancing sensitivity to the effects of photodynamic therapy; to agents that enhance interfering mRNA delivery or to agents that enhance adenovirus-mediated gene delivery (Table 12). At present there are very limited *in vivo* studies on this approach, and no studies examining their possible clinical efficacy in human diseases. Nevertheless, this approach may lead to agents that allow targeted delivery of cytotoxic agents with much less toxicity, that are either effective alone or in combination with existing treatments and therefore should be more extensively investigated. Because Bn receptors are so frequently over-expressed on various common malignancies, they are an excellent model to use to investigate this novel, therapeutic approach.

Acknowledgments

This work was partially supported by intramural research funds of NIDDK and NIH.

References

1. Breeman WA, Kwekkeboom DJ, de Blois E, de Jong M, Visser TJ, Krenning EP. Radiolabelled regulatory peptides for imaging and therapy. Anticancer Agents Med Chem. 2007; 7:345–357. [PubMed: 17504160]
2. Schroeder RP, Muller C, Reneman S, Melis ML, Breeman WA, de Blois E, Bangma CH, Krenning EP, van Weerden WM, de Jong M. A standardised study to compare prostate cancer targeting efficacy of five radiolabelled bombesin analogues. Eur J Nucl Med Mol Imaging. 2010
3. Tweedle MF. Peptide-targeted diagnostics and radiotherapeutics. Acc Chem Res. 2009; 42:958–968. [PubMed: 19552403]
4. Okarvi SM. Peptide-based radiopharmaceuticals and cytotoxic conjugates: potential tools against cancer. Cancer Treat Rev. 2008; 34:13–26. [PubMed: 17870245]
5. Gonzalez N, Moody TW, Igarashi H, Ito T, Jensen RT. Bombesin-related peptides and their receptors: recent advances in their role in physiology and disease states. Curr Opin Endocrinol Diabetes Obes. 2008; 15:58–64. [PubMed: 18185064]
6. Erspamer V, Erpamer GF, Inselvini M. Some pharmacological actions of alytesin and bombesin. J Pharm Pharmacol. 1970; 22:875–876. [PubMed: 4395815]
7. Erspamer V. Discovery, isolation and characterization of bombesin-like peptides. Ann N Y Acad Sci. 1988; 547:3–9. [PubMed: 3071223]
8. Jensen RT, Battey JF, Spindel ER, Benya RV. International Union of Pharmacology. LVIII. Mammalian Bombesin Receptors: Nomenclature, distribution, pharmacology, signaling and functions in normal and disease states. Pharmacol Rev. 2008; 60:1–42. [PubMed: 18055507]
9. McDonald TJ, Jornvall H, Nilsson G, Vagne M, Ghatei M, Bloom SR, Mutt V. Characterization of a gastrin-releasing peptide from porcine non-antral gastric tissue. Biochem Biophys Res Commun. 1979; 90:227–233. [PubMed: 496973]
10. Minamino N, Kangawa K, Matsuo H. Neuromedin B: a novel bombesin-like peptide identified in porcine spinal cord. Biochem Biophys Res Commun. 1983; 114:541–548. [PubMed: 6882442]
11. Jensen, RT.; Moody, TW. Bombesin-related peptides and neurotensin: effects on cancer growth/proliferation and cellular signaling in cancer. In: Kastin, AJ., editor. Handbook of Biologically active peptides. Vol. 1. Elsevier; Amsterdam: 2006. p. 429-434.
12. Ohki-Hamazaki H. Neuromedin B. Prog Neurobiol. 2000; 62:297–312. [PubMed: 10840151]
13. Jensen RT, Coy DH, Saeed ZA, Heinz-Erian P, Mantey S, Gardner JD. Interaction of bombesin and related peptides with receptors on pancreatic acini. Ann N Y Acad Sci. 1988; 547:138–149. [PubMed: 2467595]

14. Gonzalez N, Mantey SA, Pradhan TK, Sancho V, Moody TW, Coy DH, Jensen RT. Characterization of putative GRP- and NMB-receptor antagonist's interaction with human receptors. Peptides. 2009; 30:1473–1486. [PubMed: 19463875]
15. Weber HC. Regulation and signaling of human bombesin receptors and their biological effects. Curr Opin Endocrinol Diabetes Obes. 2009; 16:66–71. [PubMed: 19115523]
16. Zhou J, Chen J, Mokotoff M, Ball ED. Targeting gastrin-releasing peptide receptors for cancer treatment. Anticancer Drugs. 2004; 15:921–927. [PubMed: 15514561]
17. de Visser M, Verwijnen SM, de Jong M. Update: improvement strategies for peptide receptor scintigraphy and radionuclide therapy. Cancer Biother Radiopharm. 2008; 23:137–157. [PubMed: 18454684]
18. Okarvi SM. Peptide-based radiopharmaceuticals: future tools for diagnostic imaging of cancers and other diseases. Med Res Rev. 2004; 24:357–397. [PubMed: 14994368]
19. Reubi JC, Wenger S, Schumuckli-Maurer J, Schaer JC, Gugger M. Bombesin receptor subtypes in human cancers: detection with the universal radoligand (125)I-[D-TYR(6), beta-ALA(11), PHE(13), NLE(14)] bombesin(6–14). Clin Cancer Res. 2002; 8:1139–1146. [PubMed: 11948125]
20. Reubi JC, Macke HR, Krenning EP. Candidates for peptide receptor radiotherapy today and in the future. J Nucl Med. 2005; 46(Suppl 1):67S–75S. [PubMed: 15653654]
21. Moody TW, Chan D, Fahrenkrug J, Jensen RT. Neuropeptides as autocrine growth factors in cancer cells. Curr Pharm Des. 2003; 9:495–509. [PubMed: 12570813]
22. Forrer F, Valkema R, Kwekkeboom DJ, de Jong M, Krenning EP. Neuroendocrine tumors. Peptide receptor radionuclide therapy. Best Pract Res Clin Endocrinol Metab. 2007; 21:111–129. [PubMed: 17382268]
23. Van Essen M, Krenning EP, Kam BL, de Jong M, Valkema R, Kwekkeboom DJ. Peptide-receptor radionuclide therapy for endocrine tumors. Nat Rev Endocrinol. 2009; 5:382–393. [PubMed: 19488074]
24. Krenning EP, Kwekkeboom DJ, Bakker WH, Breeman WAP, Kooij PPM, Oei HY, van Hagen M, Postema PTE, de Jong M, Reubi JC, Visser TJ, Reijs AEM, Hofland LJ, Koper JW, Lamberts SWJ. Somatostatin receptor scintigraphy with [^{111}In-DTPA-D-Phe^{1}]- and [^{123}I-Tyr^{3}]-octreotide: the Rotterdam experience with more than 1000 patients. Eur J Nucl Med. 1993; 20:716–731. [PubMed: 8404961]
25. Jensen, RT. Peptide therapy. Recent advances in the use of somatostatin and other peptide receptor agonists and antagonists. In: Lewis, JH.; Dubois, A., editors. Current Clinical Topics in Gastrointestinal Pharmacology. Blackwell Science, Inc; Malden, MA: 1997. p. 144-223.
26. Gibril F, Jensen RT. Diagnostic uses of radiolabelled somatostatin-receptor analogues in gastroenteropancreatic endocrine tumors. Dig Liver Dis. 2004; 36:S106–S120. [PubMed: 15077919]
27. Kwekkeboom D, Krenning EP, de Jong M. Peptide receptor imaging and therapy. J Nucl Med. 2000; 41:1704–1713. [PubMed: 11038002]
28. Metz DC, Jensen RT. Gastrointestinal neuroendocrine tumors:; Pancreatic endocrine tumors. Gastroenterology. 2008; 135:1469–1492. [PubMed: 18703061]
29. Gibril F, Reynolds JC, Doppman JL, Chen CC, Venzon DJ, Termanini B, Weber HC, Stewart CA, Jensen RT. Somatostatin receptor scintigraphy: its sensitivity compared with that of other imaging methods in detecting primary and metastatic gastrinomas: a prospective study. Ann Intern Med. 1996; 125:26–34. [PubMed: 8644985]
30. Moody TW, Mantey SA, Pradhan TK, Schumann M, Nakagawa T, Martinez A, Fuselier J, Coy DH, Jensen RT. Development of high affinity camptothecin-bombesin conjugates that have targeted cytotoxicity for bombesin receptor-containing tumor cells. J Biol Chem. 2004; 279:23580–23589. [PubMed: 15016826]
31. Nagy A, Schally AV. Targeting cytotoxic conjugates of somatostatin, luteinizing hormone-releasing hormone and bombesin to cancers expressing their receptors: a "smarter" chemotherapy. Curr Pharm Des. 2005; 11:1167–1180. [PubMed: 15853664]
32. Schally AV. New approaches to the therapy of various tumors based on Peptide analogues. Horm Metab Res. 2008; 40:315–322. [PubMed: 18491250]

33. Moody TW, Pradhan T, Mantey SA, Jensen RT, Dyba M, Moody D, Tarasova NI, Michejda CJ. Bombesin marine toxin conjugates inhibit the growth of lung cancer cells. Life Sci. 2008; 82:855–861. [PubMed: 18336841]
34. Moody TW, Sun LC, Mantey SA, Pradhan T, Mackey LV, Gonzales N, Fuselier JA, Coy DH, Jensen RT. *In vitro* and *in vivo* antitumor effects of cytotoxic camptothecin-bombesin conjugates are mediated by specific interaction with cellular bombesin receptors. J Pharmacol Exp Ther. 2006; 318:1265–1272. [PubMed: 16766720]
35. Preston SR, Miller GV, Primrose JN. Bombesin-like peptides and cancer. Crit Rev Oncol Hematol. 1996; 23:225–238. [PubMed: 8842591]
36. Yegen BC. Bombesin-like peptides: candidates as diagnostic and therapeutic tools. Curr Pharm Des. 2003; 9:1013–1022. [PubMed: 12678868]
37. Jensen RT, Coy DH. Progress in the development of potent bombesin receptor antagonists. Trends Pharmacol Sci. 1991; 12(1):13–19. [PubMed: 1706545]
38. Wang LH, Coy DH, Taylor JE, Jiang NY, Kim SH, Moreau JP, Huang SC, Mantey SA, Frucht H, Jensen RT. Desmethionine alkylamide bombesin analogues: a new class of bombesin receptor antagonists with a potent antisecretory activity in pancreatic acini and antimitotic activity in Swiss 3T3 cells. Biochemistry (Mosc). 1990; 29(3):616–622.
39. Wang LH, Coy DH, Taylor JE, Jiang NY, Moreau JP, Huang SC, Frucht H, Haffar BM, Jensen RT. Des-Met carboxyl-terminally modified analogues of bombesin function as potent bombesin receptor antagonists, partial agonists, or agonists. J Biol Chem. 1990; 265(26):15695–15703. [PubMed: 1697594]
40. Mantey SA, Weber HC, Sainz E, Akeson M, Ryan RR, Pradhan TK, Searles RP, Spindel ER, Battey JF, Coy DH, Jensen RT. Discovery of a high affinity radioligand for the human orphan receptor, bombesin receptor subtype 3: which demonstrates it has a unique pharmacology compared to other mammalian bombesin receptors. J Biol Chem. 1997; 272(41):26062–26071. [PubMed: 9325344]
41. Ryan RR, Weber HC, Hou W, Sainz E, Mantey SA, Battey JF, Coy DH, Jensen RT. Ability of various bombesin receptor agonists and antagonists to alter intracellular signaling of the human orphan receptor BRS-3. J Biol Chem. 1998; 273:13613–13624. [PubMed: 9593699]
42. Ryan RR, Weber HC, Mantey SA, Hou W, Hilburger ME, Pradhan TK, Coy DH, Jensen RT. Pharmacology and intracellular signaling mechanisms of the native human orphan receptor BRS-3 in lung cancer cells. J Pharmacol Exp Ther. 1998; 287:366–380. [PubMed: 9765358]
43. Lin JT, Coy DH, Mantey SA, Jensen RT. Comparison of the peptide structural requirements for high affinity interaction with bombesin receptors. Eur J Pharmacol. 1996; 294:55–69. [PubMed: 8788416]
44. Ginj M, Zhang H, Waser B, Cescato R, Wild D, Wang X, Erchegyi J, Rivier J, Macke HR, Reubi JC. Radiolabeled somatostatin receptor antagonists are preferable to agonists for *in vivo* peptide receptor targeting of tumors. Proc Natl Acad Sci U S A. 2006; 103:16436–16441. [PubMed: 17056720]
45. Cescato R, Maina T, Nock B, Nikolopoulou A, Charalambidis D, Piccand V, Reubi JC. Bombesin receptor antagonists may be preferable to agonists for tumor targeting. J Nucl Med. 2008; 49:318–326. [PubMed: 18199616]
46. Mansi R, Wang X, Forrer F, Kneifel S, Tamma ML, Waser B, Cescato R, Reubi JC, Maecke HR. Evaluation of a 1,4,7,10-tetraazacyclododecane-1,4,7,10-tetraacetic acid-conjugated bombesin-based radioantagonist for the labeling with single-photon emission computed tomography, positron emission tomography, and therapeutic radionuclides. Clin Cancer Res. 2009; 15:5240–5249. [PubMed: 19671861]
47. Abd-Elgaliel WR, Gallazzi F, Garrison JC, Rold TL, Sieckman GL, Figueroa SD, Hoffman TJ, Lever SZ. Design, synthesis, and biological evaluation of an antagonist-bombesin analogue as targeting vector. Bioconjug Chem. 2008; 19:2040–2048. [PubMed: 18808168]
48. Breeman WA, Hofland LJ, de Jong M, Bernard BF, Srinivasan A, Kwekkeboom DJ, Visser TJ, Krenning EP. Evaluation of radiolabelled bombesin analogues for receptor-targeted scintigraphy and radiotherapy. Int J Cancer. 1999; 81:658–665. [PubMed: 10225459]

49. Abiraj K, Mansi R, Tamma ML, Forrer F, Cescato R, Reubi JC, Akyel KG, Maecke HR. Tetraamine-Derived Bifunctional Chelators for Technetium-99m Labelling: Synthesis, Bioconjugation and Evaluation as Targeted SPECT Imaging Probes for GRP-Receptor-Positive Tumours. Chemistry. 2010; 16:2115–2124. [PubMed: 20066690]
50. Maina T, Nock B, Mather S. Targeting prostate cancer with radiolabelled bombesins. Cancer Imaging. 2006; 6:153–157. [PubMed: 17098646]
51. Hohne A, Mu L, Honer M, Schubiger PA, Ametamey SM, Graham K, Stellfeld T, Borkowski S, Berndorff D, Klar U, Voigtmann U, Cyr JE, Friebe M, Dinkelborg L, Srinivasan A. Synthesis, 18F-labeling, and *in vitro* and *in vivo* studies of bombesin peptides modified with silicon-based building blocks. Bioconjug Chem. 2008; 19:1871–1879. [PubMed: 18754574]
52. Baidoo KE, Lin KS, Zhan Y, Finley P, Scheffel U, Wagner HN Jr. Design, synthesis, and initial evaluation of high-affinity technetium bombesin analogues. Bioconjug Chem. 1998; 9:218–225. [PubMed: 9548537]
53. Lin KS, Luu A, Baidoo KE, Hashemzadeh-Gargari H, Chen MK, Brenneman K, Pili R, Pomper M, Carducci MA, Wagner HN Jr. A new high affinity technetium-99m-bombesin analogue with low abdominal accumulation. Bioconjug Chem. 2005; 16:43–50. [PubMed: 15656574]
54. Santos-Cuevas CL, Ferro-Flores G, Arteaga de Murphy C, Ramirez Fde M, Luna-Gutierrez MA, Pedraza-Lopez M, Garcia-Becerra R, Ordaz-Rosado D. Design, preparation, *in vitro* and *in vivo* evaluation of (99m)Tc-N2S2-Tat(49–57)-bombesin: a target-specific hybrid radiopharmaceutical. Int J Pharm. 2009; 375:75–83. [PubMed: 19393305]
55. Gourni E, Paravatou M, Bouziotis P, Zikos C, Fani M, Xanthopoulos S, Archimandritis SC, Livaniou E, Varvarigou AD. Evaluation of a series of new 99mTc-labeled bombesin-like peptides for early cancer detection. Anticancer Res. 2006; 26:435–438. [PubMed: 16475730]
56. Gourni E, Bouziotis P, Benaki D, Loudos G, Xanthopoulos S, Paravatou-Petsotas M, Mavri-Vavagianni M, Pelecanou M, Archimandritis SC, Varvarigou AD. Structural assessment and biological evaluation of two N3S bombesin derivatives. J Med Chem. 2009; 52:4234–4246. [PubMed: 19522464]
57. Smith CJ, Sieckman GL, Owen NK, Hayes DL, Mazuru DG, Kannan R, Volkert WA, Hoffman TJ. Radiochemical investigations of gastrin-releasing peptide receptor-specific [(99m)Tc(X)(CO)3-Dpr-Ser-Ser-Ser-Gln-Trp-Ala-Val-Gly-His-Leu-Met-(NH2)] in PC-3, tumor-bearing, rodent models: syntheses, radiolabeling, and *in vitro*/*in vivo* studies where Dpr = 2,3-diaminopropionic acid and X = H2O or P(CH20H)3. Cancer Res. 2003; 63:4082–4088. [PubMed: 12874010]
58. Van de Wiele C, Dumont F, Vanden Broecke R, Oosterlinck W, Cocquyt V, Serreyn R, Peers S, Thornback J, Slegers G, Dierckx RA. Technetium-99m RP527, a GRP analogue for visualisation of GRP receptor-expressing malignancies: a feasibility study. Eur J Nucl Med. 2000; 27:1694–1699. [PubMed: 11105826]
59. Alves S, Correia JD, Santos I, Veerendra B, Sieckman GL, Hoffman TJ, Rold TL, Figueroa SD, Retzloff L, McCrate J, Prasanphanich A, Smith CJ. Pyrazolyl conjugates of bombesin: a new tridentate ligand framework for the stabilization of fac-[M(CO)3]+ moiety. Nucl Med Biol. 2006; 33:625–634. [PubMed: 16843837]
60. Prasanphanich AF, Lane SR, Figueroa SD, Ma L, Rold TL, Sieckman GL, Hoffman TJ, McCrate JM, Smith CJ. The effects of linking substituents on the *in vivo* behavior of site-directed, peptide-based, diagnostic radiopharmaceuticals. In Vivo. 2007; 21:1–16. [PubMed: 17354608]
61. Kunstler JU, Veerendra B, Figueroa SD, Sieckman GL, Rold TL, Hoffman TJ, Smith CJ, Pietzsch HJ. Organometallic 99mTc(III) '4 + 1' bombesin(7–14) conjugates: synthesis, radiolabeling, and *in vitro*/*in vivo* studies. Bioconjug Chem. 2007; 18:1651–1661. [PubMed: 17663527]
62. Lane SR, Veerendra B, Rold TL, Sieckman GL, Hoffman TJ, Jurisson SS, Smith CJ. 99mTc(CO)3-DTMA bombesin conjugates having high affinity for the GRP receptor. Nucl Med Biol. 2008; 35:263–272. [PubMed: 18355681]
63. Faintuch BL, Teodoro R, Duatti A, Muramoto E, Faintuch S, Smith CJ. Radiolabeled bombesin analogs for prostate cancer diagnosis: preclinical studies. Nucl Med Biol. 2008; 35:401–411. [PubMed: 18482677]
64. Shi J, Jia B, Liu Z, Yang Z, Yu Z, Chen K, Chen X, Liu S, Wang F. 99mTc-labeled bombesin(7–14)NH2 with favorable properties for SPECT imaging of colon cancer. Bioconjug Chem. 2008; 19:1170–1178. [PubMed: 18491928]

65. Retzloff LB, Heinzke L, Figureoa SD, Sublett SV, Ma L, Sieckman GL, Rold TL, Santos I, Hoffman TJ, Smith CJ. Evaluation of [99mTc-(CO)3-X-Y-Bombesin(7–14)NH2] Conjugates for Targeting Gastrin-releasing Peptide Receptors Over-expressed on Breast Carcinoma. Anticancer Res. 2010; 30:19–30. [PubMed: 20150613]

66. Garcia Garayoa E, Ruegg D, Blauenstein P, Zwimpfer M, Khan IU, Maes V, Blanc A, Beck-Sickinger AG, Tourwe DA, Schubiger PA. Chemical and biological characterization of new Re(CO)3/[99mTc](CO)3 bombesin analogues. Nucl Med Biol. 2007; 34:17–28. [PubMed: 17210458]

67. Garcia Garayoa E, Schweinsberg C, Maes V, Brans L, Blauenstein P, Tourwe DA, Schibli R, Schubiger PA. Influence of the molecular charge on the biodistribution of bombesin analogues labeled with the [99mTc(CO)3]-core. Bioconjug Chem. 2008; 19:2409–2416. [PubMed: 18998719]

68. Schweinsberg C, Maes V, Brans L, Blauenstein P, Tourwe DA, Schubiger PA, Schibli R, Garcia Garayoa E. Novel glycated [99mTc(CO)3]-labeled bombesin analogues for improved targeting of gastrin-releasing peptide receptor-positive tumors. Bioconjug Chem. 2008; 19:2432–2439. [PubMed: 19053304]

69. Maes V, Brans L, Schweinsberg C, Garcia-Garayoa E, Blauenstein P, Schubiger PA, Tourwe D. Carbohydrated [99mTc(CO)3](NalphaHis)Ac-bombesin(7–14) analogs. Adv Exp Med Biol. 2009; 611:409–410. [PubMed: 19400243]

70. Nock BA, Nikolopoulou A, Galanis A, Cordopatis P, Waser B, Reubi JC, Maina T. Potent bombesin-like peptides for GRP-receptor targeting of tumors with 99mTc: a preclinical study. J Med Chem. 2005; 48:100–110. [PubMed: 15634004]

71. Durkan K, Lambrecht FY, Unak P. Radiolabeling of bombesin-like peptide with 99mTc: 99mTc-litorin and biodistribution in rats. Bioconjug Chem. 2007; 18:1516–1520. [PubMed: 17760415]

72. Hoffman TJ, Gali H, Smith CJ, Sieckman GL, Hayes DL, Owen NK, Volkert WA. Novel series of 111In-labeled bombesin analogs as potential radiopharmaceuticals for specific targeting of gastrin-releasing peptide receptors expressed on human prostate cancer cells. J Nucl Med. 2003; 44:823–831. [PubMed: 12732685]

73. Garrison JC, Rold TL, Sieckman GL, Naz F, Sublett SV, Figueroa SD, Volkert WA, Hoffman TJ. Evaluation of the pharmacokinetic effects of various linking group using the 111In-DOTA-X-BBN(7–14)NH2 structural paradigm in a prostate cancer model. Bioconjug Chem. 2008; 19:1803–1812. [PubMed: 18712899]

74. Breeman WA, de Jong M, Bernard BF, Kwekkeboom DJ, Srinivasan A, van der Pluijm ME, Hofland LJ, Visser TJ, Krenning EP. Pre-clinical evaluation of [(111)In-DTPA-Pro(1), Tyr(4)]bombesin, a new radioligand for bombesin-receptor scintigraphy. Int J Cancer. 1999; 83:657–663. [PubMed: 10521803]

75. Bernard BF, Krenning E, Breeman WA, Visser TJ, Bakker WH, Srinivasan A, de Jong M. Use of the rat pancreatic CA20948 cell line for the comparison of radiolabelled peptides for receptor-targeted scintigraphy and radionuclide therapy. Nucl Med Commun. 2000; 21:1079–1085. [PubMed: 11192715]

76. Breeman WA, de Jong M, Erion JL, Bugaj JE, Srinivasan A, Bernard BF, Kwekkeboom DJ, Visser TJ, Krenning EP. Preclinical comparison of (111)In-labeled DTPA- or DOTA-bombesin analogs for receptor-targeted scintigraphy and radionuclide therapy. J Nucl Med. 2002; 43:1650–1656. [PubMed: 12468515]

77. de Visser M, Bernard HF, Erion JL, Schmidt MA, Srinivasan A, Waser B, Reubi JC, Krenning EP, de Jong M. Novel (111)In-labelled bombesin analogues for molecular imaging of prostate tumours. Eur J Nucl Med Mol Imaging. 2007; 34:1228–1238. [PubMed: 17287960]

78. de Visser M, van Weerden WM, de Ridder CM, Reneman S, Melis M, Krenning EP, de Jong M. Androgen-dependent expression of the gastrin-releasing peptide receptor in human prostate tumor xenografts. J Nucl Med. 2007; 48:88–93. [PubMed: 17204703]

79. Zhang H, Chen J, Waldherr C, Hinni K, Waser B, Reubi JC, Maecke HR. Synthesis and evaluation of bombesin derivatives on the basis of pan-bombesin peptides labeled with indium-111, lutetium-177, and yttrium-90 for targeting bombesin receptor-expressing tumors. Cancer Res. 2004; 64:6707–6715. [PubMed: 15374988]

80. Ho CL, Chen LC, Lee WC, Chiu SP, Hsu WC, Wu YH, Yeh CH, Stabin MG, Jan ML, Lin WJ, Lee TW, Chang CH. Receptor-binding, biodistribution, dosimetry, and micro-SPECT/CT imaging of 111In-[DTPA(1), Lys(3), Tyr(4)]-bombesin analog in human prostate tumor-bearing mice. Cancer Biother Radiopharm. 2009; 24:435–443. [PubMed: 19694578]
81. Smith CJ, Volkert WA, Hoffman TJ. Radiolabeled peptide conjugates for targeting of the bombesin receptor superfamily subtypes. Nucl Med Biol. 2005; 32:733–740. [PubMed: 16243649]
82. Ananias HJ, de Jong I, Dierck RA, Van de Wiele C, Helfrich W, Elsinga PH. Nuclear imaging of prostate cancer with gastrin-releasing-peptide-receptor targeted radiopharmaceuticals. Curr Pharm Des. 2008; 14:3033–3047. [PubMed: 18991717]
83. Rogers BE, Bigott HM, McCarthy DW, Della Manna D, Kim J, Sharp TL, Welch MJ. MicroPET imaging of a gastrin-releasing peptide receptor-positive tumor in a mouse model of human prostate cancer using a 64Cu-labeled bombesin analogue. Bioconjug Chem. 2003; 14:756–763. [PubMed: 12862428]
84. Rogers BE, Manna DD, Safavy A. *In vitro* and *in vivo* evaluation of a 64Cu-labeled polyethylene glycol-bombesin conjugate. Cancer Biother Radiopharm. 2004; 19:25–34. [PubMed: 15068608]
85. Chen X, Park R, Hou Y, Tohme M, Shahinian AH, Bading JR, Conti PS. microPET and autoradiographic imaging of GRP receptor expression with 64Cu-DOTA-[Lys3]bombesin in human prostate adenocarcinoma xenografts. J Nucl Med. 2004; 45:1390–1397. [PubMed: 15299066]
86. Yang YS, Zhang X, Xiong Z, Chen X. Comparative *in vitro* and *in vivo* evaluation of two 64Cu-labeled bombesin analogs in a mouse model of human prostate adenocarcinoma. Nucl Med Biol. 2006; 33:371–380. [PubMed: 16631086]
87. Biddlecombe GB, Rogers BE, de Visser M, Parry JJ, de Jong M, Erion JL, Lewis JS. Molecular imaging of gastrin-releasing peptide receptor-positive tumors in mice using 64Cu- and 86Y-DOTA-(Pro1, Tyr4)-bombesin(1–14). Bioconjug Chem. 2007; 18:724–730. [PubMed: 17378600]
88. Parry JJ, Andrews R, Rogers BE. MicroPET Imaging of Breast Cancer Using Radiolabeled Bombesin Analogs Targeting the Gastrin-releasing Peptide Receptor. Breast Cancer Res Treat. 2007; 18:110–117.
89. Parry JJ, Kelly TS, Andrews R, Rogers BE. *In vitro* and *in vivo* evaluation of 64Cu-labeled DOTA-linker-bombesin(7–14) analogues containing different amino acid linker moieties. Bioconjug Chem. 2007; 18:1110–1117. [PubMed: 17503761]
90. Garrison JC, Rold TL, Sieckman GL, Figueroa SD, Volkert WA, Jurisson SS, Hoffman TJ. *In vivo* evaluation and small-animal PET/CT of a prostate cancer mouse model using 64Cu bombesin analogs: side-by-side comparison of the CB-TE2A and DOTA chelation systems. J Nucl Med. 2007; 48:1327–1337. [PubMed: 17631556]
91. Prasanphanich AF, Nanda PK, Rold TL, Ma L, Lewis MR, Garrison JC, Hoffman TJ, Sieckman GL, Figueroa SD, Smith CJ. [64Cu-NOTA-8-Aoc-BBN(7–14)NH2] targeting vector for positron-emission tomography imaging of gastrin-releasing peptide receptor-expressing tissues. Proc Natl Acad Sci U S A. 2007; 104:12462–12467. [PubMed: 17626788]
92. Prasanphanich AF, Retzloff L, Lane SR, Nanda PK, Sieckman GL, Rold TL, Ma L, Figueroa SD, Sublett SV, Hoffman TJ, Smith CJ. *In vitro* and *in vivo* analysis of [(64)Cu-NO2A-8-Aoc-BBN(7–14)NH(2)]: a site-directed radiopharmaceutical for positron-emission tomography imaging of T-47D human breast cancer tumors. Nucl Med Biol. 2009; 36:171–181. [PubMed: 19217529]
93. Gasser G, Tjioe L, Graham B, Belousoff MJ, Juran S, Walther M, Kunstler JU, Bergmann R, Stephan H, Spiccia L. Synthesis, Copper(II) Complexation, (64)Cu-Labeling, and Bioconjugation of a New Bis(2-pyridylmethyl) Derivative of 1,4,7-Triazacyclononane. Bioconjug Chem. 2008; 19:719–730. [PubMed: 18254581]
94. Juran S, Walther M, Stephan H, Bergmann R, Steinbach J, Kraus W, Emmerling F, Comba P. Hexadentate bispidine derivatives as versatile bifunctional chelate agents for copper(II) radioisotopes. Bioconjug Chem. 2009; 20:347–359. [PubMed: 19173600]
95. Liu Z, Li ZB, Cao Q, Liu S, Wang F, Chen X. Small-animal PET of tumors with (64)Cu-labeled RGD-bombesin heterodimer. J Nucl Med. 2009; 50:1168–1177. [PubMed: 19525469]

96. Friedlander M, Brooks PC, Shaffer RW, Kincaid CM, Varner JA, Cheresh DA. Definition of two angiogenic pathways by distinct alpha v integrins. Science. 1995; 270:1500–1502. [PubMed: 7491498]

97. Brooks PC, Clark RA, Cheresh DA. Requirement of vascular integrin alpha v beta 3 for angiogenesis. Science. 1994; 264:569–571. [PubMed: 7512751]

98. Ma MT, Karas JA, White JM, Scanlon D, Donnelly PS. A new bifunctional chelator for copper radiopharmaceuticals: a cage amine ligand with a carboxylate functional group for conjugation to peptides. Chem Commun (Camb). 2009:3237–3239. [PubMed: 19587925]

99. Zhang X, Cai W, Cao F, Schreibmann E, Wu Y, Wu JC, Xing L, Chen X. 18F-Labeled Bombesin Analogs for Targeting GRP Receptor-Expressing Prostate Cancer. J Nucl Med. 2006; 47:492–501. [PubMed: 16513619]

100. Li ZB, Wu Z, Chen K, Ryu EK, Chen X. 18F-labeled BBN-RGD heterodimer for prostate cancer imaging. J Nucl Med. 2008; 49:453–461. [PubMed: 18287274]

101. Liu Z, Yan Y, Chin FT, Wang F, Chen X. Dual integrin and gastrin-releasing peptide receptor targeted tumor imaging using 18F-labeled PEGylated RGD-bombesin heterodimer 18F-FB-PEG3-Glu-RGD-BBN. J Med Chem. 2009; 52:425–432. [PubMed: 19113865]

102. Becaud J, Mu L, Karramkam M, Schubiger PA, Ametamey SM, Graham K, Stellfeld T, Lehmann L, Borkowski S, Berndorff D, Dinkelborg L, Srinivasan A, Smits R, Koksch B. Direct one-step 18F-labeling of peptides via nucleophilic aromatic substitution. Bioconjug Chem. 2009; 20:2254–2261. [PubMed: 19921791]

103. Zhang H, Schuhmacher J, Waser B, Wild D, Eisenhut M, Reubi JC, Maecke HR. DOTA-PESIN, a DOTA-conjugated bombesin derivative designed for the imaging and targeted radionuclide treatment of bombesin receptor-positive tumours. Eur J Nucl Med Mol Imaging. 2007; 34:1198–1208. [PubMed: 17262215]

104. Schuhmacher J, Zhang H, Doll J, Macke HR, Matys R, Hauser H, Henze M, Haberkorn U, Eisenhut M. GRP receptor-targeted PET of a rat pancreas carcinoma xenograft in nude mice with a 68Ga-labeled bombesin(6–14) analog. J Nucl Med. 2005; 46:691–699. [PubMed: 15809493]

105. Liu Z, Niu G, Wang F, Chen X. (68)Ga-labeled NOTA-RGD-BBN peptide for dual integrin and GRPR-targeted tumor imaging. Eur J Nucl Med Mol Imaging. 2009; 36:1483–1494. [PubMed: 19360404]

106. Abiraj K, Jaccard H, Kretzschmar M, Helm L, Maecke HR. Novel DOTA-based prochelator for divalent peptide vectorization: synthesis of dimeric bombesin analogues for multimodality tumor imaging and therapy. Chem Commun (Camb). 2008:3248–3250. [PubMed: 18622433]

107. Koumarianou E, Mikolajczak R, Pawlak D, Zikos X, Bouziotis P, Garnuszek P, Karczmarczyk U, Maurin M, Archimandritis SC. Comparative study on DOTA-derivatized bombesin analog labeled with 90Y and 177Lu: *in vitro* and *in vivo* evaluation. Nucl Med Biol. 2009; 36:591–603. [PubMed: 19647165]

108. Smith CJ, Gali H, Sieckman GL, Hayes DL, Owen NK, Mazuru DG, Volkert WA, Hoffman TJ. Radiochemical investigations of 177Lu-DOTA-8-Aoc-BBN[7–14]NH2: an *in vitro*/*in vivo* assessment of the targeting ability of this new radiopharmaceutical for PC-3 human prostate cancer cells. Nucl Med Biol. 2003; 30:101–109. [PubMed: 12623108]

109. Johnson CV, Shelton T, Smith CJ, Ma L, Perry MC, Volkert WA, Hoffman TJ. Evaluation of combined (177)Lu-DOTA-8-AOC-BBN (7–14)NH(2) GRP receptor-targeted radiotherapy and chemotherapy in PC-3 human prostate tumor cell xenografted SCID mice. Cancer Biother Radiopharm. 2006; 21:155–166. [PubMed: 16706636]

110. Lantry LE, Cappelletti E, Maddalena ME, Fox JS, Feng W, Chen J, Thomas R, Eaton SM, Bogdan NJ, Arunachalam T, Reubi JC, Raju N, Metcalfe EC, Lattuada L, Linder KE, Swenson RE, Tweedle MF, Nunn AD. 177Lu-AMBA: Synthesis and characterization of a selective 177Lu-labeled GRP-R agonist for systemic radiotherapy of prostate cancer. J Nucl Med. 2006; 47:1144–1152. [PubMed: 16818949]

111. Linder KE, Metcalfe E, Arunachalam T, Chen J, Eaton SM, Feng W, Fan H, Raju N, Cagnolini A, Lantry LE, Nunn AD, Swenson RE. *In vitro* and *in vivo* metabolism of Lu-AMBA, a GRP-receptor binding compound, and the synthesis and characterization of its metabolites. Bioconjug Chem. 2009; 20:1171–1178. [PubMed: 19480415]

112. Maddalena ME, Fox J, Chen J, Feng W, Cagnolini A, Linder KE, Tweedle MF, Nunn AD, Lantry LE. 177Lu-AMBA Biodistribution, Radiotherapeutic Efficacy, Imaging, and Autoradiography in Prostate Cancer Models with Low GRP-R Expression. J Nucl Med. 2009

113. Hu F, Cutler CS, Hoffman T, Sieckman G, Volkert WA, Jurisson SS. Pm-149 DOTA bombesin analogs for potential radiotherapy. *in vivo* comparison with Sm-153 and Lu-177 labeled DO3A-amide-betaAla-BBN(7–14)NH(2). Nucl Med Biol. 2002; 29:423–430. [PubMed: 12031877]

114. Varvarigou A, Bouziotis P, Zikos C, Scopinaro F, De Vincentis G. Gastrin-releasing peptide (GRP) analogues for cancer imaging. Cancer Biother Radiopharm. 2004; 19:219–229. [PubMed: 15186603]

115. Pradhan TK, Katsuno T, Taylor JE, Kim SH, Ryan RR, Mantey SA, Donohue PJ, Weber HC, Sainz E, Battey JF, Coy DH, Jensen RT. Identification of a unique ligand which has high affinity for all four bombesin receptor subtypes. Eur J Pharmacol. 1998; 343:275–287. [PubMed: 9570477]

116. Waser B, Eltschinger V, Linder K, Nunn A, Reubi JC. Selective *in vitro* targeting of GRP and NMB receptors in human tumours with the new bombesin tracer (177)Lu-AMBA. Eur J Nucl Med Mol Imaging. 2007; 34:95–100. [PubMed: 16909223]

117. Thomas R, Chen J, Roudier MM, Vessella RL, Lantry LE, Nunn AD. *In vitro* binding evaluation of 177Lu-AMBA, a novel 177Lu-labeled GRP-R agonist for systemic radiotherapy in human tissues. Clin Exp Metastasis. 2009; 26:105–119. [PubMed: 18975117]

118. Rogers BE, Rosenfeld ME, Khazaeli MB, Mikheeva G, Stackhouse MA, Liu T, Curiel DT, Buchsbaum DJ. Localization of iodine-125-mIP-Des-Met14-bombesin (7–13)NH2 in ovarian carcinoma induced to express the gastrin releasing peptide receptor by adenoviral vector-mediated gene transfer. J Nucl Med. 1997; 38:1221–1229. [PubMed: 9255155]

119. Rogers BE, Curiel DT, Mayo MS, Laffoon KK, Bright SJ, Buchsbaum DJ. Tumor localization of a radiolabeled bombesin analogue in mice bearing human ovarian tumors induced to express the gastrin-releasing peptide receptor by an adenoviral vector. Cancer. 1997; 80:2419–2424. [PubMed: 9406692]

120. Safavy A, Khazaeli MB, Qin H, Buchsbaum DJ. Synthesis of bombesin analogues for radiolabeling with rhenium-188. Cancer. 1997; 80:2354–2359. [PubMed: 9406683]

121. Moustapha ME, Ehrhardt GJ, Smith CJ, Szajek LP, Eckelman WC, Jurisson SS. Preparation of cyclotron-produced 186Re and comparison with reactor-produced 186Re and generator-produced 188Re for the labeling of bombesin. Nucl Med Biol. 2006; 33:81–89. [PubMed: 16459262]

122. Scopinaro F, Varvarigou AD, Ussof W, De Vincentis G, Sourlingas TG, Evangelatos GP, Datsteris J, Archimandritis SC. Technetium labeled bombesin-like peptide: preliminary report on breast cancer uptake in patients. Cancer Biother Radiopharm. 2002; 17:327–335. [PubMed: 12136525]

123. De Vincentis G, Scopinaro F, Varvarigou A, Ussof W, Schillaci O, Archimandritis S, Corleto V, Longo F, Delle Fave G. Phase I trial of technetium [Leu13] bombesin as cancer seeking agent: possible scintigraphic guide for surgery? Tumori. 2002; 88:S28–S30. [PubMed: 12365378]

124. Soluri A, Scopinaro F, De Vincentis G, Varvarigou A, Scafe R, Massa R, Schillaci O, Spanu A, David V. 99MTC [13LEU] bombesin and a new gamma camera, the imaging probe, are able to guide mammotome breast biopsy. Anticancer Res. 2003; 23:2139–2142. [PubMed: 12894588]

125. De Vincentis G, Remediani S, Varvarigou AD, Di Santo G, Iori F, Laurenti C, Scopinaro F. Role of 99mTc-bombesin scan in diagnosis and staging of prostate cancer. Cancer Biother Radiopharm. 2004; 19:81–84. [PubMed: 15068615]

126. Scopinaro F, De Vincentis G, Varvarigou AD, Laurenti C, Iori F, Remediani S, Chiarini S, Stella S. 99mTc-bombesin detects prostate cancer and invasion of pelvic lymph nodes. Eur J Nucl Med Mol Imaging. 2003; 30:1378–1382. [PubMed: 12920485]

127. Scopinaro F, De Vincentis G, Corazziari E, Massa R, Osti M, Pallotta N, Covotta A, Remediani S, Paolo MD, Monteleone F, Varvarigou A. Detection of colon cancer with 99mTc-labeled bombesin derivative (99mTc-leu13-BN1). Cancer Biother Radiopharm. 2004; 19:245–252. [PubMed: 15186605]

128. van de WC, Dumont F, Dierck RA, Peers SH, Thornback JR, Slegers G, Thierens H. Biodistribution and dosimetry of (99m)Tc-RP527, a gastrin-releasing peptide (GRP) agonist for

the visualization of GRP receptor-expressing malignancies. J Nucl Med. 2001; 42:1722–1727. [PubMed: 11696645]

129. Santos-Cuevas CL, Ferro-Flores G, Arteaga de Murphy C, Pichardo-Romero PA. Targeted imaging of gastrin-releasing peptide receptors with 99mTc-EDDA/HYNIC-[Lys3]-bombesin: biokinetics and dosimetry in women. Nucl Med Commun. 2008; 29:741–747. [PubMed: 18753829]
130. Dimitrakopoulou-Strauss A, Hohenberger P, Haberkorn U, Macke HR, Eisenhut M, Strauss LG. 68Ga-labeled bombesin studies in patients with gastrointestinal stromal tumors: comparison with 18F-FDG. J Nucl Med. 2007; 48:1245–1250. [PubMed: 17631559]
131. Seiz M, Mitrakopoulou-Strauss A, Schubert GA, Weinmann C, Strauss LG, Eisenhut M, Tuettenberg J. Differentiation between malignant transformation and tumour recurrence by (68)Ga-bombesin and (18)F-FDG-PET, in patients with low grade gliomas. Hell J Nucl Med. 2008; 11:149–152. [PubMed: 19081856]
132. Sekido, Y.; Fong, KM.; Minna, JD. Cancer of the lung. In: De Vita, VT.; Hellman, S.; Rosenberg, SA., editors. Cancer: Princiles and Practice of Oncology. 7. Lippincott Williams and Wilkins; Philadelphia: 2005. p. 745-752.
133. Carney DN, Moody T, Cuttitta F. Bombesin: a potent mitogen for small cell lung cancer. Ann N Y Acad Sci. 1988; 547:303–309. [PubMed: 2853594]
134. Cuttitta F, Carney DN, Mulshine J, Moody TW, Fedorko J, Fischler A, Minna JD. Bombesin-like peptides can function as autocrine growth factors in human small-cell lung cancer cells. Nature. 1985; 316:823–826. [PubMed: 2993906]
135. Pradhan TK, Katsuno T, Weber HC, Mantey SA, Coy DH, Jensen RT. Discovery of a universal ligand that interacts with high affinity with all four classes of bombesin (BN) receptors. Gastroenterology. 1997; 112:A474. Ref Type: Abstract.
136. Sun L, Fuselier JA, Coy DH. Effects of camptothecin conjugated to a somatostatin analog vector on growth of tumor cell lines in culture and related tumors in rodents. Drug Deliv. 2004; 11:231–238. [PubMed: 15371104]
137. Patterson LH, McKeown SR, Robson T, Gallagher R, Raleigh SM, Orr S. Antitumour prodrug development using cytochrome P450 (CYP) mediated activation. Anticancer Drug Des. 1999; 14:473–486. [PubMed: 10834269]
138. Fuselier JA, Sun L, Woltering SN, Murphy WA, Vasilevich N, Coy DH. An adjustable release rate linking strategy for cytotoxin-Peptide conjugates. Bioorg Med Chem Lett. 2003; 13:799–803. [PubMed: 12617894]
139. Akeson M, Sainz E, Mantey SA, Jensen RT, Battey JF. Identification of four amino acids in the gastrin-releasing peptide C receptor that are required for high affinity agonist binding. J Biol Chem. 1997; 272:17405–17409. [PubMed: 9211882]
140. Nakagawa T, Hocart SJ, Schumann M, Tapia JA, Mantey SA, Coy DH, Tokita K, Katsuno T, Jensen RT. Identification of key amino acids in the gastrin-releasing peptide receptor (GRPR) responsible for high affinity binding of gastrin-releasing peptide (GRP). Biochem Pharmacol. 2005; 69:579–593. [PubMed: 15670577]
141. Nagy A, Armatis P, Cai RZ, Szepeshazi K, Halmos G, Schally AV. Design, synthesis, and *in vitro* evaluation of cytotoxic analogs of bombesin-like peptides containing doxorubicin or its intensely potent derivative, 2-pyrrolinodoxorubicin. Proc Natl Acad Sci U S A. 1997; 94:652–656. [PubMed: 9012839]
142. Schally AV, Nagy A. Chemotherapy targeted to cancers through tumoral hormone receptors. Trends Endocrinol Metab. 2004; 15:300–310. [PubMed: 15350601]
143. Plonowski A, Nagy A, Schally AV, Sun B, Groot K, Halmos G. *In vivo* inhibition of PC-3 human androgen-independent prostate cancer by a targeted cytotoxic bombesin analogue, AN-215. Int J Cancer. 2000; 88:652–657. [PubMed: 11058885]
144. Safavy A, Raisch KP, Khazaeli MB, Buchsbaum DJ, Bonner JA. Paclitaxel derivatives for targeted therapy of cancer: toward the development of smart taxanes. J Med Chem. 1999; 42:4919–4924. [PubMed: 10579854]

145. Safavy A, Raisch KP, Matusiak D, Bhatnagar S, Helson L. Single-drug multiligand conjugates: synthesis and preliminary cytotoxicity evaluation of a paclitaxel-dipeptide “scorpion” molecule. Bioconjug Chem. 2006; 17:565–570. [PubMed: 16704191]

146. Hohla F, Schally AV, Kanashiro CA, Buchholz S, Baker B, Kannadka C, Moder A, Aigner E, Datz C, Halmos G. Growth inhibition of non-small-cell lung carcinoma by BN/GRP antagonist is linked with suppression of K-Ras, COX-2, and pAkt. Proc Natl Acad Sci U S A. 2007; 104:18671–18676. [PubMed: 18003891]

147. Stangelberger A, Schally AV, Varga JL, Hammann BD, Groot K, Halmos G, Cai RZ, Zarandi M. Antagonists of growth hormone releasing hormone (GHRH) and of bombesin/gastrin releasing peptide (BN/GRP) suppress the expression of VEGF, bFGF, and receptors of the EGF/HER family in PC-3 and DU-145 human androgen-independent prostate cancers. Prostate. 2005; 64:303–315. [PubMed: 15754342]

148. Lui VW, Thomas SM, Wentzel AM, Siegfried JM, Li JY, Grandis JR. Mitogenic effects of gastrin-releasing peptide in head and neck squamous cancer cells are mediated by activation of the epidermal growth factor receptor. Oncogene. 2003; 22:6183–6193. [PubMed: 13679857]

149. Moody TW, Berna MJ, Mantey S, Sancho V, Ridnour L, Wink DA, Chan D, Giaccone G, Jensen RT. Neuromedin B receptors regulate EGF receptor tyrosine phosphorylation in lung cancer cells. Eur J Pharmacol. 2010

150. vanderSpek JC, Sutherland JA, Zeng H, Battey JF, Jensen RT, Murphy JR. Inhibition of protein synthesis in small cell lung cancer cells induced by the diphtheria toxin-related fusion protein DAB389 GRP. Cancer Res. 1997; 57:290–294. [PubMed: 9000570]

151. Cai H, Yang H, Xiang B, Li S, Liu S, Wan L, Zhang J, Li Y, Cheng J, Lu X. Selective Apoptotic Killing of Solid and Hematologic Tumor Cells by Bombesin-Targeted Delivery of Mitochondria-Disrupting Peptides. Mol Pharm. 2010

152. Zhou J, Chen J, Zhong R, Mokotoff M, Shultz LD, Ball ED. Targeting gastrin-releasing peptide receptors on small cell lung cancer cells with a bispecific molecule that activates polyclonal T lymphocytes. Clin Cancer Res. 2006; 12:2224–2231. [PubMed: 16609038]

153. Chen J, Zhou JH, Mokotoff M, Fanger MW, Ball ED. Lysis of small cell carcinoma of the lung (SCCL) cells by cytokine-activated monocytes and natural killer cells in the presence of bispecific immunoconjugates containing a gastrin-releasing peptide (GRP) analog or a GRP antagonist. J Hematother. 1995; 4:369–376. [PubMed: 8581371]

154. Chen J, Mokotoff M, Zhou JH, Fanger MW, Ball ED. An immunoconjugate of Lys3-bombesin and monoclonal antibody 22 can specifically induce FcgammaRI (CD64)-dependent monocyte- and neutrophil-mediated lysis of small cell carcinoma of the lung cells. Clin Cancer Res. 1995; 1:425–434. [PubMed: 9816000]

155. Dubuc C, Langlois R, Benard F, Cauchon N, Klarskov K, Tone P, van Lier JE. Targeting gastrin-releasing peptide receptors of prostate cancer cells for photodynamic therapy with a phthalocyanine-bombesin conjugate. Bioorg Med Chem Lett. 2008; 18:2424–2427. [PubMed: 18329268]

156. Prasad S, Mathur A, Jaggi M, Mukherjee R. Delivering multiple anticancer peptides as a single prodrug using lysyl-lysine as a facile linker. J Pept Sci. 2007; 13:458–467. [PubMed: 17559067]

157. Singh AT, Jaggi M, Prasad S, Dutt S, Singh G, Datta K, Rajendran P, Sanna VK, Mukherjee R, Burman AC. Modulation of key signal transduction molecules by a novel peptide combination effective for the treatment of gastrointestinal carcinomas. Invest New Drugs. 2008; 26:505–516. [PubMed: 18322652]

158. Hong SS, Galaup A, Peytavi R, Chazal N, Boulanger P. Enhancement of adenovirus-mediated gene delivery by use of an oligopeptide with dual binding specificity. Hum Gene Ther. 1999; 10:2577–2586. [PubMed: 10566886]

159. Coy DH, Jiang NY, Sasaki Y, Taylor J, Moreau JP, Wolfrey WT, Gardner JD, Jensen RT. Probing peptide backbone function in bombesin. A reduced peptide bond analogue with potent and specific receptor antagonist activity. J Biol Chem. 1988; 263(11):5056–5060. [PubMed: 2451661]

160. Moody TW, Venugopal R, Hu V, Gozes Y, McDermed J, Leban JJ. BW 1023U90: a new GRP receptor antagonist for small-cell lung cancer cells. Peptides. 1996; 17:1337–1343. [PubMed: 8971929]

161. Tokita K, Hocart SJ, Katsuno T, Mantey SA, Coy DH, Jensen RT. Tyrosine 220 in the fifth transmembrane domain of the neuromedin B receptor is critical for the high selectivity of the peptoid antagonist PD168368. J Biol Chem. 2001; 276:495–504. [PubMed: 11013243]

162. Moody TW, Jensen RT, Garcia L, Leyton J. Nonpeptide neuromedin B receptor antagonists inhibit the proliferation of C6 cells. Eur J Pharmacol. 2000; 409:133–142. [PubMed: 11104826]

163. Prasad S, Mathur A, Gupta N, Jaggi M, Singh AT, Rajendran P, Sanna VK, Datta K, Mukherjee R. Bombesin analogs containing alpha-amino-isobutyric acid with potent anticancer activity. J Pept Sci. 2006

164. Okarvi SM, al-Jammaz I. Synthesis, radiolabelling and biological characteristics of a bombesin peptide analog as a tumor imaging agent. Anticancer Res. 2003; 23:2745–2750. [PubMed: 12894569]

165. Pu Y, Wang WB, Tang GC, Zeng F, Achilefu S, Vitenson JH, Sawczuk I, Peters S, Lombardo JM, Alfano RR. Spectral polarization imaging of human prostate cancer tissue using a near-infrared receptor-targeted contrast agent. Technol Cancer Res Treat. 2005; 4:429–436. [PubMed: 16029061]

166. Varvarigou AD, Scopinaro F, Leondiadis L, Corleto V, Schillaci O, De Vincentis G, Sourlingas TG, Sekeri-Pataryas KE, Evangelatos GP, Leonti A, Xanthopoulos S, Delle Fave G, Archimandritis SC. Synthesis, chemical, radiochemical and radiobiological evaluation of a new 99mTc-labelled bombesin-like peptide. Cancer Biother Radiopharm. 2002; 17:317–326. [PubMed: 12136524]

167. Ferro-Flores G, Arteaga de Murphy C, Rodriguez-Cortes J, Pedraza-Lopez M, Ramirez-Iglesias MT. Preparation and evaluation of 99mTc-EDDA/HYNIC-[Lys 3]-bombesin for imaging gastrin-releasing peptide receptor-positive tumours. Nucl Med Commun. 2006; 27:371–376. [PubMed: 16531924]

168. Achilefu S, Jimenez HN, Dorshow RB, Bugaj JE, Webb EG, Wilhelm RR, Rajagopalan R, Johler J, Erion JL. Synthesis, *in vitro* receptor binding, and *in vivo* evaluation of fluorescein and carbocyanine peptide-based optical contrast agents. J Med Chem. 2002; 45:2003–2015. [PubMed: 11985468]

169. Montet X, Weissleder R, Josephson L. Imaging pancreatic cancer with a peptide-nanoparticle conjugate targeted to normal pancreas. Bioconjug Chem. 2006; 17:905–911. [PubMed: 16848396]

170. Scopinaro F, Varvarigou A, Ussof W, De Vincentis G, Archimandritis S, Evangelatos G, Corleto V, Pulcini A, Capoccetti F, Remediani S, Massa R. Breast cancer takes up 99mTc bombesin. A preliminary report. Tumori. 2002; 88:S25–S28. [PubMed: 12365377]

171. Fragogeorgi EA, Zikos C, Gourni E, Bouziotis P, Paravatou-Petsotas M, Loudos G, Mitsokapas N, Xanthopoulos S, Mavri-Vavayanni M, Livaniou E, Varvarigou AD, Archimandritis SC. Spacer Site Modifications for the Improvement of the *in vitro* and *in vivo* Binding Properties of (99m)Tc-N(3)S-X-Bombesin[2–14] Derivatives. Bioconjug Chem. 2009

172. Scopinaro F, Massari R, Varvarigou AD, D'Alessandria C, Trotta C, Di Santo GP, Soluri A. High resolution small animal single photon emission computed tomography: uptake of [99mTc]bombesin and [123I]ioflupane by rat brain. Q J Nucl Med Mol Imaging. 2007; 51:204–210. [PubMed: 17420719]

173. Gotthardt M, van Eerd-Vismale J, Oyen WJ, de Jong M, Zhang H, Rolleman E, Maecke HR, Behe M, Boerman O. Indication for different mechanisms of kidney uptake of radiolabeled peptides. J Nucl Med. 2007; 48:596–601. [PubMed: 17401097]

174. Nock B, Nikolopoulou A, Chiotellis E, Loudos G, Maintas D, Reubi JC, Maina T. [99mTc]Demobesin 1, a novel potent bombesin analogue for GRP receptor-targeted tumour imaging. Eur J Nucl Med Mol Imaging. 2003; 30:247–258. [PubMed: 12552343]

175. Ma L, Yu P, Veerendra B, Rold TL, Retzloff L, Prasanphanich A, Sieckman G, Hoffman TJ, Volkert WA, Smith CJ. *In vitro* and *in vivo* evaluation of Alexa Fluor 680-bombesin[7–14]NH2 peptide conjugate, a high-affinity fluorescent probe with high selectivity for the gastrin-releasing peptide receptor. Mol Imaging. 2007; 6:171–180. [PubMed: 17532883]

176. Garcia Garayoa E, Schweinsberg C, Maes V, Ruegg D, Blanc A, Blauenstein P, Tourwe DA, Beck-Sickinger AG, Schubiger PA. New [99mTc]bombesin analogues with improved

biodistribution for targeting gastrin releasing-peptide receptor-positive tumors. Q J Nucl Med Mol Imaging. 2007; 51:42–50. [PubMed: 17372572]

177. Paterson BM, Karas JA, Scanlon DB, White JM, Donnelly PS. Versatile new bis(thiosemicarbazone) bifunctional chelators: synthesis, conjugation to bombesin(7–14)-NH(2), and copper-64 radiolabeling. Inorg Chem. 2010; 49:1884–1893. [PubMed: 20055473]
178. Alves S, Paulo A, Correia JD, Gano L, Smith CJ, Hoffman TJ, Santos I. Pyrazolyl derivatives as bifunctional chelators for labeling tumor-seeking peptides with the fac-[M(CO)3]+ moiety (M = 99mTc, Re): synthesis, characterization, and biological behavior. Bioconjug Chem. 2005; 16:438–449. [PubMed: 15769099]
179. Gali H, Hoffman TJ, Sieckman GL, Owen NK, Katti KV, Volkert WA. Synthesis, characterization, and labeling with 99mTc/188Re of peptide conjugates containing a dithia-bisphosphine chelating agent. Bioconjug Chem. 2001; 12:354–363. [PubMed: 11353532]
180. La Bella R, Garcia-Garayoa E, Bahler M, Blauenstein P, Schibli R, Conrath P, Tourwe D, Schubiger PA. A 99mTc(I)-postlabeled high affinity bombesin analogue as a potential tumor imaging agent. Bioconjug Chem. 2002; 13:599–604. [PubMed: 12009951]
181. La Bella R, Garcia-Garayoa E, Langer M, Blauenstein P, Beck-Sickinger AG, Schubiger PA. *In vitro* and *in vivo* evaluation of a 99mTc(I)-labeled bombesin analogue for imaging of gastrin releasing peptide receptor-positive tumors. Nucl Med Biol. 2002; 29:553–560. [PubMed: 12088725]
182. Smith CJ, Gali H, Sieckman GL, Higginbotham C, Volkert WA, Hoffman TJ. Radiochemical investigations of (99m)Tc-N(3)S-X-BBN[7–14]NH(2): an *in vitro*/*in vivo* structure-activity relationship study where X = 0-, 3-, 5-, 8-, and 11-carbon tethering moieties. Bioconjug Chem. 2003; 14:93–102. [PubMed: 12526698]
183. Bugaj JE, Achilefu S, Dorshow RB, Rajagopalan R. Novel fluorescent contrast agents for optical imaging of *in vivo* tumors based on a receptor-targeted dye-peptide conjugate platform. J Biomed Opt. 2001; 6:122–133. [PubMed: 11375721]
184. Brans L, Maes V, Garcia-Garayoa E, Schweinsberg C, Daepp S, Blauenstein P, Schubiger PA, Schibli R, Tourwe DA. Glycation methods for bombesin analogs containing the (NalphaHis)Ac chelator for 99mTc(CO)3 radiolabeling. Chem Biol Drug Des. 2008; 72:496–506. [PubMed: 19016795]
185. Schroeder RP, van Weerden WM, Bangma C, Krenning EP, de Jong M. Peptide receptor imaging of prostate cancer with radiolabelled bombesin analogues. Methods. 2009; 48:200–204. [PubMed: 19398012]
186. Melis M, Krenning EP, Bernard BF, de Visser M, Rolleman E, de Jong M. Renal uptake and retention of radiolabeled somatostatin, bombesin, neurotensin, minigastrin and CCK analogues: species and gender differences. Nucl Med Biol. 2007; 34:633–641. [PubMed: 17707803]
187. Van de Wiele C, Phonteyne P, Pauwels P, Goethals I, Van den Broecke R, Cocquyt V, Dierck RA. Gastrin-releasing peptide receptor imaging in human breast carcinoma *versus* immunohistochemistry. J Nucl Med. 2008; 49:260–264. [PubMed: 18199617]
188. Wang XL, Xu R, Lu ZR. A peptide-targeted delivery system with pH-sensitive amphiphilic cell membrane disruption for efficient receptor-mediated siRNA delivery. J Control Release. 2009; 134:207–213. [PubMed: 19135104]

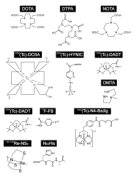

Fig. 1.
Chemical structure of common linkers used in studies to couple Bombesin (Bn) analogs to various radioisotopes for Bn-receptor-mediated imaging or cytotoxicity. For listing of abbreviations see Table 1.

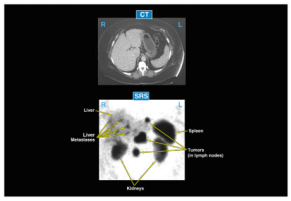

Fig. 2.

Example of usefulness of receptor-mediated imaging for targeting and imaging tumors. The upper panel shows a computed tomographic scan (CT). The lower panel shows the abdominal nuclear medicine images (SPECT image) (from a patient with metastatic neuroendocrine tumor taken 24 hours after injection of 6 mCi of [^{111}In-DTPA,DPhe^{1}]octreotide, to image over-expression of somatostatin receptors on the tumor. In this patient the CT scan was negative, whereas the somatostatin receptor scan was positive for tumor in a number of lymph nodes and the liver. This illustrates the higher sensitivity of somatostatin receptor imaging than conventional imaging (CT, MRI), the precise targeting to the tumor and the clinical usefulness of such an approach.

Table 1

Abbreviations.

(NαHis)Ac	=	Nα-histidinyl acetyl
Aba	=	γ-aminobutyric acid
Ac	=	acetyl
Aca	=	aminohexanoic acid
ACMpip	=	4-aminocarboxymethylpiperidine
Acp	=	1-aminoethy-l,4-carboxymethylpiperazine
ADS	=	amino-3-oxapentyl-succinamic acid
Ado	=	12-aminododecanoic acid
Ahx	=	6-aminohexanoic acid
AM2BA	=	p-aminomethylbenzoic acid
AMBA	=	Aminobenzoyl
Aoc	=	aminooctanoic acid
AOS	=	amino-3,6-dioxaoctyl-succinamic acid
11-Aun	=	11-aminoundecanoic acid
Ava	=	5-aminopentanoic acid
βAla	=	Beta-Alanine
Bomproamide	=	[DPhe^{6},Leu-NHEt^{13},des-Met^{14}]Bn(6-14)
Bn	=	Bombesin
BRS-3	=	Bombesin receptor subtype 3
Bzdig	=	p-aminobenzyldiglycolic acid
BZH3	=	[DTyr^{6},βAla^{11},Thi^{13},Nle^{14}]Bn(6-14)
CB-TE2A	=	1,4,8,11-tetraazabicyclo[6.6.2]hexadecane-4,11-diacetic acid
Cha	=	cyclohexylalanine
CNS	=	Central nervous system
CT	=	Computed tomography
DADT	=	diaminedithiol
DPhe	=	D-phenylalanine
Demobesin 1	=	[(N$_4$-bzlg)^{0},DPhe^{6},LeuNHEt^{13},desMet^{14}]Bn(6–14)]
Demobesin 3	=	[N$_4^{0}$,Pro^{1},Tyr^{4}]Bn
Demobesin 4	=	[N$_4^{0}$,Pro^{1},Tyr^{4},Nle^{14}]Bn
Demobesin 5	=	[(N$_4$Bzdig)^{0}]Bn(7–14)
Demobesin 6	=	[(N$_4$Bzdig)^{0},Nle^{14}]Bn(7–14)
Des-Met	=	Methionine removed
Desmosin 1	=	[N$_4^{0}$,DPhe^{6},LeuNHEt^{13},desMet^{14}]Bn(6-14)
Desmosin 4	=	[N$_4^{0}$,Pro^{1},Tyr^{4},Nle^{14}]Bn(6-14)
DMTA	=	2-(N,N″-bis(tert-butoxycarbonyl)diethylenetriamine)acetic acid
DO3A	=	1,4,7-tris(carboxymethyl)10-(aminoethyl)-1,4,7,10-tetraazacyclododecaneOH

DOTA	=	1,4,7,10-tetraazacyclododecane-N,N′,N″,N‴-tetraaceticacid
Dpr	=	1,2-diaminopropionic acid
DPR	=	2,3-diaminopropionic acid
DTPA	=	2-[bis[2-[bis(carboxymethyl)amino]ethyl]amino]acetic
EDDA	=	diorthohydroxyphenyl acetic acid
FA01010	=	(4*R*,5*S*)-4-amino-5-methylheptanoic acid
FB	=	fluorobenzoato
GABA	=	γ-aminobutyric acid
GEG	=	Glycine-Glutammate-Glycine
GI	=	Gastrointestinal
GRP	=	Gastrin-releasing peptide
GRPR	=	Gastrin-releasing peptide receptor
GSS	=	Glycine-Serine-Serine
GSG	=	Glycine-Serine-Glycine
GGG	=	Glycine-Glycine - Glycine
HSA	=	Human serum albumin
HYNIC	=	6-hydrazinonicotinic acid
Lys(Acm)	=	Amadori-Product
Lys(sha)	=	Lysine-coupled shikimic acid
Mac	=	mercaptoacetic acid
MAG3	=	mercaptoacetyltriglycine
MeGly	=	Methylglicine
Me_2Gly	=	Dimethylglicine
mIP	=	*meta*-phenylalanine
MP2248	=	DPTA-[Pro^1,Tyr^4]Bn(1-14)
MP2346	=	DOTA-[Pro^1,Tyr^4]Bn(1-14)
MP2653	=	[$ACMpip^5$,Tha^6,βAla^{11},Tha^{13},Nle^{14}]Bn(5–14)
MRI	=	Magnetic resonance imaging
MTT	=	3-(4,5-Dimethylthiazol-2-yl)-2,5-diphenyltetrazolium bromide
N_2S_2	=	Cys(Acm)-Gly-Cys(Acm)
N_3S	=	dimethylglycyl-L-seryl-L-cysteinglycinamide
N_4	=	tetramine
Nle	=	Norleucine
NMB	=	Neuromedin B
NMBR	=	Neuromedin B receptor
NOTA	=	1,4,7-triazacyclononanetriacetic acid
NO2A	=	1,4,7-triazacyclononane-1,4-diacetate
NS_3	=	2′,2″,2‴-nitrotriethanethiol
NTG	=	triazole-couple glucose
PADA	=	[pyridin-2-yl-methyl-amino]-diacetic acid

PBS	=	Phosphate buffered saline
PEG	=	ethylene glycol [2-aminoethylcarboxymethylether]
PEG_2	=	(2-aminoethyl)-carboxymethyl ether
PEG_3	=	11-amino-3,6,9-trioxaundecanoic acid
PEG_4	=	15-amino-4,7,10,13-tetraoxapentadecanoic acid
PET	=	Positron emission tomography
PNP6	=	N,N-bis[2-(bis(3-ethoxypropyl)phosphino)ethyl]ethoxyethylamine
Pra	=	Propargylglycine
PZ1	=	pyrazolyl
RGD	=	RGDyK (Arginine-Glycine-Aspartic Acid-Lysine)
RM1	=	H-DPhe-Gln-Trp-Ala-Val-Gly-His-Sta-Leu-NH_2
RP527	=	N_3S-5-Ava-Bn(7-14)
SPECT	=	Single photon emission computed tomography
SRS	=	Somatostatin receptor scintigraphy
Sta	=	Statine: (3*S*,4*S*)-4-amino-3-hydroxy-6-methylheptanoic acid
TACN	=	2-[4,7-bis(2-pyridylmethyl)-1,4,7-triazacyclononan-1-yl]acetic acid
Tat (49-57)	=	Arg-Lys-Lys-Arg-Arg-Gln-Arg-Arg-Arg (HIV-peptide)
Tha	=	β-(2-thienyl)alanine
Thi	=	3-(2-thienyl)alanine
TPPS	=	trisodium triphenylphosphine-3,3′,3″-trisulfonate
Tricine	=	N-(2-Hydroxy-1,1-bis(hydroxymethyl)ethyl)glycine
Z-070	=	DOTA-PEG_{40}[$DTyr^6$,βAla^{11},Thi^{13},Nle^{14}]Bn(6–14)

Table 2

Structure of Bn-related peptides used in various imaging studies[(a)]

Peptide		Structure (Position relative to Bn)														Ag/Ant[(b)]	RM #
N°	Name	1	2	3	4	5	6	7	8	9	10	11	12	13	14		
1	Bombesin (Bn)	Pyr	Gln	Arg	Leu	Gly	Asn	Gln	Trp	Ala	Val	Gly	His	Leu	Met-NH_2	Ag	[119,164–166]
2	GRP (13-27)	**Tyr**	**Pro**	Arg	Leu	Gly	Asn	**His**	Trp	Ala	Val	Gly	His	Leu	Met-NH_2	Ag	[48]
3	Litorin [$pGlu^6$, Phe^{13}]Bn(6-14)						**pGlu**	Gln	Trp	Ala	Val	Gly	His	**Phe**	Met-NH_2	Ag	[71]
4	Demobesin 3 [$N_4{}^0$,Pro^1,Tyr^4]Bn	**N_4 -Pro**	Gln	Arg	**Tyr**	Gly	Asn	Gln	Trp	Ala	Val	Gly	His	Leu	Met-NH_2	Ag	[70]
5	Demobesin 4 [$N_4{}^0$,Pro^1,Tyr^4,Nle^{14}]Bn	**N_4 -Pro**	Gln	Arg	**Tyr**	Gly	Asn	Gln	Trp	Ala	Val	Gly	His	Leu	**Nle**-NH_2	Ag	[70]
6	[Lys^3]Bn	Pyr	Gln	**Lys**	Leu	Gly	Asn	Gln	Trp	Ala	Val	Gly	His	Leu	Met-NH_2	Ag	[52,54,85,86,98,99,106,129,167]
7	[Tyr^4]Bn	Pyr	Gln	Arg	**Tyr**	Gly	Asn	Gln	Trp	Ala	Val	Gly	His	Leu	Met-NH_2	Ag	[48,76,102,119]
8	[εLys^3,Tyr^4]Bn	Pyr	Gln	**εLys**	**Tyr**	Gly	Asn	Gln	Trp	Ala	Val	Gly	His	Leu	Met-NH_2	Ag	[76]
9	[Gln^1,Tyr^4]Bn	**Gln**	Gln	Arg	**Tyr**	Gly	Asn	Gln	Trp	Ala	Val	Gly	His	Leu	Met-NH_2	Ag	[168]
10	[Gly^1]Bn	**Gly**	Gln	Arg	Leu	Gly	Asn	Gln	Trp	Ala	Val	Gly	His	Leu	Met-NH_2	Ag	[169]
11	[Pro^1,Tyr^4]Bn (MP2346)	**Pro**	Gln	Arg	**Tyr**	Gly	Asn	Gln	Trp	Ala	Val	Gly	His	Leu	Met-NH_2	Ag	[2,48,74,76,168]
12	[Pro^1,Tyr^4,Nle^{14}]Bn	**Pro**	Gln	Arg	**Tyr**	Gly	Asn	Gln	Trp	Ala	Val	Gly	His	Leu	**Nle**-NH_2	Ag	[45,48]
13	[Cys^0,Aca^1]Bn(2-14)	**Cys-Aca**	Gln	Arg	Leu	Gly	Asn	Gln	Trp	Ala	Val	Gly	His	Leu	Met-NH_2	Ag	[122,124,126,127,170]
14	Bn(2-14)		Gln	Arg	Leu	Gly	Asn	Gln	Trp	Ala	Val	Gly	His	Leu	Met-NH_2	Ag	[55,106,107,171]
15	[Lys^{14}]Bn(2-14)		Gln	Arg	Leu	Gly	Asn	Gln	Trp	Ala	Val	Gly	His	Leu	**Lys**-NH_2	Ag	[172]
16	[Lys^3,Tyr^4]Bn(2-14)		Gln	**Lys**	**Tyr**	Gly	Asn	Gln	Trp	Ala	Val	Gly	His	Leu	Met-NH_2	Ag	[80]
17	[mIP]Bn(2-14)	**mIP**	Gln	Arg	Leu	Gly	Asn	Gln	Trp	Ala	Val	Gly	His	Leu	Met-NH_2	Ag	[119]
18	Bn(4-14)				Leu	Gly	Asn	Gln	Trp	Ala	Val	Gly	His	Leu	Met-NH_2	Ag	[106]
19	[$Ser^{4,5,6}$]Bn(4-14)				**Ser**	**Ser**	**Ser**	Gln	Trp	Ala	Val	Gly	His	Leu	Met-NH_2	Ag	[57]
20	[ACMpip^5,Tha^6,$βAla^{11}$, Tha^{13},Nle^{14}]Bn(5–14) (MP2653)					**ACMpip**	**Tha**	Gln	Trp	Ala	Val	**βAla**	His	**Tha**	**Nle**-NH_2	Ag	[2,87]
21	[Tyr^5,$DPhe^6$,ψPhe^{14}] Bn(5-14)					**Tyr**	**DPhe**	Gln	Trp	Ala	Val	Gly	His	**Leuψ** *(c)*	**Phe**-NH_2	Ant	[48]
22	[$DPhe^6$,Leu^{13}ψPhe^{14}] Bn(6-14)						**DPhe**	Gln	Trp	Ala	Val	Gly	His	**Leuψ**	**Phe**-NH_2	Ant	[48]
23	[$DPhe^6$,Leu-$NHEt^{13}$,des-Met^{14}] Bn(6-14)*(d)*						**DPhe**	Gln	Trp	Ala	Val	Gly	His	**Leu-NHEt** *(e)*		Ant	[47]
24	[$DTyr^6$,$βAla^{11}$,Thi^{13},Nle^{14}] Bn(6-14)						**DTyr**	Gln	Trp	Ala	Val	**βAla**	His	**Thi**	**Nle**-NH_2	Ag	[50,79,104,130,173]
25	Demobesin 1 [$N_4{}^0$–1,bzdig^0,$DPhe^6$,Leu-$NHEt^{13}$,des-Met^{14}]Bn(6–13)					**N_4-bzdig**	**DPhe**	Gln	Trp	Ala	Val	Gly	His	**Leu-NHEt**		Ant	[45,174]
26	RM1 [$N_4{}^0$DPhe^6,Sta^{13},Leu^{14}] Bn(6-14)						**N_4-DPhe**	Gln	Trp	Ala	Val	Gly	His	**Sta**	**Leu**-NH_2	Ant	[46,49]

Peptide		Structure (Position relative to Bn)														Ag/Ant*(b)*	RM #
N°	Name	1	2	3	4	5	6	7	8	9	10	11	12	13	14		
27	[Lys^{6}]Bn(6-14)						**Lys**	Gln	Trp	Ala	Val	Gly	His	Leu	Met-NH_2	Ag	[168]
28	Bn(7-14)							Gln	Trp	Ala	Val	Gly	His	Leu	Met-NH_2	Ag	[2,18,46,56–62,65,66,72,73,83,84,84,86,88,91,99–101,105,108–113,116,117,121,128,168,175–183]
29	Demobesin 5 [(N$_4$Bzdig)^{0}]Bn(7–14)						**N$_4$-bzdig**	Gln	Trp	Ala	Val	Gly	His	Leu	Met-NH_{11}	Ag	[70]
30	Demobesin 6 [(N$_4$Bzdig)^{0},Nle^{14}] Bn(7–14)						**N$_4$-bzdig**	Gln	Trp	Ala	Val	Gly	His	Leu	**Nle**-NH_2	Ag	[70]
31	[Cha^{13},Nle^{14}]Bn(7-14)							Gln	Trp	Ala	Val	Gly	His	**Cha**	**Nle**-NH_2	Ant	[66,67,67,69,93,94,176,184]
32	[Cha^{13}]Bn(7-14)							Gln	Trp	Ala	Val	Gly	His	**Cha**	Met-NH_2	Ant	[66,176]
33	[Nle^{14}]Bn(7-14)							Gln	Trp	Ala	Val	Gly	His	Leu	**Nle**-NH_2	Ag	[66,176]
34	[NMeGly^{11},Sta^{13},Leu^{14}] Bn(7-14)							Gln	Trp	Ala	Val	**NMeGly**	His	**Sta**	**Leu**-NH_2	Ant	[51,102]
35	[FA01010^{13},Leu^{14}] Bn(7-14)							Gln	Trp	Ala	Val	Gly	His	**FA01010**	**Leu**-NH_2	ND*(f)*	[102]
36	[βAla^{11}, Phe^{13},Nle^{14}]Bn(7-14)							Gln	Trp	Ala	Val	**βAla**	His	**Phe**	**Nle**-NH_2	Ag	[77]
37	[His(3Me)^{11},Sta^{13},Leu^{14}]Bn(7-14)							Gln	Trp	Ala	Val	**His(3Me)**	His	**Sta**	**Leu**-NH_2	Ant	[51]
38	[des-Met^{14}] Bn(7-14)NH_2							Gln	Trp	Ala	Val	Gly	His	Leu-NH_2		Ant	[118,120]
39	[DTyr^{6},des-Met^{14}] Bn(6-13)NHEt						**DTyr**	Gln	Trp	Ala	Val	Gly	His	**Leu-NHEt**		Ant	[48]
40	[Tyr^{5},DPhe^{6}] Bn(5-13)NHEt					**Tyr**	**DPhe**	Gln	Trp	Ala	Val	Gly	His	**Leu-NHEt**		Ant	[50]
41	RC-3095 [D-Tpi^{6},Leu^{13}, ψLeu^{14}]Bn(6-14)*(g)*						**D-Tpi**	Gln	Trp	Ala	Val	Gly	His	**Leuψ** *(c)*	**Leu**-NH_2	Ant	[142,155]

All the abbreviations are listed in Table 1;

(a) Aminoacid variations compared to Bn sequence are bold;

(b) Ag: agonist; Ant: antagonist;

(c) ψindicates a reduced peptide bond (-CH_2NH- instead of –CONH-);

(d) des-Met indicates the deletion of the Bn 14th aminoacid, Methionine;

(e) NHEt, Et=ethyl;

(f) ND: no data.

(g) Tpi: 2,3,4,9-tetrahydro-1H-pyridol[3,4-b]indol-3-carboxylic acid

Table 3

In vitro studies with ^{99m}Tc bombesin analogs.

			In vitro						
			Binding Affinity						
^{99m}Tc N	Linker	Peptide	Cell used	IC_{50}	Memb bound	Stability	Amnt of Rcptr Int	Comment	Ref. N
1	DPR-βAla	Bn(7-14)	T47-D/MDA-MB-231	2.0/1.1		Stable 24 h in PBS±HSA	45 min: 80/88% 120 min: 50/69%	PZ1 Derivatives showed higher binding affinities *in vitro*	[65]
2	DPR-GGG								
3	DPR-GSG			8.1/6.1					
4	DPR-PEG5								
5	DPR-PEG8								
6	DPR-Ser-Gly-Ser			0.8/0.3					
7	DPR-Ser-Ser-Ser			5.9/2.2					
8	PZ1-βAla			0.7/0.3			45 min: 69/83% 120 min: 34/69%		
9	PZ1-Gly-Gly-Gly			6.1/2.0					
10	PZ1-Gly-Ser-Gly								
11	PZ1-PEG5			2.0/0.7					
12	PZ1-PEG8			3.2/0.3					
13	PZ1-Ser-Gly-Ser								
14	PZ1-Ser-Ser-Ser			1.4/0.5					
15	N4-Gly-4-aminobenzoyl	[HDPhe^{6},Sta^{13},Leu ^{14}]Bn(6-14) "RM1" [Antagonist]	GRPR binding by autoradiography on cancer sections of prostate.	3.7±1.3	40% (2h)		Low internalization (10%, 2 h). Antagonist		[49]
16	NS3-Gly-Gly-Cys	Bn(2-14)	PC-3	3.0±0.7	17% (2h)	After 2 h stability in plasma 60%, in PC-3 30%. Kidney homogenates, after 5 min 40% intact, after 15 min 20%. Liver homogenates, after 5 min, almost totally degradated.	78% (2 h)	Introduction of the spacer Orn-Orn-Orn compared to non spacer produced a higher stability and internalization into the cells.	[171]
17	NS3-Gly-Gly-Cys-Orn-Orn-Orn			2.2±0.1	4%(2h)	After 2 h stability in plasma 60%, in PC-3 50%. Kidney homogenates, after 5 min 45% intact, after 15 min 30%. Liver homogenates, after 5 min, 60% intact.	88% (2 h)		
18	Gly-Gly-Cys-Aca	BN(2-14)	PC-3	1.1±0..1		In human plasma 2h: 80%. Kidney and liver homogenates: total degradation after 15 min.	75% (30 min)	The length of the Bn sequence did not alter binding, internalization or efflux rate.	[56]
19		BN(7-14)		1.9±0.1		In human plasma 2h: 35%. Kidney and liver homogenates: total degradation after 15 min.	65% (30 min)		
20	(NαHis)Ac-Pra(Glu)-βAla-βAla	[Cha^{13},NLe^{14}]Bn(7-14)	PC-3	IC_{50}:4.2±0.1, K_D: 0.3±0.1					[69]
21	EDDA/HYNIC	[Lys^{3}]Bn(1-14)	PC-3/MCF7/MDA-MB231				17.6±1.9(4h)/19.0±0.9(2h)/5.5±0.2(1h)/	The hybrid Tat-Bn analog's cell binding and internalization is higher than with the Bn analog.	[54]

			In vitro						
			Binding Affinity						
^{99m}Tc N	Linker	Peptide	Cell used	IC_{50}	Memb bound	Stability	Amnt of Rcptr Int	Comment	Ref. N
22	N_2S_2	[Tat(49-57)-Gly-Gly-Cys-Gly-[Lys^3]]Bn(1-14)	PC-3/MCF7/MDA-MB231			65% in human serum (24h); 41% after cys challenge in molar ratio 500:1 (cys:pept)	28.1±3.9(4h)/18.3±2.1(2h)/19.4±1.3(1h)		
23	Tetraamine-benzylaminodiglycolic acid	Demobes0in 1 (Antagonist)	PC-3/GRPR-HEK293/human prostate cancer	2.1±0.5/2.4±0.5/2.6±0.2	25% (2h)		No internalization (Antagonist)		[45]
24		Demobesin 4		0.8±0.1/2.1±0.3/2.0±0.5	10% (2h)		0.2±0.1 (30min)(Agonist)		
25	≡N(PNP6)-Cys-βAla-	Bn(7-14)	PC-3			After 4h cys challenge in molar ratio 100:1 (cys:pept): 93.6%	15.5% (2h)		[63]
26	HYNIC-βAla					After 4h cys challenge in molar ratio 100:1 (cys:pept): 98.3%	18.5% (2h)		
27	(NαHis)Ac-β^{3}hGlu-β^{3}Glu-β^{3}Glu	[Cha^{13},NLe^{14}]Bn(7-14)	PC-3	IC_{50}:634±221.7 k_D:nd		$t_{1/2}$ human plasma: 16h; in PC-3: 30–40min	1% (1h)	A positive charge may favor internalization of the tricarbonyl-labeled analogues, while more than one negative charge would have an adverse influence.	[67]
28	(NαHis)Ac-β^{3}hGlu-β^{3}Glu-βAla			IC_{50}:16.3±8.3 k_D:0.4±0.1			15% (1h)		
29	(NαHis)Ac-β^{3}hGlu-βAla-βAla			IC_{50}:13.3±3.0 k_D: 0.08±0.01			30% (1h)		
30	(NαHis)Ac-β^{3}hLys-βAla-βAla			IC_{50}:23.6±12.0 k_D:0.14±0.06		$t_{1/2}$ human plasma: 16h; in PC-3: 80min	40% (1h)		
31	(NαHis)Ac-β^{3}hSer-βAla-βAla			IC_{50}:6.8±3.2 k_D:0.05±0.03		$t_{1/2}$ human plasma: 16h; in PC-3: 30–40min	30% (1h)		
32	(NαHis)Ac-βAla-βAla			IC_{50}:5.1±1.7 k_D: 0.19±0.12			30% (1h)		
33	DTMA-βAla-	Bn(7-14)	PC-3	0.28±0.02			23.8±0.003% (2h)	βAla analog had the highest IC50 and internalization rates.	[62]
34	DTMA-Gly-Gly-Gly			2.56±1.3			2.37±0.01% (2h)		
35	DTMA-Gly-Ser-Gly			0.68±0.3			6.59±0.04% (2h)		
36	DTMA-Ser-Ser-Ser			0.74±0.2			11.46±0.03% (2h)		
37	(NαHis)Ac-βAla-βAla	[Cha^{13},NLe^{14}]Bn(7-14)	PC-3	IC_{50}:5.1±1.7 k_D:0.18±0.12		$t_{1/2}$ in PC-3: 30±6 min	29–37% of the total radioactivity/mg		[68]
38	(NαHis)Ac-Lys(sha)-βAla-βAla			IC_{50}:6.5±1.7 k_D:0.02±0.01		$t_{1/2}$ in PC-3: 35±11 min			
39	(NαHis)Ac-Lys(Amd)-βAla-βAla			IC_{50}:3.7±1.7 k_D:0.18±0.03		$t_{1/2}$ in PC-3: 37±8 min			
40	(NαHis)Ac-Ala(NTG)-βAla-βAla			IC_{50}:3.2±1.2 k_D:0.29±0.16		$t_{1/2}$ in PC-3: 38±5 min			
41		Litorin				67.5±5.0% in human plasma after 24h. 83.2±2.7% after cys challenge ratio molarity 1:1000			[71]
42	(NαHis)Ac	Bn(7-14)	PC-3	IC_{50}:1.9±0.7 k_D:0.19±0.09		$t_{1/2}$ human plasma: 0.5±0.2h, in PC-3: <0.1h	Internalization increased in the first 30 min and remained constant for 2 h. Cell related activity: 71–92% was internalized after 2 h.	The difference in the linker did not have a significant effect on stability or receptor affinity. However,	[66]
43		[Cha^{13}]Bn(7-14)		IC_{50}:5.1±1.4 k_D:0.08±0.04		$t_{1/2}$ human plasma:16±3h, in PC-3:0.3±0.1h			

			In vitro						
			Binding Affinity						
^{99m}Tc N	Linker	Peptide	Cell used	IC_{50}	Memb bound	Stability	Amnt of Rcptr Int	Comment	Ref. N
44		[Cha^{13},NLe^{14}]Bn(7-14)		IC_{50}:14.2±3.0 k_D:0.39±0.23		$t_{1/2}$ human plasma:6±1.5h, in PC-3:0.25±0.1h		substitutions in 13 and 14 positions increased stability.	
45		[NLe^{14}]Bn(7-14)		IC_{50}:15.7±6.0 k_D:0.51±0.28		$t_{1/2}$ human plasma:16±3h, in PC-3:0.25±0.1h			
46	(NαHis)Ac-βAla-βAla	[Cha^{13},NLe^{14}]Bn(7-14)		IC_{50}:5.1±1.7 k_D:0.18±0.12		$t_{1/2}$ human plasma: 10±1.45h, in PC-3:0.5±0.1h			
47	(NαHis)Ac-NH-CH_2-CH_2-O-CH_2-CH_2-O-	[Cha^{13},NLe^{14}]Bn(7-14)		IC_{50}:8.9±0.5 k_D:0.25±0.06		$t_{1/2}$ human plasma:8±3h, in PC-3:0.35±0.1h			
48	NS$_3$-4-(isocyanomethyl)benz oic acid-βAla	Bn(7-14)	PC-3	0.20±0.04			10–20% (2h)		[61]
49	NS$_3$-4-(isocyanomethyl)benz oic acid-Gly-Gly-Gly			1.9±0.4					
50	NS$_3$-4-(isocyanomethyl)benz oic acid-Ser-Ser-Ser			1.2±0.1					
51	NS$_3$-4-isocyanobutanoic acid-βAla			0.35±0.03			65% (2h)		
52	NS$_3$-4-isocyanobutanoic acid-Gly-Gly-Gly			1.4±0.1			10–20% (2h)		
53	NS$_3$-4-isocyanobutanoic acid-Ser-Ser-Ser			0.65±0.32					
54	DPR-Asn-Asn-Asn	Bn(7-14)	PC-3	1.3±0.2	20% (2h)	>75% after 4h in human serum		The different spacer linker used did not produce changes in the binding or stability characteristics between them.	[60]
55	DPR-Asn-Asn-Asn-βAla			2.2±0.1					
56	DPR-Asn-Asn-Asn-5Ava			3.6±2.2					
57	DPR-Arg-Arg-Arg			0.6±0.1					
58	DPR-Arg-Arg-Arg-βAla			0.2±0.02					
59	DPR-Arg-Arg-Arg-5Ava			0.4±0.1					
61	HYNIC/Tricine/TPPS–βAla	Bn(7-14)	PC-3/HT-29	38±1 in PC-3		In saline solution with Cys after 12h incubation, 95% stable.	20±3% (1h)		[64]
62	EDDA-HYNIC	[Lys^3]Bn	PC-3			>90% after 24h in human serum. >91% after cys challenge ratio molarity 1:500	11.5% (4h)		[167]
63	Gly-Gly-Cys-Aca	Bn(2-14)	PC-3	1.13					[55]
64	MeGly-Gly-Cys-Aca			0.76					
65	Me$_2$Gly-Gly-Cys-Aca			0.76					
66	Mac-Gly-Cys-Aca			1.42					
67	PZ1-βAla	Bn(7-14)	PC-3	0.7±0.04	25% (2h)		90% (90min)		[59]
68	PZ1-Gly-Gly-Gly			0.2±0.02	53% (2h)		56% (90min)		
69	PZ1-Ser-Ser-Ser			1.9±0.1	30% (2h)		48% (90min)		
70	Pm-DADT	[DTPA^1,Lys^3,Tyr^4]Bn	PC-3	Ki^{α} (nM): 4.1±1.4		>90% after 6h in human serum.			[53]
71		Demobesin 3	PC-3/autoradiography in human tumor biopsy samples.	0.06±0.04/0.47		In mouse plasma: 50% (2h)	75% (2h)		[70]

			In vitro						
			Binding Affinity						
^{99m}Tc N	Linker	Peptide	Cell used	IC_{50}	Memb bound	Stability	Amnt of Rcptr Int	Comment	Ref. N
72		Demobesin 4		0.15±0.04/1.94					
73		Demobesin 5		0.08±0.05/0.65					
74		Demobesin 6		0.60±0.05/1.3					
75		Demobesin 1 (Antagonist)	PC-3/AR42J/autoradiography in human prostate cancer samples/mouse pancreas	PC-3=0.35±0.32AR42J=0.45±0.18, human tumor: 3.2±0.7, mouse pancreas: 7.1±1.1.			PC-3=37% (6h), AR42J=19% (6h)	Demobesin 1 had IC_{50} 11-14 fold lower than Z-070 in PC-3	[50] see also ^{111}In tables
76	$^{99m}Tc(H_2O)(CO)_3$-Dpr-Ser-Ser-Ser	Bn(7-14)	PC-3	0.86±0.22	16% (40min)		55% (90min)		[57]

All peptides not indicated as antagonist are agonist at human Bn receptors.

Abbreviations: T47-D, MDA-MB-231, MCF7=human breast cancer cell line, PC-3=human prostate cancer cell line, HEK293=transformed human embryonic kidney cell line, HT29=colon rectal adenocarcinoma cell line.

Abbreviations see Table 1; Structures see Table 2 and Fig. 1.

Table 4

In vivo studies with ^{99m}Tc bombesin analogs.

			In vivo					
^{99m}Tc N	**Linker**	**Peptide**	**Stability**	**Animal**	**Biodistribution**	**Imaging**	**Comment**	**Ref. N**
1	DPR-βAla	Bn(7-14)		Normal CF-1 and SCID bearing T47D or MDA-MB-231 tumors	High level of pancreas uptake12.2–15.0±0.7/2.7% ID/g in normal CF-1 mice, but low tumor uptake.		DPR showed superior target tissue accumulation and pharmacokinetic properties *in vivo*.	[65]
2	DPR-GGG							
3	DPR-GSG					SPECT, favorable tumor/background ratio, clear visualization of tumor tissue. Kidneys (1.0–1.8) and GI (2.3–4.8) predominant source of radioactivity.		
4	DPR-PEG5							
5	DPR-PEG8							
6	DPR-Ser-Gly-Ser							
7	DPR-Ser-Ser-Ser				High level of pancreas uptake12.2–15.0±0.7/2.7% ID/g in normal CF-1 mice. High tumor upake. Selected for imaging study due to good tumor uptake and retention, and rapid elimination from non-target tissue by the renal-urinary system.	Favorable tumor/ background ratio, clear visualization of tumor tissue. Kidneys (0.8–0.9) and GI (1.3–2.7) predominant source of radioactivity.		
8	PZ1-βAla			Normal CF-1	8.5±0.2.2% ID/g pancreas uptake, but low tumor uptake.			
9	PZ1-Gly-Gly-Gly				Low pancreas uptake			
10	PZ1-Gly-Ser-Gly							
11	PZ1-PEG5							
12	PZ1-PEG8							
13	PZ1-Ser-Gly-Ser							
14	PZ1-Ser-Ser-Ser							
15	N4-Gly-4-aminobenzoyl	[HDPhe^{6},Sta^{13},Leu^{14}]Bn(6-14)“RM1” [Antagonist]		Human PC-3 xenograft-bearing nude mice	Tumor uptake at 4 h:29.9±4.0 %IA/g. Rapid and very high uptake in the pancreas and other GRPR expressing organs was also found but it washes out from these abdominal organs quickly, which results in good tumor/	SPECT/CT after 12 h injection of radiopeptide. Clear delineation of the tumor, low abdominal		[49]

			In vivo					
^{99m}Tc N	**Linker**	**Peptide**	**Stability**	**Animal**	**Biodistribution**	**Imaging**	**Comment**	**Ref. N**
					non-tumor tissue ratios at early time points.	uptake, kidneys faintly visible.		
16	NS3-Gly-Gly-Cys	Bn(2-14)		Normal Swiss and PC-3 tumor-bearing SCID mice	In normal mice: fast blood clearance, no uptake or retention in the stomach, low accumulation in liver and GI, excretion by kidneys and high accumulation in pancreas. In PC-3 tumor bearing SCID mice: “NS3-Gly-Gly-Cys” showed lower accumulation in pancreas and tumor than “NS3-Gly-Gly-Cys-Orn-Orn-Orn” which shows higher tumor/non-tumor ratios.		Introduction of the spacer Orn-Orn-Orn compared to non spacer produced a better uptake in target specific pancreatic and tumor tissue, and also higher quality SPECT images.	[171]
17	NS3-Gly-Gly-Cys-Orn-Orn-Orn					Dynamic γ camera: The PC-3 tumor was visible as early as 10 min after injection and remained observable up to 120 min p.i. Prominent uptake was also observed in the kidneys. Clearance of the radioactivity through the urinary bladder was evident.		
18	Gly-Gly-Cys-Aca	BN(2-14)		Normal Swiss and PC-3 tumor-bearing SCID mice	In normal mice: fast blood clearance, no uptake or retention in the stomach, low accumulation in liver but high uptake by intestine for 4 h, and high accumulation in pancreas. In PC-3 tumor bearing SCID mice: good tumor uptake by both analogs.	Dynamic planar view: tumors clearly viewed from min 15 in both cases.	Bn (7-14) radiolabeled analog had a slower washout from pancreas, but a slightly higher liver excretion rate.	[56]
19		BN(7-14)						
20	(NαHis)Ac-Pra(Glu)-βAla-βAla	[Cha^{13},NLe^{14}]Bn(7-14)		Nude mice bearing PC-3 tumors	Introduction of carbohydrate moiety Pra(Glu) produces an increase in the tumor uptake and retention.			[69]
21	EDDA/HYNIC	[Lys^3]Bn(1-14)		Balb C normal mouse and athymic mice bearing PC-3 tumors.	^{99m}Tc-Tat-BN clearance is predominantly renal. Pancreas shows higher uptake than non-excretory organs such as muscle. The tumor/ muscle ratio for ^{99m}Tc-BN was 7 and for ^{99m}Tc-Tat-BN was 8.5	γ camera: Clear tumor uptake and a dissection process to eliminate internal viscera, highlighted the ^{99m}Tc-BN and ^{99m}Tc-Tat-BN uptake in tumor PC-3 cells..	Although ^{99m}Tc-Tat-BN has better tumor/muscle ratio, it also has a high uptake by kidneys and non-target organs that should be reduced for a lower background.	[54]
22	N_2S_2	[Tat(49-57)-Gly-Gly-Cys-Gly-[Lys^3]]Bn(1-14)						
23	Tetraamine-benzylaminodiglycolic acid	Demobesin 1 (Antagonist)		PC-3 tumor-bearing SCID mice	Both Bn analogs targeted well the pancreas and PC-3 tumor. [^{99m}Tc]Demobesin1 showed higher PC-3 tumor accumulation at all times. Pancreas uptake/accumulation of [^{99m}Tc]Demobesin1 declined faster. Blood and background clearance was fast for both agents, excreted predominantly via kidneys. [^{99m}Tc]Demobesin1 showed a higher of hepatobiliary excretion with higher liver and bowel values.		The radiolabeled Bn antagonist (Demobesin1) may be is a preferable tool for radioimagining due to its higher tumor accumulation and uptake.	[45]
24		Demobesin 4						
25	≡N(PNP6)-Cys-βAla-	Bn(7-14)		Normal Swiss and PC-3 tumor-bearing SCID mice	Both analogs had rapid blood clearance. High uptake	Scintigraphy: Tumor uptake was higher	The best radiotracer was ^{99m}Tc-HYNIC due	[63]

			In vivo					
^{99m}Tc N	Linker	Peptide	Stability	Animal	Biodistribution	Imaging	Comment	Ref. N
26	HYNIC-βAla				of ^{99m}TcN(PNP6) by liver, pancreas and intestine expected considering the lipophilic character of the conjugate. ^{99m}Tc-HYNIC excreted primarily by the renal-urinary system and ^{99m}TcN(PNP6) via the hepatobiliary system. The highest tumor uptake using the HYNIC conjugate: 3.0±0.5%ID/g *vs* 1.2±0.3%ID/g for nitrido conjugate. The best ratios tumor/non tumor achieved with ^{99m}Tc-HYNIC.	with ^{99m}Tc-HYNIC than ^{99m}TcN(PNP6). Higher uptake of ^{99m}TcN(PNP6) by the hepatobiliary excretory system.	its high radiochemical yield, fast radiolabeling procedure without need of purification step, and more consistent tumor uptake.	
27	(NαHis)Ac-β^{3}hGlu-β^{3}Glu-β^{3}Glu	[Cha^{13},NLe^{14}]Bn(7-14)		PC-3 tumor-bearing SCID mice		No tested	A positive charge in the linker resulted in higher uptake in kidney and liver. A hydroxyl group and especially a single negative charge in form of a β^{3}homoglutamic acid considerably ameliorated the biodistribution profile, with higher tumor uptake, and significantly improved tumor-to-background ratios. However, additional negative charges led to a loss of affinity and internalization, and unfavorable biodistribution.	
28	(NαHis)Ac-β^{3}hGlu-β^{3}Glu-βAla					SPECT/CT: high uptake in the kidneys, pancreas, and bowel.		
29	(NαHis)Ac-β^{3}hGlu-βAla-βAla				Highest tumor uptake with a longer retention. Fast clearance from normal tissues. Higher pancreas and tumor uptake	SPECT/CT: Clearer visualizatin of tumors xenograft, lower renal and hepatic uptakes, abdominal uptake corresponds to pancreas and intestinal tract.		
30	(NαHis)Ac-β^{3}hLys-βAla-βAla				Not tested	Not tested		
31	(NαHis)Ac-β^{3}hSer-βAla-βAla					Not tested		
32	(NαHis)Ac-βAla-βAla					SPECT/CT: high uptake in the abdominal cavity due to the high hepatic, pancreatic, and intestinal uptakes.		
33	DTMA-βAla-	Bn(7-14)		Normal CF-1 and PC-3 tumor-bearing SCID mice	Normal CF-1 mice: rapid clearance from blood in the 4 analogs, except in the case of Ser-Ser-Ser. βAla and Gly-Gly-Gly analogs excreted by hepatobiliary system, Ser-Ser-Ser and Gly-Ser-Gly analogs by the kidneys. βAla has the highest uptake by the pancreas. In PC-3 bearing tumor mice: βAla was the only one tested, high tumor uptake and very rapid clearance from the whole body.		Although βAla analog has the higher tumor uptake rate, it had low accumulation in tumor tissue due to rapid accumulation in the hepatobiliary system.	[62]
34	DTMA-Gly-Gly-Gly							
35	DTMA-Gly-Ser-Gly							
36	DTMA-Ser-Ser-Ser							
37	(NαHis)Ac-βAla-βAla	[Cha^{13},NLe^{14}]Bn(7-14)		CF-1 nu/nu PC-3 tumor bearing mice	All new analogs exhibited higher tumor/background ratios compared to	SPECT/CT: reduction of abdominal	The introduction of a carbohydrated linker	[68]
38	(NαHis)Ac-Lys(sha)-βAla-βAla							

			In vivo					
^{99m}Tc N	Linker	Peptide	Stability	Animal	Biodistribution	Imaging	Comment	Ref. N
39	(NαHis)Ac-Lys(Amd)-βAla-βAla				the nonglycated peptide. The best results were obtained with the triazole coupled glucose with a 4-fold increased uptake and retention in tumor tissue and a significantly reduced accumulation in the liver. Apart from higher tumor-to-liver ratios, both tumor-to-kidney and tumor-to-blood ratios could be significantly improved.	background, tumor xenografts could clearly be visualized.	improved the biodistribution of Bn analogues labeled with the ^{99m}Tc-tricarbonyl core.	
40	(NαHis)Ac-Ala(NTG)-βAla-βAla							
41		Litorin		Normal Wistar rat		High and specific pancreas uptake. Excretion by kidneys.		[71]
42	(NαHis)Ac	Bn(7-14)		CF-1 nu/nu PC-3 tumor bearing mice	All analogues had low blood and stomach accumulation. Higher kidney uptake than liver and high colon and pancreas uptake. Tumor uptake was lower than pancreas in all cases.		The analogues including a spacer (46 and 47) had an improved biodistribution, and higher tumor-to-blood ratios. Tumor-to-kidney and tumor-to-liver ratios also increased when the -βAla βAla-spacer was used.	[66]
43		[Cha^{13}]Bn(7-14)						
44		[Cha^{13},NLe^{14}]Bn(7-14)						
45		[NLe^{14}]Bn(7-14)						
46	(NαHis)Ac-βAla-βAla	[Cha^{13},NLe^{14}]Bn(7-14)						
47	(NαHis)Ac-NH-CH_2-CH_2-O-CH_2-CH_2-O-CH_2CO	[Cha^{13},NLe^{14}]Bn(7-14)						
48	NS_3-4-(isocyanomethyl)benzoic acid-βAla	Bn(7-14)		CF-1 mice	Minimal uptake by stomach, rapid accumulation in the liver and excretion to the intestines, and low accumulation in pancreas after 1h. No good candidate.			[61]
51	NS_3-4-isocyanobutanoic acid-βAla							
54	DPR-Asn-Asn-Asn	Bn(7-14)		Normal CF-1 and PC-3 tumor-bearing SCID mice	In Normal CF-1: Highest pancreas uptake after 1h by Bn analog 56 and 55. At 4h and 24h pancreas uptake was higher with 55 analog. In PC-3 tumor-bearing SCID mice: the analog tested was number 55 and showed a good tumor uptake.		Analogs including Asn had no liver accumulation but kidney clearance, the contrary was observed in Arg derivatives. Among them the more promising is number 55.	[60]
55	DPR-Asn-Asn-Asn-βAla					SPECT/CT and MRI: Clearly visualized the tumors, but GI uptake was higher than with a previous described analog (DPR-Ser-Ser-Ser).		
56	DPR-Asn-Asn-Asn-5Ava							
57	DPR-Arg-Arg-Arg							
58	DPR-Arg-Arg-Arg-βAla							
59	DPR-Arg-Arg-Arg-5Ava							
60	Cys-Aca-Gln-Arg-Leu-Gly-Asn	[Lys^{14}]Bn(2-14)		Normal rats		SPECT: amygdala is clearly visualized.		[172]

			In vivo					
^{99m}Tc N	**Linker**	**Peptide**	**Stability**	**Animal**	**Biodistribution**	**Imaging**	**Comment**	**Ref. N**
61	HYNIC/Tricine/TPPS –βAla	Bn(7-14)	This analog was completely metabolized in urine, kidney, and liver samples at 1 h p.i. The majority of the radioactivity was found in the urine sample at 1 h p.i.	BALB/c normal and BALB/c nude mice bearing HT-29 tumors	The analog had a rapid renal clearance. Tumor uptake was the highest at 30 min p.i., with a steady decrease over the 4 h. study period. It had good T/B ratios for blood, liver and muscle at 1 h p.i	γ camera: Tumor is clearly visualized at 1 h p.i. with excellent tumor/background contrast. At 1h p.i., the highest uptake areas were tumor, kidneys, and bladder. By 4h p.i., the radioactivity in the chest region almost completely disappears while the tumor is still clearly seen.		[64]
62	EDDA-HYNIC	[Lys^3]Bn		Athymic mice bearing PC-3 tumors.	2 h p.i. the analog exhibited a rapid renal clearance. The highest non-specific uptake was found in kidneys. A significant uptake of radioactivity was observed in pancreas. Tumor also exhibited specific uptake of radioactivity.	γ camera: clear tumor uptake and a dissection process to eliminate internal viscera, highlighted the Bn analog uptake in tumor.		[167]
63	Gly-Gly-Cys-Aca	Bn(2-14)		Normal Swiss mice	The 4 Bn analogs showed renal clearance. Pancreas uptake was high and specific. Intestinal uptake can be attributed mainly to the GRP-R expressed in this tissue.			[55]
64	MeGly-Gly-Cys-Aca							
65	Me_2Gly-Gly-Cys-Aca							
66	Mac-Gly-Cys-Aca							
67	PZ1-βAla	Bn(7-14)		PC-3 tumor-bearing SCID mice	Tumor uptake and retention were lower when compared to other ^{99m}Tc-Bn conjugates of this type. The 3 analogs tested showed comparable accumulation of radiotracers in PC-3 xenografted tumors. The uptake of radioactivity in a normal pancreas was not different from other studies with ^{99m}Tc-Bn conjugates.			[59]
68	PZ1-Gly-Gly-Gly							
69	PZ1-Ser-Ser-Ser							
70	Pm-DADT	[DTPA^1,Lys^3,Tyr^4]Bn		CD-1 normal mice and PC-3 tumor-bearing SCID mice	In normal mice: fast clearance with low radioactivity excreted through the hepatobiliary system. Small amount of radioactivity was found in stomach, but high uptake in the pancreas. In C3 tumor-bearing SCID mice: specific and clear uptake by the tumor.	γ camera: clear and specific tumor uptake after 12h.	DTPA or its combination with Pm-DADT is important for the analog to be excreted by kidneys produces a low background imaging in the abdominal region.	[53]
71		Demobesin 3	In urine samples from animal	PC-3-tumor-bearing CD-1 nu/nu	Demobesin 5 and 6 were rapidly cleared via the liver and Demobesin 3 and 4 via kidneys, showing low	γ camera:clear tumour uptake, low		[70]

			In vivo					
^{99m}Tc N	Linker	Peptide	Stability	Animal	Biodistribution	Imaging	Comment	Ref. N
			after being inyected with the analogs showed the presence of 3 metabolites and no intact analog.	mice;human ileal carcinoids	background activity. [^{99m}Tc]Demobesin 5 and 6 show a high percentage of intestinal uptake. All four radiopeptides had high and slowly declining pancreas uptake. Uptake of radiopeptides in the PC-3 human prostate cancer xenograft was high, especially for [^{99m}Tc]Demobesin 3 and 4 (9–11%ID/g at 1 h pi), remaining high (7–9%ID/g) at 4 h pi.	background and low kidney uptake.		
72		Demobesin 4						
73		Demobesin 5						
74		Demobesin 6						
75		Demobesin 1 (Antagonist)		Nude mice bearing PC-3 and AR42J tumors.	In both cases rapid blood clearance, Demobesin1 is excreted by renal and hepatobiliar systems. In AR4-2J and PC-3 tumor-bearing mice, [^{99m}Tc]Demobesin 1 and [111In]Z-070 displayed similar uptake in the rat tumor. However, in the human PC-3 xenografts, [^{99m}Tc]Demobesin 1 showed a 2- to 3-fold higher uptake than [111In]Z-070.		Tumor uptakes depends on the origin of the tumor, this should be taking into account in the selection of experimental tools.	[50] see also ^{111}In tables
76	$^{99m}Tc(H_2O)(CO)_3$-Dpr-Ser-Ser-Ser	Bn(7-14)		Normal CF-1 and PC-3 tumor-bearing SCID mice	In normal mice: in both cases, fast clearance from blood, with no uptake or retention in the stomach, very high uptake by normal pancreas, excretion by renal system. In PC-3 tumor bearing mice: high uptake and accumulation in the tumor. Being the tumor uptake by $^{99m}Tc(H_2O)(CO)_3$-analog higher than than the other analog and than the previously described in ^{99m}Tc-N_3S-analog.			[57]
77	^{99m} $TC(CH_2CH_3)(CO)_3$-Dpr-Ser-Ser-Ser							

All peptides not indicated as antagonist are agonist at human Bn receptors.

Abbreviations see Table 1 and 3; Structures see Table 2 and Fig. 1.

Table 5

In vitro studies with ^{111}In bombesin analogs.

			In vitro						
			Binding affinity						
^{111}In N	Linker	Peptide	Cell used	IC 50/Kd (nM)	Membrane bound	Stability	Amount of Receptor Internalization	Comment	Ref. N
1	DO3A-CH2CO-G-4-aminobenzoyl	Bn(7–14) “AMBA”	GRPR binding by autoradiography on cancer sections of prostate.	0.8±0.1	4.3±0.3% (4h)		29±2.3% (4h)		[46]
2		[HDPhe^{6}, Sta^{13}, Leu^{14}]Bn(6–14) “RM1” [Antagonist]		35±13	21.8±0.93% (4h)		4.7±0.1% (4h)		
3	DOTA	[Pro^{1}, Tyr^{4}]Bn	CA20948 and AR42J	IC$_{50}$: 3–9 for the 4 Bn analogs. Binding and internalization depends on temperature. DPTA-[Pro^{1}, Tyr^{4}]Bn has highest binding and internalization.					[76]
4		[ε-Lys^{3}, Tyr^{4}]Bn							
5	DPTA	[Pro^{1}, Tyr^{4}]Bn				Stable after heating for 25 min 100 °C			
6		[ε-Lys^{3}, Tyr^{4}]Bn							
7	DOTA$^{0–1}$PEG$_{4}^{0}$	[DTyr^{6}, *β* Ala^{11}, Thi^{13}, Nle^{14}]Bn(6–14) “Z-070”	PC-3 and AR42J	PC-3=3.87±0.97, AR42J=0.17±0.04	PC-3<7.5%, AR42J<7.5% (both 6 h)		PC-3=37% AR42J=19% (both 6h)	Demobesin1= affinity 11–14 fold>Z-070 (PC3)	[50]
12	DOTA	Bn(7–14)	PC-3	110.6±32.3					[72]
13	DOTA-βAla			2.1±0.3					
14	DOTA-5-Ava			1.7±0.4					
15	DOTA-8-Aoc			0.6±0.1	26% (1 h)	t$_{1/2}$: 17.3 h in human serum	72% (1 h)		
16	DOTA-11-Aun			64±11.2					
17	DOTA-GABA	[DTyr^{6},βAla^{11}, Thi^{13}, Nle^{14}]Bn(6–14): “BZH2”	Autoradiography on sections of cancers with BnRs	GRPR: 1.4±0.1, NMBR: 4.93±1.03, BRS-3: 10.7±4.2	AR42J<7%.	t$_{1/2}$: 2.3 h in human serum	35% (6 h).		[79]
18	DPTA-GABA	[DTyr^{6},βAla^{11}, Thi^{13}, Nle^{14}]Bn(6–14): “BZH1”		GRPR: 3.47±0.32, NMBR: 10.5±3.03, BRS-3: 41.7±22.2	AR42J<7%	t$_{1/2}$: 2.0 h in human serum	40% (6 h).		
19	DOTA-8-Aoc	Bn(7–14)	PC-3	0.5±0.1					[73]
20	DOTA-5-ADS			3.2±0.3					
21	DOTA-8-AOS			6.2±0.3					
22	DOTA-AMBA			1.1±0.1					
23	DOTA-Gly-AMBA			1.9±0.1			Lowest internalization		

			In vitro						
			Binding affinity						
^{111}In N	Linker	Peptide	Cell used	IC 50/Kd (nM)	Membrane bound	Stability	Amount of Receptor Internalization	Comment	Ref. N
24	DOTA-Gly-AM2BA			0.7±0.1					
26	DOTA-aminohexanoyl	[DPhe^{6}, Leu-NHEt^{13}, des-Met^{14}]Bn(6–14): “Bomproamide” [Antagonist]	PC-3	1.4±0.1	>internalizated		14% (45 min)		[47]
30	DPTA	[Lys^{3}, Tyr^{4}]Bn(2–14)	PC-3	K_d: 22.9±6.8 B_{max}: 880 fmol per 10^6 PC-3 cells	After 1 h incubation: 17% radiactivity in cell surface	87.0±5.7% (72 h normal saline),66.0 ±5.35% and 59.4±3.40 % (8 h in human or rat plasma, respectively)	83% (1 h)		[80]
33	DPTA	[Pro^{1}, Tyr^{4}]Bn(1–14)	Autoradiography in 12 different prostate tumor xenografts in male nuce mice	High-density of GRPR in androgen-dependent tumors, low GRPR in androgen-responsive and -independent tumors. Castration results in GRPR downregulation in the 3 androgen-dependent tumors.					[78]
34	DTPA	[Pro^{1}, Tyr^{4}]Bn	7315b rat pituitary tumor cells	8 nM	With AR42J and CA20948 cells, binding with agonist>antagonist. Agonist was internalized, not antagonist.				[48]
35		[Tyr^{5}, DPhe^{6}]Bn(5–13)NHEt [Antagonist]		11 nM					
36	DPTA	[Pro^{1}, Tyr^{4}]Bn	PC-295 human prostate tumor xenografts and rat colon sections.	Rat: 2.4±0.6, human: 1.4±0.6		human serum: 67% (4 h)			[77]
37	DDpr(DPTA)	[βAla^{11}, Phe^{13}, Nle^{14}]Bn(7–14)		Rat:0.2±0.1, human: 0.5±0.1					
38	DPTA-ACMpip-Tha	[βAla^{11}, Phe^{13}, Nle^{14}]Bn(7–14)		Rat: 0.1±0.01, human: 0.4±0.1		human serum: 74% (4 h)			
39	DPTA-ACMpip-Tha	[βAla^{11}, Tha^{13}, Nle^{14}]BN(7–14)		Rat: 0.3±0.1, human: 0.4±0.01					
40	DPTA-Acp	[βAla^{11}, Phe^{13}, Nle^{14}]Bn(7–14)		Rat: 0.4±0.1, human: 2.5±0.3					
41	DPTA-DTha	[βAla^{11}, Tha^{13}, Nle^{14}]BN(7–14)		Rat: 1.2±0.1, human: 15.4±2.8					

All peptides not indicated as antagonist are agonist at human Bn receptors.

Cell line: CA20948 (rat pancreatic tumor cell line), AR42J (rat acinar pancreatic tumor cell line), PC-3 (human prostate cancer), 7315b (rat pituitary tumor cell line), PC-295 (human prostate cancer).

Abbreviations see Table 1; Structures see Table 2 and Fig. 1.

Table 6

In vivo studies with ^{111}In bombesin analogs.

			In vivo					
^{111}In N	Linker	Peptide	Stability	Animal	Biodistribution	Imaging	Comment	Ref. N
1	DO_3A-CH2CO-G-4-aminobenzoyl	Bn(7–14) "AMBA"		Nude mice+PC-3	RM1 has a higher tumor uptake than AMBA (13.4±0.8% *vs* 3.7±0.8% IA/g at 4 h after inyection) as well as to all tumor-to-normal tissues ratio.			[46]
2		"RM1" [HDPhe^6, Sta^{13}, Leu^{14}]Bn(6–14) [Antagonist]				SPECT showed a high uptake by the tumor lasting more than 72 h		
3	DOTA	[Pro^1, Tyr^4]Bn		Nude rats+AR42J	Although [^{111}In-DOTA-Pro^1, Tyr^4]Bn showed the highest uptake, of radioactivity in GRP receptor-positive tissues as well as higher target-to-blood ratios, ^{111}In-DTPA [Pro^1, Tyr^4]Bn was easier to handle and is more practical to use.			[76]
4		[ε-Lys^3, Tyr^4]Bn						
5	DPTA	[Pro^1, Tyr^4]Bn				^{111}In-DPTA-[Pro^1, Tyr^4]Bn can visualized tumor in rat by scintigraphy.		
6		[ε-Lys^3, Tyr^4]Bn						
7	DOTA$^{0–1}$-PEG$_4{}^0$	[DTyr^6, *β* Ala^{11}, Thi^{13}, Nle^{14}]Bn(6–14): Z-070		Normal Lewis rats and Nude mice+AR42J and PC-3 xenografts	In AR4-2J and PC-3 tumor-bearing mice, [^{99m}Tc]Demobesin 1 and [^{111}In]Z-070 have a similar tumor uptake. PC-3 xenografts, [^{99m}Tc]Demobesin 1 showed a 2–3x> uptake than [^{111}In]Z-070.			[50]
8	DOTA	PESIN	23.3±1.4% (5 min), 1.8±0.6% (15 min)	Swiss nu/nu mice+PC-3	PC-3 uptake at 1 h was comparable for Demobesin1, AMBA, PESIN and MP2346 (3.0±0.4, 2.7±0.5,	All analogues visualised PC-3 tumours by SPECT/CT and autoradiography.	Comparing this Bn analogs with ^{99m}Tc-Desmosin 1: Stability:	[2]

			In vivo					
^{111}In N	Linker	Peptide	Stability	Animal	Biodistribution	Imaging	Comment	Ref. N
					2.3±0.5 and 2.1±0.9%ID/g, respectively). AMBA, MP2346 and PESIN revealed favourable increases in tumor to blood ratios over time.		64.1±1.6% (5 min) and 41.5±0.5 (15 min). Changes in tumor to kidney and pancreas ratios for Demobesin1 from 1 to 24 h after injection were significantly better than for the other analogues.	
9		AMBA	36.1±2.7% (5 min), 9.8±0.5% (15 min)					
10		MP2346	21.2±0.8% (5 min), 3.4±1.3% (15 min)		High tumor uptake: 2.1±0.9%ID/g (1h), but high uptake by the kidneys (7.9±1.9%ID/g)			
11		MP2653	9.8±0.5% (5 min), 2.8±0.4% (15 min)		Very low tumor uptake: 0.9±0.25ID/g (1h)			
12	DOTA	Bn(7–14)		CF-1 healthy mice and PC-3 in ICR SCID mice for DOTA-8-Aoc	Radioactivity was cleared efficiently from blood by renal/urinary pathway. Pancreatic uptake increased as a function of hydrocarbon spacer length. ^{111}In-DOTA-8-Aoc-BBN(7–14) conjugate conducted on PC-3 xenografts in SCID mice showed a specific uptake of radioactivity in tumor, with 3.63±1.11 %ID/g observed 1 h after injection. High			[72]
13	DOTA-βAla							
14	DOTA-5-Ava							
15	DOTA-8-Aoc							
16	DOTA-11-Aun							

			In vivo					
^{111}In N	Linker	Peptide	Stability	Animal	Biodistribution	Imaging	Comment	Ref. N
					tumor-to-blood and tumor-to-muscle ratios (6:1 and 45:1, respectively) were achieved at 1 h after injection. Radioactivity in the tumor was 43,19, and 9% of the radioactivity retained 24, 48, and 72 h after injection *vs* 1h.			
17	DOTA-GABA	[DTyr^{6},βAla^{11}, Thi^{13}, Nle^{14}]Bn(6–14): BZH2		Lewis rats+ARJ42	Biodistribution studies of ^{111}In-BZH1 and ^{111}In-BZH2 (^{177}Lu-BZH2) in AR4–2J tumor-bearing rats showed specific and high uptake in GRPR–positive organs and in the AR4–2J tumor. A fast clearance from blood and all of the non-target organs except the kidneys was found.			[79]
18	DPTA-GABA	[DTyr^{6},βAla^{11}, Thi^{13}, Nle^{14}]Bn(6–14): BZH1						
19	DOTA-8-Aoc	Bn(7–14)		Normal CF-1 mice and SCID mice+PC-3 xenografts	In CF-1 mice, the BB2R uptake in the pancreas of radioconjugates containing aromatic linking groups was found to be significantly higher at 1 h postinjection than with radioconjugates with ether linker moieties. By 24 h postinjection, the radioconjugates containing aromatic groups exhibited the	Fused Micro-SPECT/CT imaging studies at 24 h showed accumulation of radioactivity in the tumor with all radioconjugates. In both biodistribution and Micro-SPECT/CT imaging studies, the radioconjugates containing aromatic linking groups typically		[73]
20	DOTA-5-ADS							
21	DOTA-8-AOS							
22	DOTA-AMBA							
23	DOTA-Gly-AMBA							
24	DOTA-Gly-AM2BA							

Curr Drug Deliv. Author manuscript; available in PMC 2012 January 1.

			In vivo					
^{111}In N	Linker	Peptide	Stability	Animal	Biodistribution	Imaging	Comment	Ref. N
					highest percentage tumor retention.	exhibited higher G.I. retention than hydrocarbon or ether linking moieties.		
25	DOTA-Sar5	[DTyr^{5,6},βAla^{11}, Thi^{13}, Nle^{14}]Bn(6–14)		Normal Wistar rat and autoradiography of kidney slides	Injection of polyglutamic acid or gelofusine but not that of Lys reduce kidney accumulation of the radiopeptide.			[173]
26	DOTA-aminohexanoyl	[DPhe^{6}, Leu-NHEt^{13}, des-Met^{14}]Bn(6–14): Bomproamide [Antagonist]		Normal CF-1 mice and SCID mice with PC-3 xenografts	Rapid (0.25 h p.i.) and high (12.2±3.2%ID/g) pancreatic uptake was observed in healthy CF-1 mice. Rapid (0.25 h p.i.) and high uptake (6.9± 1.1%ID/g) was observed in PC-3 prostate cancer xenografts in SCID mice.	PC-3 xenografts were well observed in SCID mice by SPECT/CT.		[47]
27	DPTA	[Pro^{1}, Tyr^{4}]Bn: MP2248		Nude NMRI mice, with or without surgical castration and resupplementation of testosterone with PC-82, PC-295 and PC-310 xenografts	Expression of human GRPR in androgen-dependent PC xenografts is reduced by androgen ablation and is reversed by restoring the hormonal status of the animals.			[185]
28	No linker	[ACMpip^{5}, Tha^{6},βAla^{11}, Tha^{13}, Nle^{14}]Bn(5–14): MP2653						
29	DPTA	[Pro^{1}, Tyr^{4}]Bn		Lewis rats with CA20948 and AR42J	CA20948 tumor, both in cell culture and as solid tumor in rats, is a very useful model for peptide receptor scintigraphy and radionuclide therapy studies.		This radiopeptde was compared with CCK, substance P and octreotide radiopeptide.	[75]

			In vivo					
^{111}In N	Linker	Peptide	Stability	Animal	Biodistribution	Imaging	Comment	Ref. N
30	DPTA	[Lys^3, Tyr^4]Bn(2–14)		SCID mice with PC-3 xenografts	Accumulated in tumor, adrenal, pancreas, small intestine, and large intestine. Fast blood clearance and fast excretion from the kidneys were observed. The levels of radioactivity within the tumor peaked at 8 hours and then declined rapidly.	Micro-SPECT/CT showed uptake in the tumors at 8 and 24 h. High accumulation in the kidney, pancreas, and GI at 4, 8, 24, and 48 h. The trend of uptake seen in the imaging data was similar to the results of the biodistribution study.		[80]
31	DPTA	[Pro^1, Tyr^4]Bn: MP2248		Lewis rats+CC531 (Colon CAR.) or CA20948 xenografts	Highest uptake by pancreas and kidneys. Rapid clearance of radioactivity from blood. Urinary excretion amounted to 70% ID after 24 hr, with a total body retention of 10% ID. Specific uptake was found in the CA20948 pancreas tumour and CC531 colon carcinoma in tumour bearing rats.	The CA20948 tumour, inoculated in the hindleg, was also visualized scintigraphically.		[74]
32	DPTA	[Pro^1, Tyr^4]Bn(1–14)		Lewis rats and C57B16 or NMRI nude mice	Kidney uptake is higher in mouse than in rat males.	Autoradiography in kidney slices showed, in both mice and rats, high uptake in cortex, less in outer medulla and none in inner medulla.		[186]
34	DTPA	[Pro^1, Tyr^4]Bn		Bufallo rats+7315b prolactinoma xenografts	The agonist [^{111}In-DTPA-Pro^1, Tyr^4]Bn showed much higher specific uptake in	Scintigraphy of isolated 7315b tumors from rat		[48]
35		[Tyr^5, DPhe^6]Bn(5–13)NHEt [Antagonist]						

			In vivo					
^{111}In N	Linker	Peptide	Stability	Animal	Biodistribution	Imaging	Comment	Ref. N
					Bn receptor-positive tissues and tumor than the antagonist [^{111}In-DTPA-Tyr^{5}, DPhe^{6}]Bn(5–13)NHEt, with concordant target to background ratios.	showed tumor uptake		
36	DPTA	[Pro^{1}, Tyr^{4}]Bn		Rats bearing CA20948 tumors and Nude mice bearing PC-3 tumors.	High receptor-mediated uptake in receptor-positive organs and tumors.	Using this Bn analog tumours could be visualised using planar gamma camera and microSPECT/CT imaging after 1 min during 4 h.		[77]
38	DPTA-ACMpip-Tha	[βAla^{11}, Phe^{13}, Nle^{14}]Bn(7–14)						

All peptides not indicated as antagonist are agonist at human Bn receptors.

Abbreviations see Table 1 and 5; Structures see Table 2 and Fig. 1.

Table 7

In vitro studies with ^{125}I, $^{185/187}Re$, ^{18}F, ^{64}Cu, ^{68}Ga and ^{90}Y bombesin analogs.

Peptide #	Iso.	Linker	Peptide	In vitro					Comment	Ref. N
				Binding affinity		Membrane bound	Degrad.	Receptor Intern.		
				Cell used	IC_{50}/K_d (nM)	Amnt.(%)		Amnt.(%)		
1	^{125}I	no	[Tyr^4]Bn	SKOV3.ip1-AdCMV-GPRR	no	80.3±5.9	no	no	Exp. Performed over-expressing AdCMVGRPR construct in each cell line	[119]
2	^{131}I	mIP	Bn		no	no	no	no		
3	^{125}I	no	[Tyr^4]Bn	SKOV3.ip1-AdCMV-GPRR	no	~ 75	no	no		[118]
4	^{125}I	no		Balb/B1 GRPR, (BnR11)	no	25.6±1.6	no	37.3±10.9 (4h)		
5	^{125}I	no		Hela	no	~70	no	no		
6	^{125}I	no		A427	no	~ 88	no	no		
7	^{125}I	mIP	[des Met^{14}]Bn [Antagonist]	SKOV3.ip1-AdCMV-GPRR	no	~ 68	no	no		
8	^{125}I	mIP		Balb/B1 GRPR, (BnR11)	no	38.3±11.6	no	32±9 (4h)		
9	^{125}I	mIP		Hela	no	~ 60	no	no		
10	^{125}I	mIP		A427	no	~ 65	no	no		
11	$^{185/187}Re$	Aca-Gly-Gly-Cys(Bn1.1)	Bn(2–14)	PC-3	1.13	no	no	no	High affinity for Bn1.1 cmpd	[55]
12	$^{185/187}Re$	Aca-MeGly-Gly-Cys (Bn1.2)			0.76	no	no	no		
13	$^{185/187}Re$	Aca-Me$_2$Gly-Gly-Cys (Bn1.3)			nd	no	no	no		
14	$^{185/187}Re$	Aca-Mac-Gly-Cys (Bn1.4)			1.42	no	no	no		
18	^{188}Re	Tris	[des Met^{14}] Bn(7–14) [Antagonist]	BnR-11	no	13.9±0.1	no	no		[120]
19	^{188}Re	Tris-C$_6$			no	12.8±0.2	no	no		
20	^{188}Re	Tris		PC-3	no	9.9±0.3	no	no		
21	^{188}Re	Tris-C$_6$			no	nd	no	no		
22	^{18}F	3-Cyano-4-[^{18}F] fluorobenzoyl-Ava	[NMeGly^{11}, Sta^{13}, Leu^{14}] Bn(7–14) [Antagonist]	PC-3	2.71	no	~ 100 (2h)	no	High affinity and plasma stability	[102]
23	^{18}F		[FA(01010)^{13}, Leu^{14}] Bn(7–14)	PC-3	9.2	no	~ 100 (2h)	no		
24	^{18}F	2-(4-(di-tert-butylfluorosilyl)phenyl) acetyl-Arg-Ava-	[NMeGly^{11}, Sta^{13}, Leu^{14}] Bn(7–14) (4b)[Antagonist]	PC-3	22.9	no	no	no	4b has higher affinity, lower stability both *in vitro* and ex vivo experiments than 3b cmpd	[51]
25	^{18}F		[His(3Me)^{11}, Sta^{13}, Leu^{14}] Bn(7–14) (3b) [Antagonist]	PC-3	267.7	no	no	no		

Peptide #	Iso.	Linker	Peptide	In vitro					Comment	Ref. N
				Binding affinity		Membrane bound	Degrad.	Receptor Intern.		
				Cell used	IC_{50}/K_d (nM)	Amnt.(%)		Amnt.(%)		
26	^{18}F	FB	Bn	PC-3	no	no	no	7 (30 min)	FB-dual GRPR/integrin avb3 cmpd, has slighty lower uptake than FB-Bn compd.	[100]
27	^{18}F		Bn (7–14)-RGD	PC-3	no	no	no	6 (30 min)		
28	^{18}F	FB-PEG_3-Glu	Bn (7–14)-RGD	PC-3	73.3±1.6	no	no	6.65±0.3 (2h)	Rapid internalization. Similar affinity.	[101]
29	^{18}F	PEG_3-Glu		PC-3	85.4± 1.9	no	no			
30	^{18}F	FB	[Lys^3]Bn	PC-3	5.3±0.6	no	no	61 (2h)	Aca-linker reduces affinity and uptake of Bn(7–14)	[99]
31	^{18}F	FB-Aca	Bn(7–14)		48.7± 0.1	no	no	50 (2h)		
32	^{18}F	no	[Lys^3]Bn		3.3± 0.4	no	no	no		
33	^{18}F	Aca	Bn(7–14)		20.8± 0.3	no	no	no		
34	^{64}Cu	DOTA	MP2346	PC-3	no	no	no	34 (1h)	Lower internalization and retention compared to the same cmpd Labeled with ^{86}Y.	[87]
35	^{64}Cu	DOTA	[Lys^3]Bn	PC-3	2.2±0.5	no	no	65±10 (30min)	DOTA-[Lys^3]Bn has affinity and internalization rate similar to Bn	[85]
37	^{64}Cu	DOTA-8-Aoc	Bn(7–14)	PC-3	1.4±0.1	no	no	no	Both cmpds have a steady increase in the amount of activity in the cell over time	[90]
38	^{64}Cu	CB-TE2A-8-Aoc			0.5±0.01	~600cpm	no	~1000cpm		
39	^{64}Cu	TACN-βAla-βAla	[Cha^{13}, Nle^{14}] Bn(7–14)	No	no	no	*in vitro*/*in vivo*	no	Stable in presence of a large excess of a competing ligand or copper seeking superoxide dismutase and in rat plasma.	[93]
40	^{64}Cu	bispidine derivatives	[Cha^{13}, Nle^{14}] Bn(7–14)	no	no	no	*in vitro*/*in vivo*	no	Cmpd Show high stability both *in vitro* and *in vivo*.	[94]
41	^{64}Cu		[Cha^{13}, Nle^{14}] Bn(7–14)	no	no	no	no	no		
42	^{64}Cu	DOTA	Bn (7–14)-RGD	PC-3	85.8± 2.1	no	no	3.7±0.02	NOTA cmpd has faster *in vitro* kinetic than DOTA cmpd	[95]
43	^{64}Cu	NOTA			92.7± 3.5	no	no	2.9±0.5		
44	^{64}Cu	cage amine ligand (CuL1)	[Lys^3] Bn(1–14)	no	no	no	no	no	High serum stability.	[98]
45	^{64}Cu	DOTA-GGG	Bn(7–14)	PC-3	50±16.2	no	no	670 fmol/mg (20h)	The presence of glutamic acids in the linker reduces binding affinity and internalization	[89]
46	^{64}Cu	DOTA-GSG			81.8± 34.3	no	no	830 fmol/mg (20h)		
47	^{64}Cu	DOTA-GSS			31.7±6	no	no	1550 fmol/mg (20h)		
48	^{64}Cu	DOTA-GEG			2160± 718	no	no	160 fmol/mg (20h)		
49	^{64}Cu	DOTA-GEE			19300±4050	no	no	no sign.		

Peptide #	Iso.	Linker	Peptide	In vitro					Comment	Ref. N
				Binding affinity		Membrane bound	Degrad.	Receptor Intern.		
				Cell used	IC_{50}/K_d (nM)	Amnt.(%)		Amnt.(%)		
50	^{64}Cu	DOTA-Aba	Bn(7–14)	T-47D	78.5± 15.1	no	no	1300±198 fmol/mg (4h)	Low binding affinity values. The longer linker Ado allows binding but interferes with internalization	[88]
51	^{64}Cu	DOTA-Ava			41.5± 7.8	no	no	n.d.		
52	^{64}Cu	DOTA-Ahx			15.8± 5.4	no	no	1312±100 fmol/mg (4h)		
53	^{64}Cu	DOTA-Aoc			6.7±1.1	no	no	1419±109 fmol/mg (4h)		
54	^{64}Cu	DOTA-Ado			27±5.4	no	no	5.6 fmol/mg (2h)		
55	^{64}Cu	NOTA-8-Aoc	Bn(7–14)	PC-3	3.1±0.5	no	no	no	NOTA chelator improves binding affinity.	[91]
57	^{64}Cu	NO_2A-8-Aoc	Bn(7–14)	T-47D	7.6±2.2	no	no	90 (45min)	Promising pharmacokinetic values.	[92]
59	^{64}Cu	DOTA-Aoc	Bn(7–14)	PC-3	K_d 6.1±2.5	3.3 to 4.6	no	18.2±0.4 (2h)	High affinity and internalization rates.	[83]
60	^{64}Cu	DOTA-PEG	Bn(7–14)	PC-3	3.9±0.6 mM	9.3 to 12.4	no	~ 45 (2h)	Differences in internalization due to different affinity.	[84]
61	^{64}Cu	DOTA-Aoc			90.5±22	2.4 to 3.1	no	~ 12 (2h)		
62	^{64}Cu	DOTA	[Lys^3]Bn	PC-3	2.2±0.5	no	no	~ 84 (2h)	DOTA- Aca compd has reduced pharmacokinetic properties.	[86]
63	^{64}Cu	DOTA-Aca	Bn(7–14)		18.4±0.2	no	no	~ 75 (2h)		
66	^{68}Ga	NOTA	Bn (7–14)-RGD	PC-3	55.9±4.2	no	no	1.7±0.3 (15 min)	High affinity and internalization rates.	[105]
68	^{68}Ga	DOTA-PEG2	[DTyr^6,βAla^{11}, Thi^{13}, Nle^{14}] Bn(6–14) (BZH3)	AR42J	K_d 0.5	no	no	88 (2h)	Good affinity. Rate of internalization shows an agonistic nature of the compd.	[104]
69	^{68}Ga	DOTA-PEG4	Bn(7–14)	human cancer tissue	6.6±0.1	no	no	43.7±1.8 (6h)	Affinity analysis for receptor subtypes [NMBR 12.5±0.5; GRPR 10±0.0;BB3R >1000]	[103]
70	^{90}Y	DOTA-GABA	[DTyr^6,βAla^{11}, Thi^{13}, Nle^{14}] Bn(6–14) (BZH2)	human cancer tissue	4.9±1 NMBr; 1.4±0.1 GRPr; 10.7±4.2 BB3	no	no	no	^{90}Y-BHZ2 had significantly higher affinity for all receptor subtypes, due to the extra negative charge at the NH_2 terminus.	[79]
71	^{90}Y	DOTA-GABA	[DTyr^6,βAla^{11}, Thi^{13}, Nle^{14}] Bn(6–14) (BZH2)	ARJ42	no	no	no	Rapidly internalyzed		
72	^{86}Y	DOTA	MP2346	PC-3	no	no	no	13 (1h)	Long incubation period shows higher levels of internalization	[87]
74	^{90}Y	DOTA	Bn(2–14)	PC-3	1.99±0.1	no	79.1 (24h)	23.3±0.03 (4h)		[107]

All peptides not indicated as antagonist are agonist at human Bn receptors.

Abbreviations see Table 1; Structures see Table 2 and Fig. 1.

Cell lines: SKOV3.ip1, Ovarian carcinoma; Hela, Human cervical cancer; A427, Human lung carcinoma; BnR11, Mouse embryonic fibroblast cell line stably transfected with GRP receptor; PC-3, Human prostate cancer cells; T47D, Human breast cancer cells; AR42J, Rat pancreatic acinar cell tumor

Table 8

In vivo studies with ^{125}I, $^{185/187}Re$, ^{18}F, ^{64}Cu, ^{68}Ga and ^{90}Y bombesin analogs.

Peptide #	Isotope	Linker	Peptide			In vivo		Ref. N
				Animal	Biodistribution	Imaging	Comment	
1	^{125}I	mIP	Bn	SKOV3.ip1-AdCMV-GRPR tumor bearing Athymic nu/nu mice BALB/c	Similar biodistribution between 125I and 131I.	no	^{131}I cmpd has good tumor uptake but a short effective half life in tumor, too. Therapeutic response with repeated administration.	[119]
2	^{131}I		Bn			no		
6	^{125}I	no	[Tyr^4]Bn	SKOV3.ip1 tumor bearing athymic nude mice	In normal mice clearance for both cmpds was rapid. mIp cmpd undergoes a slower deiodination than the other cmpd In tumor bearing mice mIP showed a faster and better tumor uptake than the other cmpd	no	SKOV3.ip1 injected in mice oveexpressed AdCMVGRPR construct. Difference in tumor uptake between two cmpds is likely due to the different rate of deiodination,	[118]
7	^{125}I	no		Balb/c mice		no		
8	^{125}I	mIP	[des-Met^{14}]Bn [Antagonist]			no		
9	^{125}I	mIP		SKOV3.ip1 tumor bearing athymic nude mice		no		
15	^{188}Re	N_3S-5-Ava	Bn(7–14)	CF-1 mice	Similar distribution for all compd. Differences observed at 4h PI. Clearance via renal and liver pathways.	no	$^{188,186}Re$ coniugates are useful targeting GRPR +tissues. NCA^{186,18}8Re have higher specificity than CA ^{186}Re	[121]
16	^{186}Re	N_3S-5-Ava carried				no		
17	^{186}Re	N_3S-5-Ava non-carried				no		
24	^{18}F	2-(4-(di-tert-butylfluorosilyl)phenyl)acetyl-Arg-Ava-	[NMeGly^{11}, Sta^{13}, Leu^{14}] Bn(7–14) (4b) [Antagonist]	PC-3 tumor bearing nude mice	Low uptake and clearance. High accumulation in liver, gallbladder, intestine	no	Cmpd synthesized by silicon-based one-step labeling protocols a new labeling method for synthesis of new ^{18}F-labeled Bn derivatives.	[102]
26	^{18}F	FB	Bn	PC-3 tumor bearing nude mice	High tumor specificity of dual FB-Bn/ RGD cmpd	microPET for distribution and metabolic stability	dual tracer has more than additive effect *in vivo* for tumor uptake.	[100]

Peptide #	Isotope	Linker	Peptide			In vivo		Ref. N
				Animal	Biodistribution	Imaging	Comment	
28	^{18}F	FB-PEG_3-Glu	Bn (7–14)-RGD	PC-3 tumor bearing nude mice	Hight tumor specificity. Low liver uptake. Excretion by kidney	microPET for distribution and metabolic stability	PEG_3 spacer improves renal clearance respect to non-PEGylated cmpd (see [100])	[101]
30	^{18}F	FB	[Lys^3]Bn	PC-3 tumor bearing nude mice	Tumor-to-nontarget ratios of Lys3-Bn cmpd were higher that those of Aca-Bn(7–14) cmpd Renal clearance, with higher hepatobiliary accumulation for Aca-Bn(7–14).	microPET 10 min after injection. PET and CT imaging of orthopic PC-3 tumor model 17min after injection.	FB-Lys^3Bn has higher efficacy in targeting the tumor. Useful for orthopic prostate Ca. imaging and GRPR+ tumors.	[99]
31	^{18}F	FB-Aca	Bn(7–14)					
34	^{64}Cu	DOTA	MP2346	PC-3 tumor athymic nude mice	Rapid clearance, within 24h. Uptake and specificity lower than ^{86}Y-labeled cmpd	PET/CT imaging 1 and 24 h after injection.	Low tumor/non-tumor ratios. High background and liver accumulation.	[87]
35	^{64}Cu	DOTA	[Lys^3]Bn	PC-3 tumor athymic nude mice	Rapid and predominant renal clearance. Significant uptake in tumor and pancreas.	microPET and autoradiographic imaging. Comparable uptake indices between microPET ROI and quantitative autoradiography analyses.	PET imaging of prostate Ca. with 64Cu-labeled Bn analogs is useful to determine dosimentry and tumor response to the same ligand labeled with therapeutic amounts of ^{67}Cu for internal radiotherapy.	[85]
36	^{64}Cu			CWR22 tumor athymic nude mice				
37	^{64}Cu	DOTA-8-Aoc	Bn(7–14)	PC-3 tumor bearing SCID mice	Clearance through renal system.	microPet, fused microPET/CT and axial images. Significantly reduced activity of CB-TEA-8-Aoc cmpd in kidney and gastrointestinal tract	Better clearance of CB-TEA-8-Aoc than DOTA-8-Aoc cmpd Even the last shows an higher retention.	[90]
38	^{64}Cu	CB-TE2A-8-Aoc						

Peptide #	Isotope	Linker	Peptide			In vivo		Ref. N
				Animal	Biodistribution	Imaging	Comment	
39	^{64}Cu	TACN-β Ala-β Ala	[Cha^{13}, NLe^{14}] Bn(7–14)	Wistar rats	high uptake and rapid renal clearance 5′ and 60′ single ID	PET images 60′ after single ID	Further exp. are necessary to evaluate specificity of the binding and tumor uptake. TACN as linker showed interesting results for developing new Cu-radiopharmaceuticals.	[93]
40	^{64}Cu	bispidine derivatives	[Cha^{13}, NLe^{14}] Bn(7–14)	Wistar rats	Significant retention in kidney; high stability	no	Bifunctional bispidine cmpds are new versatile Bn-derivatives of copper radiopharmaceuticals useful for both diagnosis and therapy.	[94]
41	^{64}Cu			PC-3 tumors bearing mice	no	PET imaging.		
42	^{64}Cu	DOTA	Bn (7–14)-RGD	PC-3 tumors bearing mice and Balb normal mice	Analysis in Balb normal mice. High pancreatic uptake.	Small animal PET in PC-3 tumor bearing mice. Rapid clearance by blood. High kidney uptake and tumor/non-tumor ratio.	NOTA-RGD-Bn has an higher tumor uptake and tumor/non-tumor ratio and lower liver uptake than DOTA-RGD-Bn cmpd	[95]
43	^{64}Cu	NOTA						
45	^{64}Cu	DOTA-GGG	Bn(7–14)	PC-3 tumors bearing mice	Good blood clearance except for GSG cmpd which has constant but low values. GSG cmpd has a low tumor uptake	Small animal PET/CT images 1 and 24h after I.V.	Agreement bethween biodistribution and imaging studies. Additional serines in the linker cause lower liver uptake.	[89]
46	^{64}Cu	DOTA-GSG						
47	^{64}Cu	DOTA-GSS						
50	^{64}Cu	DOTA-Aba	Bn(7–14)	T-47D tumor bearing SCID mice	Rapid bood clearance. High pancreas and tumor uptake. Very similar tumor/non tumor ratios between cmpds	no	A reduced carbon linker length reduced both liver uptake and tumor uptake.	[88]
52	^{64}Cu	DOTA-Ahx				MicroPET imaging 1h after I.V.		
53	^{64}Cu	DOTA-Aoc				no		
54	^{64}Cu	DOTA-Ado						
55	^{64}Cu	NOTA-8-Aoc	Bn(7–14)	CF-1 mice	Rapid blood clearance and excretion by kidney.	no	Promising cmpd for both molecular imaging and therapy.	[91]

Peptide #	Isotope	Linker	Peptide			In vivo		Ref. N
				Animal	Biodistribution	Imaging	Comment	
56	^{64}Cu			PC-3 tumors bearing SCID mice	Good tumor uptake. High specificity and affinity	MicroPET 24h after P.I. Strong site direct PET targeting agent for prostate Ca.		
57	^{64}Cu	NO_2A-8-Aoc	Bn(7–14)	CF-1 mice	High pancreas uptake after 1h I.V.	no	NO_2A-compd. useful for breast therapeutic analyses. Very fine structure.	[92]
58	^{64}Cu			T-47D tumor bearing SCID mice	High pancreas uptake with a low intestine uptake.	MicroMR and microPET/CT imaging analyses. Pancreas most visible.		
59	^{64}Cu	DOTA-Aoc	Bn(7–14)	PC-3 tumors bearing mice	Excellent liver and pancreas uptake. Good tumor uptake. Rapid blood clearance.	MicroPET imaging. Clear tumor visualization	Necessary to reduce liver and normal tissue uptake for imaging and therapeutic purposes.	[83]
60	^{64}Cu	DOTA-PEG	Bn(7–14)	Normal athymic nude mice	Only significant difference in uptake and retention is in the bone, kidneys and blood. High pancreas uptake.	no	Higher PEG-cmpd uptake than expected.	[84]
61	^{64}Cu	DOTA-Aoc				no		
62	^{64}Cu	DOTA	[Lys^3]Bn	PC-3 tumor athymic nude mice	Obtained by PET images. Liver uptake higher that other organs. Aca-linker reduces pancreas affinity	micoPET images	DOTA-[Lys^3]Bn has high affinity and moderate metabolic stability. Specific tumor localization with good tumor/non tumor ratios. It is superior to DOTA-Aca-Bn(7–14) cmpd	[86]
63	^{64}Cu	DOTA-Aca	Bn(7–14)					
64	^{64}Cu	DOTA	[Lys^3]Bn	22Rv1 tumor athymic nude mice				
65	^{64}Cu	DOTA-Aca	Bn(7–14)					
66	^{68}Ga	NOTA-Aca	Bn (7–14)-RGD	PC-3 tumor bearing mice	High tumor and pancreas uptake.	MicroPET images. Low uptake in PC-3 tumors. Excretion by kidneys.	Dual receptor binding cmpd Demonstrated to be useful in tumors where only one of the receptors is over-expressed.	[105]
67	^{68}Ga			MDA-MB-435 tumor bearing mice		MicroPET images. Low expressing		

Peptide #	Isotope	Linker	Peptide			In vivo		Ref. N
				Animal	Biodistribution	Imaging	Comment	
						GRPR system. Good tumor uptake.		
68	^{68}Ga	DOTA-PEG$_2$	[D-Tyr^6,β-Ala^{11}, Thi^{13}, Nle^{14}] Bn(6–14) (BZH3)	AR42J tumor bearing mice	Dose dependent uptake of high expressing GRPR tissues. Fast blood clearance.	PET images 1h after injection. Clear definition of tumor tissue and low uptake of non target tissues.	With well defined and low background images, BZH3 has prerequisites as a helpful cmpd in GRPR+ tumors.	[104]
69	^{68}Ga	DOTA-PEG$_4$	Bn(7–14)	PC-3 tumor bearing mice	Rapid blood clearance. High uptake in tumor and pancreas. High retention in kidneys.	PET and Scintigraphy imaging show high uptake in tumor, pancreas and kidneys. Scintigraphy	PEG$_4$ spacer form suitable cmpd for clinical studies.	[103]
72	^{86}Y	DOTA	MP2346	PC-3 tumor bearing athymic mice	High level of tumor/non tumor ratios. Specific uptake. No optimal kidneys uptake. More favorable distribution than 64Cu cmpd	PET/CT images. Low background uptake. Results consistent with biodistribution studies.	To reduce renal uptake and improve clearance ^{86}Y-MP2346 has to be altered to have a neutral or negative charge.	[87]
73	^{86}Y	DOTA		AR42J tumor bearing rats		PET/CT images. Low bakcground uptake. Higher quality than 64Cu cmpd		
74	^{90}Y	DOTA	Bn(214)	normal Swiss mice	Efficent clearance from blood Excretion by kidneys. Good pancreatic uptake.	no	Preference toward ^{177}Lu cmpd rather than ^{90}Y cmpd	[107]

All peptides not indicated as antagonist are agonist at human Bn receptors.

Abbreviations see Table 1 and 7; Structures see Table 2 and Fig. 1.

Cell lines: SKOV3.ip1, Ovarian carcinoma; T47D, Human breast cancer cell; CWR22, Human prostate cancer cells; 22RV1, Human prostate carcinoma; PC-3, Human prostate cancer cells; AR42J, Rat pancreatic acinar cell tumor

Table 9

In vitro studies with ^{177}Lu bombesin analogs.

^{177}Lu-Peptide#	Linker	Peptide	In vitro					Comment	Ref. N
			Binding affinity		Membrane bound	Degrad.	Receptor Intern.		
			Cell used	IC_{50}/K_d (nM)	Amnt.(%)		Amnt.(%)		
1	DOTA	di=[Lys^3] Bn(1–14)(09)	PC-3	no	no	no	35.9±1.5	08 and 09 cmpd. are divalent. Increased targeting propertes. Potential probes for MRI	[106]
2	DOTA	mono=[Lys^3] Bn(1–14)(07)					18.3± 1.1		
3	DOTA-Ahx	mono=Bn(4–14)(06)					26.5± 0.8		
4	DOTA-Ahx	di=Bn(4–14)(08)					41.9± 2.1		
7	DOTA	Bn(2–14)	PC-3	1.3±0.1	5.2±0.01	85.6% after 24h in h. serum	30.7±0.07 (4h)	Adding ^{177}Lu increases affinity compared to 90Y-labeling	[107]
8	Bn8 (DO_3A-CH_2CO-8-Aminooctanoyl)	Bn(714)	PC-3	3.1±1	34.6	no	72.9±0.08 (40min)	^{177}Lu-Amba displays high affinity, retention rather than other pan-Bn or Bn8	[110]
9	DO_3A-CH_2CO-G-(4-aminobenzoyl) [AMBA]	Bn(7–14)	PC-3	2.5±0.5/K_d 1.02	34.1	$t_{1/2}$=38.8h (h) 3.1h (m)	76.8±1.8 (40min)		
10	DOTA-8-Aoc	Bn(7–14)	PC-3	0.3± 0.1	10 (40min)	no	85 (40min)	Superior pharmacokinetic properties to ^{99}Tc-N_3S-5-Ava-Bn (7–14)	[108]
11	DOTA-PEG_4	Bn(7–14)	h. cancer tissues	6.1±3.0	no	no	39.1±1.1 (6h)	Low affinity respect to unlabeled cmpd.	[103]
12	DO_3A-CH_2CO-G-4-aminobenzoyl [AMBA]	Bn(7–14)	PC-3	5	no	$t_{1/2}$=38.8±1.3h (human); 8.1±3.8h (rat); 3.1±0.1h (mouse)	no	*In vitro* slow degradation	[111]
13	DO_3A-CH_2CO-G-4-aminobenzoyl [AMBA]	Bn(7–14)	LNCaP	K_d 0.6±0.2	19.6±3.3 (2h)	no	47.9±5.3	Good affinity even in low expressing GRPR tumors (LNCaP and DU145)	[112]
14		Bn(7–14)	DU145	K_d 0.5±0.1	16.4±3.4 (2h)		63.9±6.9		
15		Bn(7–14)	PC-3	no	15.3±2.3 (2h)		74.7±15.3		
16	DOTA-GABA	[DTyr^6, β Ala^{11}, Thi^{13}, Nle^{14}] Bn(6–14): “BZH2” [Antagonist]	Autoradiography on sections of cancers with BnRs	no	no	no	no		[79]
17	DO_3A-CH_2CO-G-4-aminobenzoyl [AMBA]	Bn(7–14)	Autoradiography on sections of cancers with BnRs	no	no	no	no	^{177}Lu-AMBA identifies hGRPR and hNMBR, but not BRS-3.	[116]
18	DO_3A-CH_2CO-G-4-aminobenzoyl [AMBA]	Bn(7–14)	CHO expr. hNMBR;	K_d 0.025	no	no	no	No BRS-3 specific binding observed. Competition exp. On hunan cancer tissue	[117]
19			HEK293 expr. hGRPR	K_d 0.035	no	no	no		

^{177}Lu-Peptide#	Linker	Peptide	In vitro					Comment	Ref. N
			Binding affinity		Membrane bound	Degrad.	Receptor Intern.		
			Cell used	IC_{50}/K_d (nM)	Amnt.(%)		Amnt.(%)		
20			BALB 3T3 exp. BRS-3	K_d>1000	no	no	no	revealed high GRPR affinity over NMBR and BRS-3.	
21 (^{149}Pm)	DO_3A-amide	Bn(7–14)	PC-3	no	no	~95 (more 5 days)	no	β-alanine increasaes affinity	[113]
22 (^{149}Pm)	DO_3A-amide-β-Ala	Bn(7–14)		no	no	~95 (more 5 days)	no		
23 (^{153} Sm)	DO_3A-amide-β-Ala	Bn(7–14)		59.8± 23.1	no	~95 (more 5 days)	no		
24 (^{153} Sm)	DO_3A-amide	Bn(7–14)		1.8±0.2	no	~95 (more 5 days)	no		

All peptides not indicated as antagonist are agonist at human Bn receptors.

Abbreviations see Table 1; Structures see Table 2 and Fig. 1.

Cell lines: SKOV3.ip1, Human ovarian carcinoma; AR42J, Rat pancreatic acinar cell tumor; LNCaP, Human prostate cancer cells; DU145, Human metastatic prostate cancer cells; PC-3, Human prostate cancer cells; HEK293, Human Embryonic kidney cells; CHO, Chinese hamster ovary; BALB 3T3, Mouse embryonic fibroblast cell line

Table 10

In vivo studies with ^{177}Lu bombesin analogs.

^{177}Lu-Peptide #	Linker	Peptide	In vivo				Ref. N
			Animal	Biodistribution	Imaging	Comment	
5	DO_3A-amide-β-Ala	Bn(7–14)	CF-1 mice	Only with the β-Ala cmpd. Rapid tissue clearance	no	β-Ala increases lipophilicity with faster clearance	[113]
6	DOTA-8-Aoc	Bn(7–14)	PC-3-tumor-bearing SCID mice	no	scintigraphy 48hr post IV.	GRPR radiolabeled cmpd.+chemo suppressed prostate Ca.	[109]
7	DOTA	Bn(2–14)	mice	Cleared from the blood within 24hr; rapidly excreted in urine; low kidney retention	no	^{177}Lu compd. had slower kinetics.	[107]
8	Bn8 (DO_3A-CH_2CO-8-Aminooctanoyl)	Bn(7–14)	PC-3-tumor-bearing SCID mice	40–50% excreted by urine after 24hr. High cellular retention.	no	^{177}Lu-Amba better biodistribution for radiotherapeutic purpose than pan-Bn or Bn8	[110]
9	DO_3A-CH_2CO-G-(4-aminobenzoyl) [AMBA]						
10	DOTA-8-Aoc	Bn(7–14)	CF-1 and PC-3-tumor-bearing SCID mice	Cleared from blood within 1 h, mainly renal. High pancreatic accumulation in CF-1 and specific tumor targeting in PC-3 xenografts.	no	Potential peptide for therapeutic radiopharmaceuticals for GRPR+ cancers.	[108]
11	DOTA-PEG_4	Bn(7–14)	PC-3 tumor bearing athymic nude mice	Blood clearance at 1 h post IV; faster from pancreas than tumor. Excreted by kidney and high pancreas and tumor uptake.	PET and scintigraphic images; accumulation mostly in pancreas, kindey and tumor.	^{177}Lu AMBA is more effective for clinical studies than ^{99}Tc-labelled Bn analogues.	[103]
12	DO_3A-CH_2CO-G-$_4$-aminobenzoyl [AMBA]	Bn(7–14)	PC-3 tumor bearing nude mice	Renal excretion. High uptake in pancreas and tumors.	no	Rapidly metabolized *in vivo* but strong efficacy in targeting GRPR+ tumors.	[111]
13	DO_3A-CH_2CO-G-$_4$-aminobenzoyl [AMBA]	Bn(7–14)	LNCaP tumor bearing nude mice	Renal clearance (50% after 24hr). Main targets= pancreas and tumor for PC-3 tumor bearing	γ-imaging for tumor uptake and retention; Autoradiography for for viable tumor cells.	Limits cell proliferation and re-establish the normal vascular phenotype in LNCaP and DU145 xenografts. Therapeutic	[112]
14			DU145 tumor bearing nude mice				

^{177}Lu-Peptide #	Linker	Peptide	In vivo				Ref. N
			Animal	Biodistribution	Imaging	Comment	
15			PC-3 tumor bearing nude mice	mice. For the others types of xenograft the principal target is only the pancreas		potential in low-GRPR expressing prostate Ca.	
16	DOTA-GABA	[DTyr^{6},β Ala^{11}, Thi^{13}, Nle^{14}] Bn(6–14): "BZH2" [Antagonist]	ARJ42 tumor bearing Lewis rats	^{177}Lu-BHZ2 showed specific and high uptake in GRPR–positive organs and in the AR42J tumor. A fast clearance from blood and all of the non-target organs except the kidneys was found.	no		[79]
18	DO_3A-CH_2CO-G-$_4$-aminobenzoyl [AMBA]	Bn(7–14)	Autoradiography on human neoplastic and non-neoplastic tissues	no	no	Specific binding of various types of tumor tissues and chroinc pancreatitis pancreas.	[117]
22 (^{149}Pm)	DO_3A-amide-β-Ala	Bn(7–14)	CF-1 mice	Only with the β-Ala cmpd. Rapid tissue clearance	no	Same retention compared to other tho lanthanides. (see in this table peptide #6.). Potential therapeutic cmpd.	[113]
23 (^{153} Sm)					no	See peptide # 6 and 17.	

All peptides not indicated as antagonist are agonist at human Bn receptors.

Abbreviations see Table 1 and 9; Structures see Table 2 and Fig. 1.

Cell lines: SKOV3.ip1, Human ovarian carcinoma; AR42J, Rat pancreatic acinar cell tumor; LNCaP, Human prostate cancer cells; DU145, Human metastatic prostate cancer cells; PC-3, Human prostate cancer cells.

Table 11

Studies in human using radiolabeled bombesin analogs.

Isotope	Linker	Peptide	No	Patients studied	Imaging technique	Results	Ref. N
^{99m}Tc	Cys^0-Aca^1	"[Leu^{13}]Bn" [Cys^0-Aca^1, Bn(2–14)]	**1**	3 normal; 1 **prostate cancer**, 1 **SCLC**	SPECT and planar scintigraphy	No side effects, visualization of both tumors for 3h, radioactivity accumulation in liver, kidneys and thyroid gland. Tumor uptake higher than with ^{99m}Tc sestamibi alone.	[123]
			2	Biopsies from 5 **suspicious** for **breast cancer**	Biopsy driven by Imaging Probe combined with X-ray	48/48 biopsies high, 19/21 intermediate and 2/8 low radioactivity uptake positive for cancer.	[124]
			3	14 patients positive for **prostatic lesions**	SPECT and planar scintigraphy	100% cancer and lymph nodes visualized. Results confirmed by pathologic evaluation while ^{111}In-Octreotide only detected 2/3 cases.	[125]
			4	5 **suspicious** for **breast cancer**	Planar scintigraphy	No sides effects. 100% cancer and lymph nodes visualized. Radioactivity accumulated in liver, kidneys and thyroid gland. Tumor/breast uptake ratio higher than with ^{99m}Tc sestamibi alone.	[122]
			5	10 **suspected** and 1 proven with **prostate cancer**	SPECT and planar scintigraphy	100% cancer and lymph nodes visualized. Results confirmed by pathologic evaluation. Detection of the lymph nodes affected better than with MRI.	[126]
			6	13 (6 **suspected**+7 known to have **rectal cancer**)	SPECT and planar scintigraphy	Cancer detected in 11/13 and 2 false positives. 5/5 positive lymph nodes detected. Results confirmed by pathologic evaluation. After 60 min all radiopeptide is in intestine.	[127]
^{99m}Tc	EDDA/HYNIC	[Lys^3]Bn	**7**	11 (3 with proven **breast cancer** and 8 with possible cancer)	SPECT and planar scintigraphy	No side effects. Predominant renal clearance. Patients with breast cancer showed asymmetrical uptake by breast tissue, with higher accumulation in patients with breast cancer.	[129]
^{99m}Tc	N_3S	"RP527" 5-Ava-Bn(7–14)	**8**	4 patients with bone metastasis with androgen-resistant **prostate cancer** + 6 suspected **breast carcinoma**	SPECT and planar scintigraphy	No side effects. Hepatic and renal clearance non blood accumulation. Radiopeptide uptake in 1/4 prostate cancer bone metastases and 4/6 breast cancer metastases and affected lymph nodes.	[58]
			9	6 **healthy** subjects	Study of dosimetry by time/course (planar scintigraphy, blood and urine samples)	No side effects. Hepatobiliary and renal clereance, non blood accumulation. Low uptake by brain, myocardium, lungs, brest and testes. Possible radiotracer for the supradiaphragmatic region and favorable dosimetry for SPECT.	[128]
			10	14 patients (9 suspected **breast carcinoma**+5 tamoxifen-resistant bone	Planar scintigraphy	8/9 suspected patients tumor and lymph nodes were detected. 0/5 resistant patients detected.	[187]

Isotope	Linker	Peptide	No	Patients studied	Imaging technique	Results	Ref. N
				metastasized breast carcinoma)			
^{68}Ga	DOTA-PEG$_2$	"BZH3" [DTyr^6,β Ala^{11}, Thi^{13}, Nle^{14}] Bn(6–14)	**11**	17 **GIST** patients	PET scans comparing ^{68}Ga-BZH3 to ^{18}F-FDG	FDG discovered 25/30 lessions, BZH3 8/30. Tumor uptake is lower with BZH3 than with FDG. In 1 case the lesion was seen with BZH3 and not with FDG.	[130]
			12	9 low grade glioma patients	PET scans comparing ^{68}Ga-BZH3 to ^{18}F-FDG	6/6 patients with increase with BZH3 and FDG uptake had malignant transformation. 2/2 with decreased BZH3 and no FDG uptake had malignant transformation.	[131]

All peptides not indicated as antagonist are agonist at human Bn receptors.

Abbreviations see Table 1; Structures see Table 2 and Fig. 1.

Table 12

Studies with Bn analogs conjugated to non-radioactive cytotoxic agents.

					In vitro				
N	**Drug**	**Linker**	**Bn Analog**	**Cell used**	**Binding affinity IC_{50} (nM)**	**Stability**	**Amnt of Rcptr Int**	**Cytotoxicity**	**Ref. N**
1	Camptothecin	N-(N-Me-aminoethyl)-glycine carbamate	[$DTyr^6$, β Ala^{11}, Phe^{13}, Nle^{14})Bn(6–14)]	Balb 3T3, NCI-H1299, MOLT-4, HT-29, PC-3, NCI-H69, SKNSH	K_i: GRPR=0.012±0.001; NMBR= 0.035±0.003; BRS-3=0.031±0.008.	20 min half life in mouse plasma	33±2% (1h)	Reduced cell growth depends on the cell expression of GRPR, NMBR or BRS-3. Tumoricidal IC_{50} from 90 to 1923 nM. In NCI-H1299, CFPAC-1 or PC-3 xenografted nude mice reduced tumor growth 55–84%.	[30,34]
2	Camptothecin	[N-(N-methyl-amino-ethyl)-glycine carbamate	[$DSer^5$, $DTyr^6$, β Ala^{11}, Phe^{13}, NLe^{14}]Bn(5–14)	HUVECs, PC-3, MCF-7, H29, SKNSH	IC_{50} for cytotoxicity: PC-3=429.85 nM, MCF-7: 1.70 μM, NCI-H69= 2.71 μM, H29= 2269 nM, SKNSH= 1610 nM			Bn conjugated in PC-3 inhibits adhesion to collagen type I, $\alpha v\beta 3$ and $\alpha v\beta 5$, dose 10–20 μM. In HUVECs inhibits capillary-like tube formation and *in vivo* angiogenesis, dose 10–20 μM and 40 μM, respectively.	[136]
3	Paclitaxel	PEG	Bn(7–13)	H1299	24h incubation=14±1.1 nM, 96h=6±0.9 nM	$T_{1/2}$ in PBS: 154 min, $t_{1/2}$ in human plasma 113 min		Conjugated tumoricidal IC_{50} is 2.5-fold lower than with Paclitaxel alone	[144]
4		Glu and PEG	Bn(6–14)	MO59J, JNPRSLT1, Hutu-80, FADU, SKNAS				Addition of PEG as linker produces an increase in the solubility but a decrease in the cytotoxicity. The best cytotoxicity results were obtained with Paclitaxel-Glu-$(Bn(6–14)_2)$: 64–93%	[145]
5	2-Pyrrolino-DOX	Glutaric acid	[$DTpi^6$, Leu^{13}, ψiLeu^{14}]Bn(6–14) (Antagonist) and 15 other [Leu^{13}, ψiLeu^{14}]Bn(6–14) analogs	CFPAC-1, DMS-53, PC-3 and MKN-45 cells	2-pyrrolino-DOX-14-O-glt-[$^{13}\psi^{14}$, CH_2-NH, Leu^{14}]Bn(6–14) Ki: 1.6 in Bn/GRP Swiss 3T3 cells			Tumoricidal IC_{50} of 2-pyrrolino-DOX-14-O-glt-[$^{13}\psi^{14}$, CH_2-NH, Leu^{14}]Bn(6–14) ranges from 0.4 to 6.8 nM in cell tested, and 2-Pyrrolino-DOX from 0.22–3.6 nM	[141]
6	Hemiasterlin	ALALAEGEGEG	[$DPhe^6$, βAla^{11}, Phe^{13}, Nle^{14})Bn(6–14)	NCI-H1299	15±2			From 0.1–1 μM inhibited proliferation in a dose-related manner.	[33]
		ALALANG			25±3				
	Dolastatin	LALAEGEGEG			150±18			No cytotoxic activity in NCI-H1299 cells.	
		G			20±2				
		LALAG			15±1				
7	KLAKLAKKLAKLAKGG (KLA)		Bn(2–14)	Raji, NB4, CEM, K562, Molt4 and Jurkat				Tumoricidal IC_{50} in μM range in all tumor cell line, from solid tumors or leukemia. *In vivo* K562 xenografted BALB/C nude mice treatment with each Bn conjugated produce a reduction in tumor volume.	[151]
	GRFKRFRKKFKKLFKKLS (B27)								
	GGLRSLGRKILRAWKKYG (B28)								
8	DAB_{389}		GRP	AR42J, HuTu 80				GRP conjugated peptide inhibited protein synthesis in cell lines expressing GRPR or NMBR.	[150]
9	OKT3 (anti-CD3 antibody)	SPDP	[Cys^5, $DPhe^6$, Leu-$NHEt^{13}$, des-Met^{14}] Bn(5-14) (Antagonist)	NCI-H345, DMS273	Specific binding of Bn conjugated to NCI-H345 and DMS273			Specific and dose dependent inhibition of SCLC growth by Bn conjugate, increasing apoptosis by cleavage of caspase-3, -9 and PARP. *In vivo* DMS276 xenografted mice treated with the Bn conjugated showed a reduction of tumor size.	[152]
10	FcγT	SATA/Sulfo-SMCC	[Lys^3]Bn	NCI-H69, NCI-H345, SHP-77, DMS273	NCI-H69 binds 5036 immnuconjugates/cell, NCI-H345 binds 6116, SHP-77 binds 2399 and DMS273 to 9473 5–50 μg/ml FcγT-[Lys^3]Bn =50–85% positive cells		The amount of compound internalized remain inside the cells for 4 h	Co-culture of tumor cells line with activated monocytes and immunoconjugate produces >80% of cell tumor lysis, and 75% with neutrophils and SHP-77 cells.	[154]
11	FcγT or FcγTII	SATA/SMCC	[$DTrp^6$, Leu^{13}-ψ(CH_2NH)Phe^{14}]Bn(6–14) (Antagonist)	NCI-H69, NCI-H345, SHP-77, DMS273	Both immnunoconjugates binds in a dose related manner to the SCLC cells, 50–85% positive cells			Bn agonist immunoconjugated has no effect on clonogenic growth of SCCL cells. Both (agonist and antagonist) immunoconjugated produced the lysis of SCLC when incubated with monocytes previously activated	[153]
12			Lys^3]Bn						
13			[$DPhe^6$, $desMet^{14}$]Bn(6–14)	MiaPaCa-2, SW620, HT29, PTC				*In vitro* MTT results: in MiaPaCa-2 cell best cytotoxicity with analog 17 at 0.1 nM, SW620 analog 18 at 0.1 nM, HT29 analog 16	[163]

					In vitro				
N	Drug	Linker	Bn Analog	Cell used	Binding affinity IC_{50} (nM)	Stability	Amnt of Rcptr Int	Cytotoxicity	Ref. N
14			[DPhe^{6}, Aib^{11}, desMet^{14}]Bn(6–14)					at 1 μM. PTC analog 19 at 0.01 nM. *In vivo* PTC cell tumor xenofraft mice analog 18 produced a inhibition of tumor growth of 44.3%	
15			[DPhe^{6}, Aib^{9}, desMet^{14}]Bn(6–14)						
16			[DPhe^{6}, Aib^{9}, Ile^{13}, desMet^{14}]Bn(6–14)						
17			[DPhe^{6}, Aib^{11}, Ile^{13}, desMet^{14}]Bn(6–14)						
18			[DPhe^{6}, Aib^{9}, Aib^{11}, Ile^{13}, desMet^{14}]Bn(6–14)						
19			Butanoyl[DPhe^{6}, Aib^{11}, desMet^{14}]Bn(6–14) (All antagonists)						
20		Lys-Lys between peptides	SS analog-Substance P antagonist-VIP receptor binding inhibitor-Bn antagonist	MOLT-4, MCF-7, MiaPaCa-2, KB, PTC				EC_{50} (μM) for MTT assay: MOLT-4=0.29, MCF-7=0.34, MiaPaCa-2=0.21, KB=2.1, PTC>10. *In vivo* experiments with PTC tumor bearing mice showed a 73.7% tumor regression.	[156]
				Colo-205, MiaPaCa-2, ECV304				Analog 20 decreases cAMP, EGF stimulated growth and pMAPKs, also reduces p53 and Bcl-2 but increases caspase 3. It also inhibits capillary-like tube formation and secretion of VEGF in endothelial cells.	[157]
21	Mono-carbohexyl-tetrasulfonated aluminium phthalocyanine		8-Aoc-Bn(7–14)	PC-3	8-Aoc-Bn(7–14)=3.73×10^{-10} M $AlPcS_4$-8-Aoc-Bn(7–14)=2.94×10^{-8} M			$AlPcS_4$-8-Aoc-Bn(7–14) showed higher phototoxicity than $AlPcS_4$ alone and 2–3 fold increase photodynamic efficacy over $AlPcS_4$ at lower doses.	[155]
22	Maleimide-PEG		Bn(7–14)	CHO-d1EGFP				Bn analog combined with EHCO/siRNA nanoparticles produces a high efficient cell-specific siRNA system (cell uptake=73.9%; gene silencing effiency=91.9%)	[188]
23			GRP-MH20 (GRP bound to the N′ side of MH20)	HeLa, Colo 205, Swiss 3T3 ans NIH 3T3				It showed a significant enhancement (8–15- fold) of adenovirus mediated gene transfer in the 3 cell lines. This increase is proportional to the GRPR in cell.	[158]
24			MH20-GRP (GRP bound to the C′ side of MH20)					It had not activity on adenovirus infection and gene transfer.	

All peptides not indicated as antagonist are agonist at human Bn receptors.

Abbreviations: SATA= N-succinimidyl S-acetylthioacetate; Sulfo-SMCC= sulfosuccinimidyl 4-(N-maleimidomethyl) cyclohexane-1-carboxylate; Ail= α-aminoisobutyric acid; EHCO= 1(-aminoethyl)imino-bis[N-(oleicyl-cysteinyl-histinyl-1-aminoethyl)propio-n-amide for peptide 19: Somatostain analog= D-Phe-Cys-Tyr-D-Trp-Orn-CyLeu-Pen-Thr-NH_2; Substance P antagonist= D-Arg-Pro-Lys-Pro-DPhe-Gln-D-Trp-Phe-D-Trp-Leu-CyLeu-NH_2 VIP receptor binding inhibitor=Leu-Met-Tyr-Pro-Thr-Tyr-Leu-Lys-OH; Bn anatagonist=[DPhe^{6},Aib^{11},desMet^{14}]Bn(6–14); MH-20=Lys-Met-Tyr-Pro-Arg-Gly-Asn-Hys-Trp-Ala-Val-Gly-His-Leu-Met; SPDP= N-succinimidyl 3-[2-pyridyldithio] propionate. OKT3= anti-CD3 monoclonal antibody; DOX= doxorubicin. **Cell lines:** Rat pancreatic cancer= AR42J, mouse embryonic fibroblasts= Balb-3T3 and Swiss 3T3 and Chinese hamster ovary cell line= CHO.

Human breast cancer= MCF-7, colon cancer= Colo-205, HT29 and SW620, epidermoid carcinoma= KB, gastric cancer= MKN-45, gliobalstoma= MO59J, hypopharyngeal carcinoma=FADU, intestine carcinoma= Hutu, leukemia= CEM, Jurkat, KS62, MOLT-4 and NB4, lymphoma= Raj, neuroblastoma= SKNAS and SKNSH, pancreatic cancer= CFPAC-1 and MiaPaCa-2, papillary thyroid cancer= PTC, prostate cancer=PC-3, small cancer lung cell= DMS273, DMS-53, JNPRSLT1, NCI-H345, NCI-H69 and SHP-77, umbilical vein endothelial cell= ECV304 and HUVECS, non-small cell lung cancer cell line= NCI-H1299, human cervical adenocarcinoma cell line= HeLa

Abbreviations see Table 1; Structures see Table 2 and Fig. 1.